Función de la SUMOilación en el desarrollo del sistema nervioso central de vertebrados

Function of SUMOylation during development of the central nervous system in vertebrates

Trabajo de tesis para el acceso al título de
Doctor en Biología Molecular y Biomedicina
por la Universidad de Sevilla.
En Sevilla, a … de …… de 2017.

Director del trabajo:

Fdo: Mario García Domínguez

Tutor del trabajo:

Fdo: Andrés Aguilera López

Autor del trabajo:

Fdo: Francisco de Paula Juárez Vicente

Table of Contents

1 Resumen 7

2 Abstract 9

3 Introduction 11

3.1 The Central Nervous System (CNS) in vertebrates 11

3.1.1 Morphogenesis of the central nervous system 12

3.1.2 Neurogenesis in the central nervous system 19

3.2 SUMO (Small Ubiquitin-like MOdifier) 26

3.2.1 The SUMOylation pathway 28

3.2.2 Role of SUMOylation in the cell 35

3.3 Objectives 39

4 Results 41

4.1 Study of the role of SUMO during hindbrain formation. 42

4.1.1 Krox20 interacts with Ubc9. 42

4.1.2 Krox20 functions as a SUMO ligase. 44

4.1.3 Nab mediates SUMO recruitment to the chromatin. 52

4.1.4 Nab SUMOylation modulates Krox20 activity in vivo. 53

4.2 Study of the components of the SUMOylation pathway in the process of neuronal differentiation. 58

4.2.1 Retinoic acid-mediated neuronal differentiation results in free SUMO pool changes. 58

4.2.2 SUMO overexpression impairs neuronal differentiation. 60

4.2.3 Neuronal differentiation proceeds without significant changes in gene expression of SUMO ligases and basic pathway components. 65

4.2.4 The SUMO proteases Senp5 and Senp7 are upregulated during neuronal differentiation. 67

4.2.5 Senp7 is required for proper neuronal differentiation. 69

4.2.6 The Senp7 promoter is transiently activated following induction of neuronal differentiation. 73

4.3 Identification of proteins that exhibit changes in their SUMOylation state during P19 neuronal differentiation. 77

4.3.1 P19 cells undergo neuronal differentiation when grown under SILAC conditions. 77

4.3.2 SUMO immunoprecipitation and peptide elution effectively enriches P19 cell extracts with endogenously SUMOylated proteins. 81

4.3.3 Several proteins are identified as differentially SUMOylated targets between proliferative and differentiating P19 cells. 84

4.3.4 SUMOylation analysis by SDS-PAGE of identified proteins validates the SILAC protocol on proliferating and differentiating P19 cells. 91

5 Discussion 93

5.1 The transcription factor Krox20 as an E3 SUMO ligase. 93

5.2 Regulation of the hindbrain development by SUMO. 94

5.3 SUMOylation as a regulated process during neurogenesis. 96

5.4 Senp7 accounting for proper neuronal differentiation. 98

5.5 Cellular functions of SUMO targets in the process of neuronal differentiation 101

6 Conclusions 108

7 Materials and Methods 111

7.1 Materials 111

7.1.1 Vectors 111

7.1.2 Oligonucleotides 114

7.1.3 Antibodies and peptides 116

7.1.4 Organisms 118

7.2 Methods 119

7.2.1 Culture conditions of employed organisms 119

7.2.2 DNA/RNA techniques 120

7.2.3 Model organisms 128

7.2.4 Protein techniques 131

7.2.5 Other techniques 140

7.2.6 Data processing 141

8 Abbreviations.....143

9 Appendix.....148

10 Bibliography.....150

11 Agradecimientos.....172

1 Resumen

La formación del Sistema Nervioso Central (SNC) y la diferenciación de neuronas, células gliales y otros tipos celulares que lo conforman, son procesos esenciales que implican un gran número de eventos celulares que tienen lugar durante el desarrollo en los eucariotas superiores. Estos eventos incluyen la activación de varias rutas de señalización o el control transcripcional de un gran número de genes, siendo todos ellos mecanismos que tienen que ser regulados de una forma muy precisa en la célula. Muchos son los procesos celulares en los que la modificación post-traduccional por SUMO se ha visto implicada, pero todavía no se ha establecido una función clara de la SUMOilación en el desarrollo neural, constituyendo el establecimiento de esta función el objetivo principal de esta tesis.

En una primera parte de este trabajo, nuestros estudios se han centrado en el factor de transcripción Krox20, el cual regula la formación del rombencéfalo o cerebro posterior y cuya interacción con la enzima de conjugación de SUMO Ubc9 ha sido previamente descrita. Los resultados obtenidos a partir de experimentos realizados *in vitro* e *in vivo* nos han permitido determinar la función de Krox20 como ligasa E3 en la SUMOilación de sus correpresores, las proteínas Nab. Experimentos posteriores nos han permitido establecer una función para la SUMOilación de Nab *in vivo*, reprimiendo la regulación transcripcional que Krox20 ejerce sobre varios genes y sobre sí mismo.

En una segunda aproximación hemos detectado una mayor acumulación de SUMO libre en diferenciación neuronal, asociada a un menor nivel de SUMOilación de proteínas, lo que nos ha llevado a estudiar la regulación de la ruta de SUMOilación en este proceso de diferenciación. Tras un análisis de la expresión de los distintos componentes de la ruta de SUMOilación en neurogénesis, nuestros resultados muestran un aumento en la expresión de las proteasas específicas de SUMO *Senp5* y *Senp7* en células que se están diferenciando. Experimentos adicional han puesto de manifiesto que, de hecho, este aumento en la expresión de Senp7 es necesario al comienzo de la diferenciación neuronal para su correcta progresión.

Una vez hemos establecido cómo la ruta de SUMOilación se regula en neurogénesis, hemos querido determinar si existe un cambio en el patrón de SUMOilación de proteínas diana entre condiciones de proliferación y de diferenciación neuronal. Con este objetivo,

hemos utilizado la técnica del SILAC (Stable Isotope Labelling with Amino acids in Cell culture) para posteriormente purificar proteínas SUMOiladas en estas dos condiciones, empleando un protocolo de inmuno-precipitación que utiliza péptidos correspondientes a los epítopos reconocidos por los anticuerpos empleados, permitiendo así la elución específica de proteínas que han sido modificadas por SUMO de forma endógena. Tras la posterior identificación de proteínas por espectrometría de masas (MS), el análisis y validación de los datos obtenidos entre condiciones de proliferación y diferenciación nos ha permitido detectar cambios en el estado de SUMOilación de un gran número de proteínas que, de forma interesante, corresponden en gran medida con factores que presentan funciones relacionadas con la transcripción o su regulación.

Por tanto, el uso de distintas aproximaciones durante el desarrollo de este trabajo nos ha permitido demostrar que la SUMOilación es fundamental para el desarrollo neural, ejerciendo funciones críticas y actuando a distintos niveles durante este proceso.

2 Abstract

Morphogenesis of the Central Nervous System (CNS), as well as differentiation of the neurons, glia and other cell types that comprise it, is an essential process involving a great number of cellular events that take place during development of higher eukaryotes. These events include activation of a variety of signalling pathways and the transcriptional control of several genes, all comprising mechanisms that need to be tightly regulated in the cell. Many are the cellular processes regulated by the post-translational modification of proteins by SUMO, but a role for SUMOylation in neuronal development remains unestablished and, therefore, constitutes the aim of this thesis.

In the first part of this work, we have centered our investigations on the transcription factor Krox20, which regulates hindbrain formation and was previously shown to interact with the SUMO conjugating enzyme Ubc9. Results obtained in experiments performed *in vitro* and *in vivo* have evidenced that this interaction is due to the role of Krox20 as an E3 ligase for SUMOylation of its coregulators, the Nab proteins. Further experiments have permitted to us the establishment of a functional role for Nab SUMOylation *in vivo*, repressing the transcriptional activity of Krox20, which in a latter manner reverts in *Krox20* own repression.

In a second scientific approach, we have encountered that neuronal differentiation proceeds with net SUMO deconjugation in the cell, which has prompted us to study how the SUMO modification pathway is regulated during this differentiation process. After a wide expression analysis of the different components from the SUMOylation pathway during neurogenesis, our results show how the SUMO-specific proteases *Senp5* and *Senp7* are upregulated in differentiating cells. Further experiments have elucidated that Senp7 upregulation at the onset of neuronal differentiation is indeed required for proper progression of this process.

Once establishing how the SUMOylation pathway is regulated during neurogenesis, we also wanted to determine whether there is a change in the SUMOylation pattern of target proteins between proliferative and neuronal differentiating cells. For this purpouse, we have performed a Stable Isotope Labelling with Amino acids in Cell culture (SILAC) experiment to purify SUMOylated proteins in these two conditions, employing an

immunoprecipitation protocol using peptides corresponding to the epitopes recognized by the employed antibodies that permits the specific elution of endogenously SUMOylated proteins for their subsequent mass spectrometry (MS) identification. After analysis and validation of the obtained data between proliferation and neuronal differentiation, we have detected changes in the SUMOylation state of several proteins that, interestingly, correspond in a great number with factors related to transcription or transcriptional regulation.

Thus, by different approaches we have demonstrated that SUMOylation is fundamental for neural development, playing critical roles and acting at different levels during this process.

3 Introduction

Cell differentiation processes are essential during development and adult life of an organism. Alterations of these processes have critical consequences such as malformations, tumour development or degenerative diseases. Understanding the precise control of cell differentiation is necessary for the introduction of advanced therapies for these alterations. In this context, the study of neuronal differentiation is outstanding, as the results obtained may be of value for the cure of nervous system lesions and neurodegenerative diseases that show an increasing incidence in our population. A great number of proteins, mostly transcription factors, participate in neurogenesis, both in the earlier cell cycle exit and the later differentiation process. Our knowledge regarding factors implicated in the transcriptional regulation that leads to neuronal differentiation is increasing, but the signalling mechanisms involved need of further investigation.

A signalling system that is acquiring more relevance regarding transcriptional control is the post-translational modification by SUMO. SUMO (Small Ubiquitin-like MOdifier) is a small polypeptide similar to ubiquitin that covalently binds to other proteins, modifying them in a post-translational way. While ubiquitylation is usually related to protein degradation via the proteasome, SUMOylation use to have a regulatory function. In this manner, a relevant role in neuronal functioning has been described, highlighting its implication in neuron synapsis and protein aggregates associated to neurodegenerative diseases. However, its implication in neural development has been only briefly studied.

3.1 The Central Nervous System (CNS) in vertebrates

The nervous system in vertebrates is divided into two clearly differentiated structural groups attending to their embryological origin: the central nervous system (CNS), comprised by the encephalon and the spinal cord, and the peripheral nervous system (PNS), comprised by cranial and spinal nerves, as well as the peripheral ganglia. Both systems are derived from the ectoderm during a complex and tightly regulated developmental process. In this work, we will focus in the events that take place during formation of the CNS.

3.1.1 Morphogenesis of the central nervous system

During the early embryonic development, a portion of the dorsal ectoderm (also named neural ectoderm) specializes to give rise to the neural plate, constituted by cells with columnar morphology. The neural plate then thickens and neural groove starts to deepen, while neural folds rise and eventually converge in the middle line, closing the plate to form the neural tube in a process known as neurulation (Figure I-1). The neural tube will give rise to the CNS through embryogenesis. The dorsal part of the neural tube is populated by a number of cells with self-renewal potential and high migration and differentiation capabilities that will give rise to the neural crest. During embryogenesis, this structure will constitute the PNS and other structures.

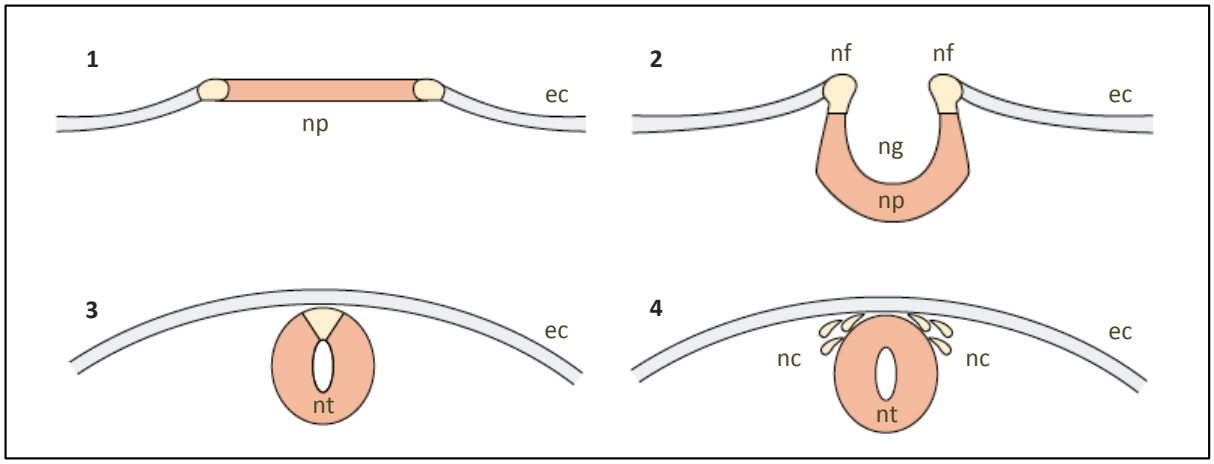

Figure I-1: neural tube closure. Neurulation in vertebrates, in which a subset of cells from the ectoderm (ec) forms the neural plate (np) (1). Then, invagination of the neural plate leads to the formation of the neural groove (ng) and neural folds (nf) (2), which latterly will close dorsally to form the neural tube (nt) (3). A subset of cells dorsally close to the neural tube form the neural crest (nc) (4), which eventually will migrate for the establishment of the dorsal root ganglia (modified from (Knecht, AK and Bronner-Fraser, M, 2002)).

The neural tube is separated from the ectodermal epidermis and is originally comprised by a single layer of columnar shaped cells called neuroepithelial cells. All neurons and macroglial cells from the CNS are derived from these cells, which exhibit stem cell characteristics like self-renewal capacity and certain degree of pluripotency (Yamashita, M,

2013). Though nuclear staining of the neuroepithelial cells shows dispersed cell nuclei at different levels, these cells form a unique layer of polarized cells whose nuclei distribute along their apical-basal axis, thus forming a pseudostratified monoepithelium (Chenn, A *et al.*, 1998). Neuroepithelial cells connect themselves to the basal or apical face of the neuroepithelium through specialized junctions towards the apical side, which comprises the neural tube lumen (Schoenwolf, GC and Kelley, RO, 1980), or through less specialized junctions towards the basal side (Rodriguez-Boulan, E and Nelson, WJ, 1989). As mentioned, the pseudostratified shape of this cell layer is caused by nuclei displacement through the apical-basal axis, a process coupled to the cell cycle progression. This displacement is also known as interkinetic nuclear migration (Chenn, A and McConnell, SK, 1995), in which major part of mitotic cells locate to the apical surface of the neuroepithelium and cells in S-phase locate to the basal side (reviewed in (Gotz, M and Huttner, WB, 2005). This way, following mitosis of each cell, cell nucleus moves from the apical side of the neuroepithelium to the basal side, where DNA duplication takes place and then, during G2 phase, the nucleus comes back to the apical side, where cell division takes place (Figure I-2).

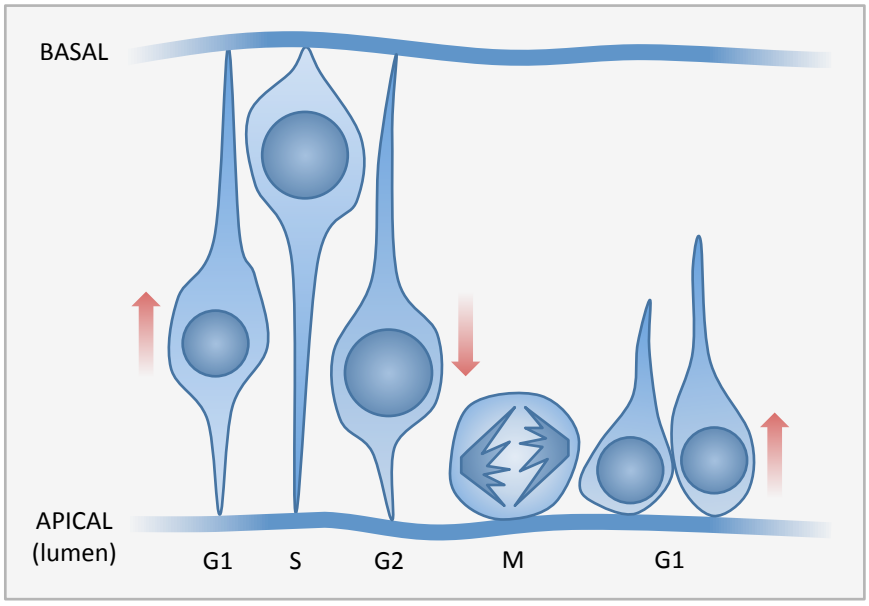

Figure I-2: interkinetic nuclear migration of neuroepithelial cells. Schematic design of the relationship between cell-cycle progression of neuroepithelial cells and migration of their nuclei along their apical-basal axis, as indicated by arrows. During G1-phase, cell nuclei migrate to the basal surface of the cell to duplicate DNA. Then, during G2-phase, the nucleus returns to the apical surface, where mitosis takes place.

There are lot of works describing cytoskeletal components and proteins implicated in the regulation of this migrating process and associated defects have also been established. However, the triggering mechanisms involved in interkinetic nuclear migration, its regulation and the consequences over neuroepithelial cells fate have not been yet clarified (Willardsen, MI and Link, BA, 2011).

Neuroepithelial cells will differentiate to give rise to four regions of the neural tube, which will eventually form distinct parts of the CNS: the forebrain (prosencephalon), the midbrain (mesencephalon), the hindbrain (rhombencephalon) and the spinal cord. Two transiently formed structures can be identified during neural tube development, which are comprised by postmitotic cells and constitute signalling cores that are critical for neuronal differentiation of neuroepithelial cells. These structures are known as the roof plate at the dorsal side, and the floor plate at the ventral side (Figure I-3) and, together with the notochord, coordinate neuronal differentiation in a spatial-temporal manner, depicting the previously mentioned regions. Thus, neuronal differentiation follows in a ventral-dorsal manner in the spinal neural tube, whereas in the brain-related parts, neurons originate first in inner layers and newly differentiated progenitors occupy outer layers as they differentiate into new neurons (McConnell, SK, 1988). After generation of the firsts neurons, neuroepithelium give rise to a new compartmentalized region, where two main structures can be recognized: the ventricular zone, facing to the lumen, and the mantle layer or pial surface, located to the outer part of the neural tube and where neuroepithelial cells have migrated and differentiate into neurons (Figure I-3). There is also an intermediate layer called subventricular zone, comprised by the postmitotic cells that migrate to the mantle layer and have just exited cell cycle, though they still do not express specific markers for fully differentiated neurons. In the spinal neural tube, neural development progression maintains this basic compartmentalization, while regions that will give rise to forebrain, midbrain and hindbrain exhibit a more complex territory patterning that in part will be further explained (below). A dorsal-ventral gradient of extracellular signals also generates different sub-populations of neurons that distribute with a territory patterning in the neural tube (reviewed in (Lewis, KE, 2006)). Previously mentioned structures in the ventral region like the notochord first and the floor plate in further stages secrete the Sonic hedgehog (Shh) protein, while dorsal structures, like the ectoderm first and the roof plate lately, secrete bone morphogenetic (BMP) proteins. Another common signalling molecule is the retinoic

acid (RA), which acts over the Wnt signalling pathway that has been associated to the proper establishment and differentiation of neuronal populations (Maden, M, 2006). In fact, RA has been described to differentiate mouse pluripotent cells into a neuronal phenotype (MacPherson, PA *et al.*, 1997). All together, these signals orchestrate the territory patterning of the different types of neurons that accumulate in the developing neural tube. As an example, in the spinal neural tube, only neural progenitors from the ventral section of the ventricular zone will differentiate into motor neurons, while dorsal progenitors will give rise to different types of interneurons (reviewed in (Lewis, KE, 2006)).

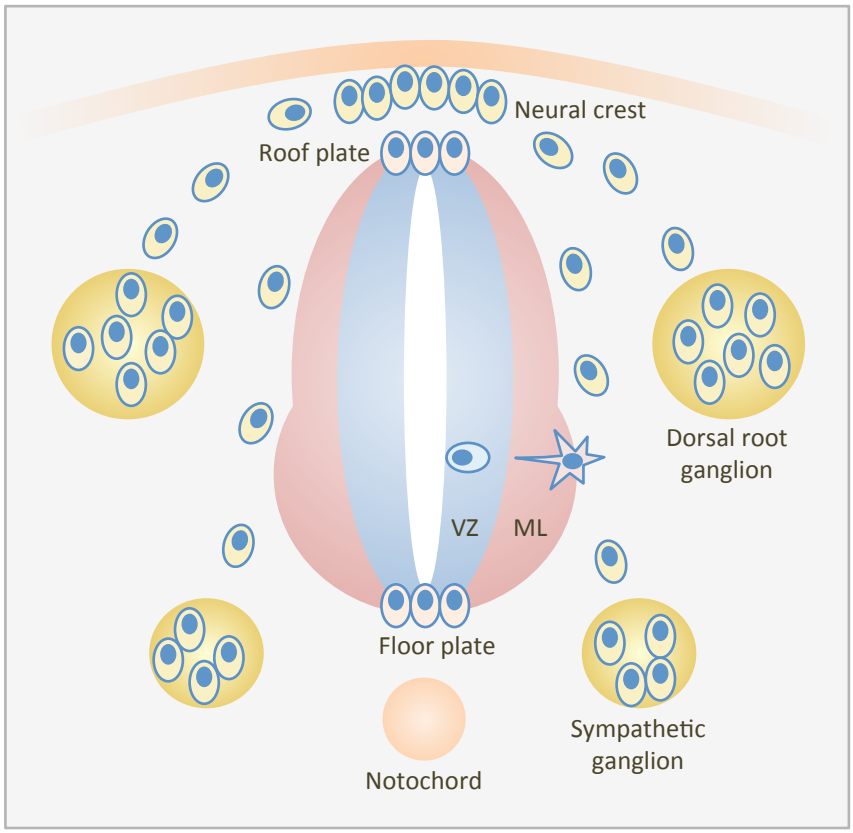

Figure I-3: structure specification of the neural tube. Representation of a transversal section from the neural tube in vertebrates during neuronal differentiation and neural crest formation and the associated structures that can be observed. Neural progenitors migrate from the ventricular zone (VZ) to the pial surface or mantle layer (ML) while they differentiate to glial cells or neurons. Additionally, cells from the neural plate migrate and differentiate to form the dorsal root ganglia and sympathetic ganglia. Structures like the roof or floor plate and the notochord are responsible of dorsal-ventral signalling for the proper development of the neural tube and the adjacent ganglia.

3.1.1.1 Hindbrain formation and Krox20 regulation

As previously mentioned, neuron territory patterning is very complex during development of the neural tube in those parts that will give rise to the brain and the cerebellum (forebrain, midbrain and hindbrain). The transcription factor Krox20 has a critical role in hindbrain segmentation during neural development of vertebrates. This segmentation process consists on the formation of 7 to 8 segments denominated rhombomeres that distribute along the rostral-caudal axis of the embryo (Lumsden, A and Krumlauf, R, 1996). This division permits the differentiation of neural progenitors located in the hindbrain into different subtypes of neurons, organization of the brachial nerves and the establishment of the neural crest. Given the hindbrain complexity, its formation depends on a really strict transcriptional control and gene expression pattern associated to each of the rhombomeres, which present unique characteristics that vary through the rostral-caudal axis (Figure I-4). A high number of genes are implicated in this segmentation, showing complex expression patterns whose regulation has not been completely elucidated.

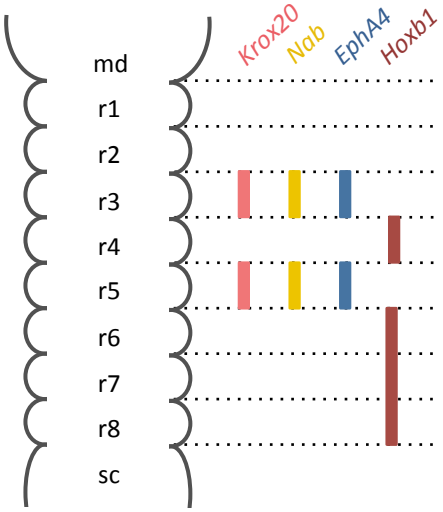

Figure I-4: territory expression pattern of *Krox20* and related genes. During formation of the hindbrain, the transcription factor *Krox20* is expressed in r3 and r5, together with its corregulators *Nab1* and *Nab2* (*Nab*) and *EphA4*. The transcription factor *Hoxb1* is expressed in r4 and all along r6, r7 and r8.

Krox20, also known as Egr2, is a transcription factor belonging to the family of Early Growth Response (Egr) factors and is expressed in the rhombomeres 3 (r3) and 5 (r5), being essential for the establishment and maintenance of these segments during hindbrain formation (Figure I-4) (Schneider-Maunoury, S *et al.*, 1993). The Egr family of proteins is

comprised by four factors, firstly described by their association with cellular proliferation response to different growth factors (Chavrier, P *et al.*, 1988). A common feature of this family of proteins is the presence of three zinc-finger domains to bind DNA, located to the C-terminal part of the proteins (Figure I-5). Each of these zinc-finger domains allows for the recognition of nine base pairs, also called Egr-response elements, which localize in the promoter regions of Egr-regulated genes. Most of the proteins from this family also have an R1 repressor domain upstream to the zinc-finger domains (Figure I-5). The R1 domain is responsible for Krox20 interaction with NGFI-A/Egr1-binding (Nab) proteins, Nab1 and Nab2, which were initially identified as corepressors of Egr factors (Russo, MW *et al.*, 1995). To this point, the I268F single mutation in this domain has been reported to abrogate interaction with Nab proteins (Svaren, J *et al.*, 1998). Additionally, two acidic regions located towards the N-terminal part of the protein and an intermediate region between R1 and one of these acidic domains (Figure I-5) have been described to mediate transcriptional regulation from a number of target genes; as an example, the intermediate domain between both acidic domains and R1 has been associated to transcriptional activation of *EphA4* and repression of *follistatin* (Desmazieres, A *et al.*, 2009).

Nab proteins have a critical role over the control of different inflammatory processes and during development of the embryo, especially on CNS formation and myelinisation (Le, N *et al.*, 2005; Mager, GM *et al.*, 2008). Regarding their relationship with Krox20, a mainly corepressive function has been established, though they have also been occasionally described as transcriptional coactivators (Russo, MW *et al.*, 1995; Svaren, J *et al.*, 1996). Nab1 and Nab2 show NLS sequences and share a high sequence identity, showing in their N-terminal part two Nab corepressor domains (NCD), each one being related with specific functions (Figure I-5). As an example, the NCD1 has been associated to the interaction with Egr factors and also to homo- and heterodimerization between Nab proteins. In fact, the double mutation Q64R/H95Q has been shown to disrupt the interaction with Krox20 through this domain (Svaren, J *et al.*, 1998). On the other hand, the NCD2, together with the C-terminal part of the protein (CID), has been implicated in the transcriptional repressor activity (Figure I-5). This C-terminal domain interacts with the chromodomain helicase DNA-binding protein 4 (CHD4) subunit of the chromatin remodelling complex NuRD, resulting in transcriptional repression. Nevertheless, interaction with CHD4 seems not to be sufficient for the full repressive activity associated to Nab (Srinivasan, R *et al.*, 2006).

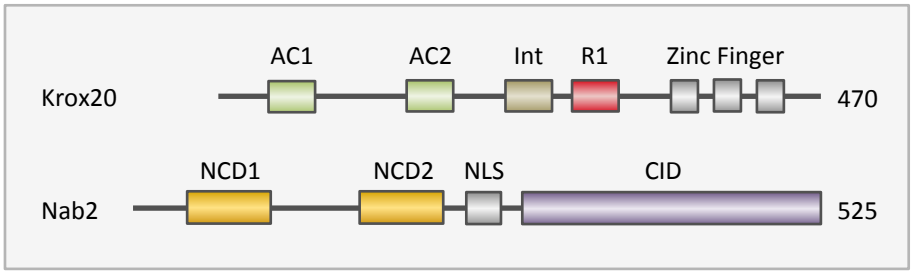

Figure I-5: structural domains from Krox20 and Nab2 proteins. Krox20 structural domains comprise two acidic domains (AC1 and AC2) and an intermediate region (Int) involved in transcriptional regulation of various target genes, a repressor R1 motif that also binds to Nab proteins and three zinc-finger domains for DNA binding. Structural domains of Nab2 are also represented, showing an NLS domain, together with the NCD1 domain for interaction with Krox20 and the NCD2 and CID motifs, which have been associated to repressor activity.

As previously mentioned, some of the structural domains present in Krox20 have been described to control in a positive or a negative way the expression of some genes during the establishment of rhombomeres 3 and 5. This group of genes include *Krox20* itself, the genes for *Nab1* and *Nab2* corepressors and also Hox genes associated to the establishment of the rostral-caudal axis of the embryo, the follistatin glycoprotein that has been implicated in rhombomere-to-rhombomere signalling, and adhesion factors from the Eph family of proteins that are necessary for the control of cellular segregation and the establishment of frontiers between adjacent rhombomeres ((Chomette, D *et al.*, 2006; Theil, T *et al.*, 1998) and reviewed in (Mellitzer, G *et al.*, 2000)). It has been specifically described how Krox20 directly controls in a positive sense the expression of *EphA4* in r3 and r5 (Figure I-6) (Desmazieres, A *et al.*, 2009), while *Hoxb1* is indirectly controlled in a negative sense (Garcia-Dominguez, M *et al.*, 2006). Finally, *Nab1* and *Nab2* genes are also activated by Krox20 in r3 and r5, thus indicating the presence of a negative regulatory feedback by which Krox20 activates the expression of its own corepressors (Figure I-6) (Mechta-Grigoriou, F *et al.*, 2000).

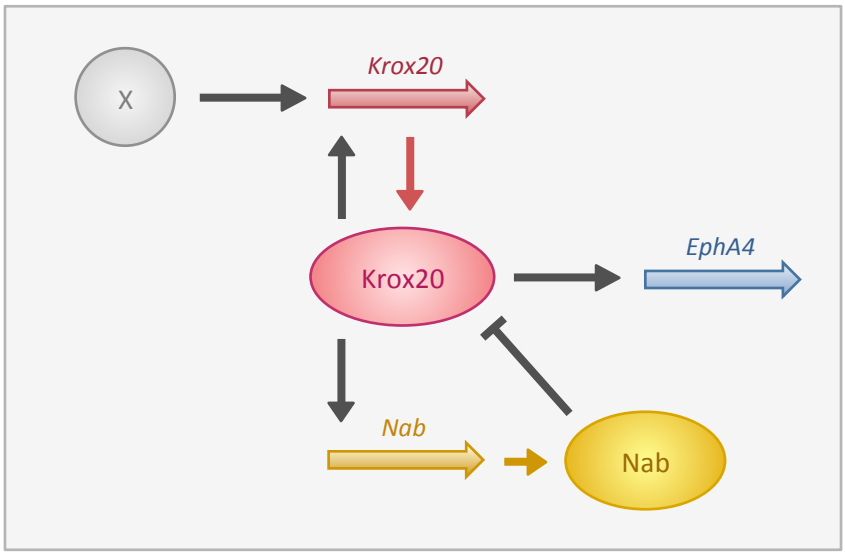

Figure I-6: Krox20 regulation in r3 and r5 specification and maintenance during hindbrain development. Expression of *Krox20* is initially activated by various factors (X). Then, the transcription factor activates its own expression together with the *EphA4* gene. Krox20 also activates the expression of genes encoding its Nab corepressors, thus establishing a negative feedback in which Nab proteins repress the transcriptional activity of Krox20, eventually leading to its own inactivation. Coloured arrows indicate protein biosynthesis, black arrows indicate transcriptional activation and flat-end arrow indicates corepressor activity.

3.1.2 Neurogenesis in the central nervous system

During morphogenesis of the CNS, neuroepithelial cells under nuclear interkinetic migration undergo proliferation while they remain in the ventricular zone of the neural tube. As previously mentioned, under certain circumstances, they enter in cell-cycle arrest and start migrating to the mantle layer while get differentiated into neuron or glial cells. Taking into consideration that differentiation of neural progenitors requires cell-cycle arrest after G1-phase, the interaction and proper coordination between neurogenic factors and cell cycle progression machinery is critical for the establishment of functional neuronal populations ((Willardsen, MI and Link, BA, 2011) and reviewed in (Swiss, VA and Casaccia, P, 2010)).

Another key feature during CNS development is the balance between proliferation of neural progenitors and differentiation to neurons, which needs to be tightly maintained. For this, three different types of cellular divisions have been described: symmetric proliferative

(producing two new proliferative progenitors), asymmetric neurogenic (producing one proliferative progenitor and one postmitotic cell) and symmetric neurogenic (producing two postmitotic cells). The best-studied cellular feature known to affect neurogenesis during these divisions is the partitioning of determinants at cytokinesis, where certain factors are distributed equally or unequally in daughter cells, thus creating either symmetric or asymmetric divisions, respectively (reviewed in (Willardsen, MI and Link, BA, 2011)). At this point, proteins like epidermal growth factor receptor (EGFR) or TRIM32 proteins have been unequally detected in both offspring cells after asymmetric neurogenic divisions (Schwamborn, JC *et al.*, 2009; Sun, Y *et al.*, 2005). Tissue specificity of the factors involved in controlling these divisions has also been described, as neuroepithelial cortical cells that undergo mitosis and receive the new centrosome are prone to migrate and differentiate into neurons, while cells with the former centrosome remain located in the ventricular zone (Wang, X *et al.*, 2009). Another factor controlling proliferative or differentiating state of the neural progenitors is the G1-phase duration, as the specifying action of determinants after mitosis would need a certain duration time of the G1-phase. To this point, it has been described how shortening G1-phase reverts in delayed neurogenesis, with the resulting increased generation of neural progenitors (Lange, C *et al.*, 2009).

A major regulator of the neural progenitors fate is the Notch signalling pathway. In this pathway, receptor and ligand are both transmembrane proteins that confer specificity to neighbouring cells (reviewed in (Bray, SJ, 2006)). Notch ligands are represented by Delta and Serrate/Jagged transmembrane factors that belong to the DSL (Delta, Serrate and LAG-2) family of proteins. DSL is an extracellular domain present in these proteins that is essential to interact with the Notch receptor. The Notch receptor contains an extracellular domain comprising a variable number of epidermal growth factor (EGF) repeats and a linker region that connects to the transmembrane domain and the Notch intracellular domain (Nicd). This way, in a group of neuroepithelial cells, when the Notch receptor from one of the cells interacts with a DSL ligand from other cell, the Nicd domain is cleavaged and translocated to the nucleus, where it binds to the DNA-binding protein CSL (CBF1, Su(H) and LAG-1) and, together with Mastermind (Mam), induces CSL-mediated transcriptional activation of the E(spl)/HES class of genes (*Hes*/*Her*/*Esr*) to maintain the proliferative state of neural progenitors (reviewed in (Bray, SJ, 2006)). Regulation of the Notch pathway is related to the fate establishment of neural progenitors. An interesting regulator of this process is

Numb, a well-characterized inhibitor of the Notch pathway that induces Notch receptor endocytosis. It has been described how Numb is unequally distributed into neural progenitors from *Drosophila*, leading to a misbalance of the Notch pathway between the two newly generated neural progenitors (Berdnik, D *et al.*, 2002). Interplay between the Notch signalling pathway and some basic helix-loop-helix (bHLH) proteins has been established to occur during both invertebrate and vertebrate neural development.

Genes encoding bHLH transcription factors were originally described in *Drosophila melanogaster* and related genes were further discovered in vertebrates (reviewed in (Bertrand, N *et al.*, 2002; Guillemot, F, 1999)). These genes have a common bHLH structural motif that is present in many transcription factors, which is characterized by two α-helices separated by a loop. The helices have been associated to dimerization, while the upstream basic region is required for binding to specific DNA sites with the sequence CANNTG, also named as E-box. Various families of Class II bHLH genes have been established in vertebrates, showing similarities with *Drosophila* bHLH genes and specificities between them. Thus, bHLH vertebrate genes with similarities with *Drosophila ato* (*atonal*) would be grouped in the Atonal family (*Math1* and *Math5*), the Neurogenin family (*Ngn1, Ngn2 and Ngn3*), the NeuroD family (*NeuroD*, *NeuroD2, Math2* and *NeuroM*) and the Olig family (*Olig1*, *Olig2* and *Olig3*). Genes related to *Drosophila asc* (*achaete-scute*) are classified in the Achaete-Scute family (*Mash1* and *Mash2*) (Table I-1). These previously mentioned proteins form heterodimers with ubiquitously expressed Class I bHLH proteins or E proteins, encoded by *E2A* (with its two alternative products E12 and E47), *HEB* and *E2-2* in vertebrates (Johnson, JE *et al.*, 1992; Massari, ME and Murre, C, 2000). When heterodimers are formed, they bind to the previously mentioned E-boxes to activate transcription of target genes. Most bHLH proteins act as transcriptional activators, with only few exceptions like Olig2 (Mizuguchi, R *et al.*, 2001; Novitch, BG *et al.*, 2001). As their action depends on hetero-dimerization, a regulation system for bHLH proteins has been identified, consisting on HLH-containing proteins that compete for binding to E proteins. These competitors lack a basic region to interact with DNA, thus preventing transcriptional activation. To this point, the inhibitor of differentiation (Id) group of proteins have been described to act as regulators of bHLH proteins in vertebrates (reviewed in (Massari, ME and Murre, C, 2000; Yokota, Y, 2001)).

Table I-1: Neural development-associated bHLH (basic helix-loop-helix) proteins. bHLH proteins described in invertebrates (yellow) and vertebrates (green), grouped in distinct families according to sequence similarities in their bHLH domains.

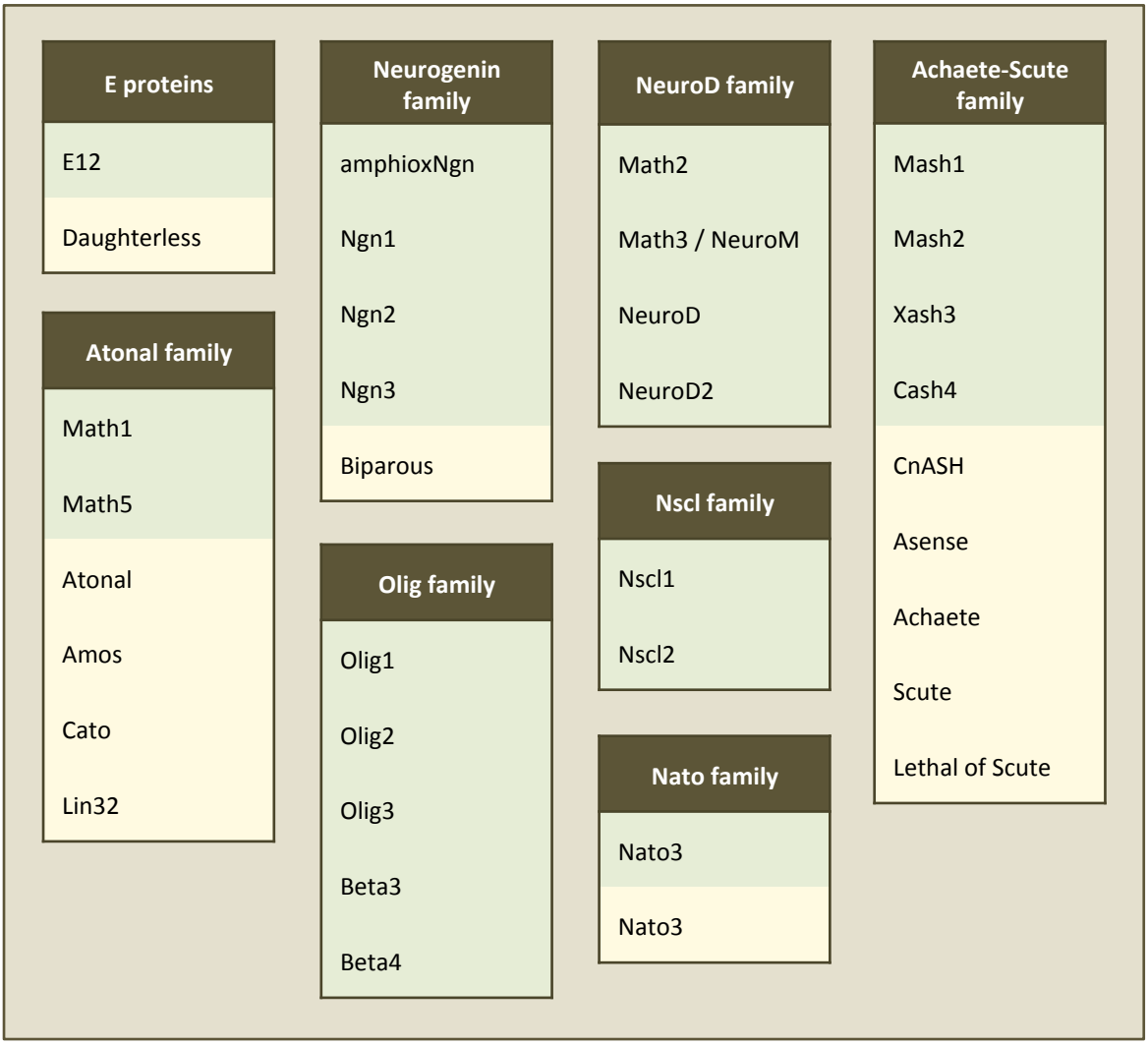

bHLH proteins are functionally heterogeneous, playing distinct roles during invertebrate and vertebrate neural differentiation pathways, in a fashion that often depends on the cellular lineage and localization. Studies of the function of these genes have, in general, supported the division of bHLH genes into early acting determination genes and late acting differentiation genes. In vertebrates, early acting determination genes or proneural genes are expressed in proliferative neuroepithelial cells and are necessary and sufficient to promote the generation of neural progenitors in the ventricular zone of the neural tube (Figure I-7).

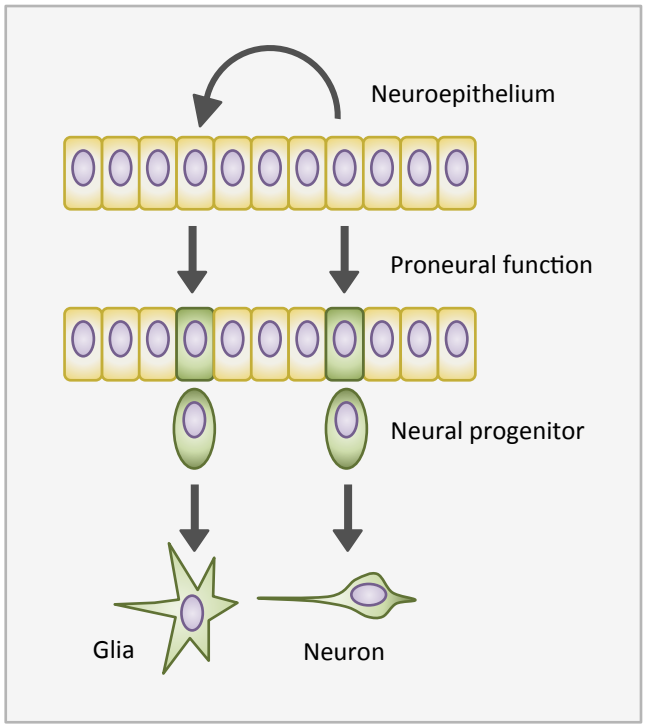

Figure I-7: Neural progenitors commitment and differentiation. In vertebrates, neuro-epithelial cells are already specified for a neural fate while they proliferate. Activation of proneural bHLH genes in these cells leads to their commitment into neural progenitors with limited mitotic potential that, following subsequent activation of other bHLH genes, will finally differentiate into glial cells or neurons (adapted from (Bertrand, N *et al.*, 2002)).

Proneural genes comprise the Achaete-Scute genes *Mash1* together with the Neurogenin genes *Ngn1* and *Ngn2* and the Atonal gene *Math1* (reviewed in (Bertrand, N *et al.*, 2002)). An additional characteristic of proneural genes is their ability to induce the expression of Notch ligands Delta and Serrate/Jagged, as well as activating the Notch signalling pathway (Figure I-8) (reviewed in (Bertrand, N *et al.*, 2002)). Proneural genes are subjected to repression by inhibitors Hes, Her and Esr, previously mentioned to be under the control of Notch signalling pathway (Figure I-8) (Davis, RL and Turner, DL, 2001; Kageyama, R and Nakanishi, S, 1997). It is also interesting to mention that the cell cycle controlling cyclin D1 has been related to regulation of proneural genes (Lukaszewicz, AI and Anderson, DJ, 2011) and that expression of Cdk (cyclin-dependent kinases) inhibitors such as p27 has been reported following induction of bHLH proteins in mouse cells (Farah, MH *et al.*, 2000), to induce cell-cycle arrest (Figure I-8).

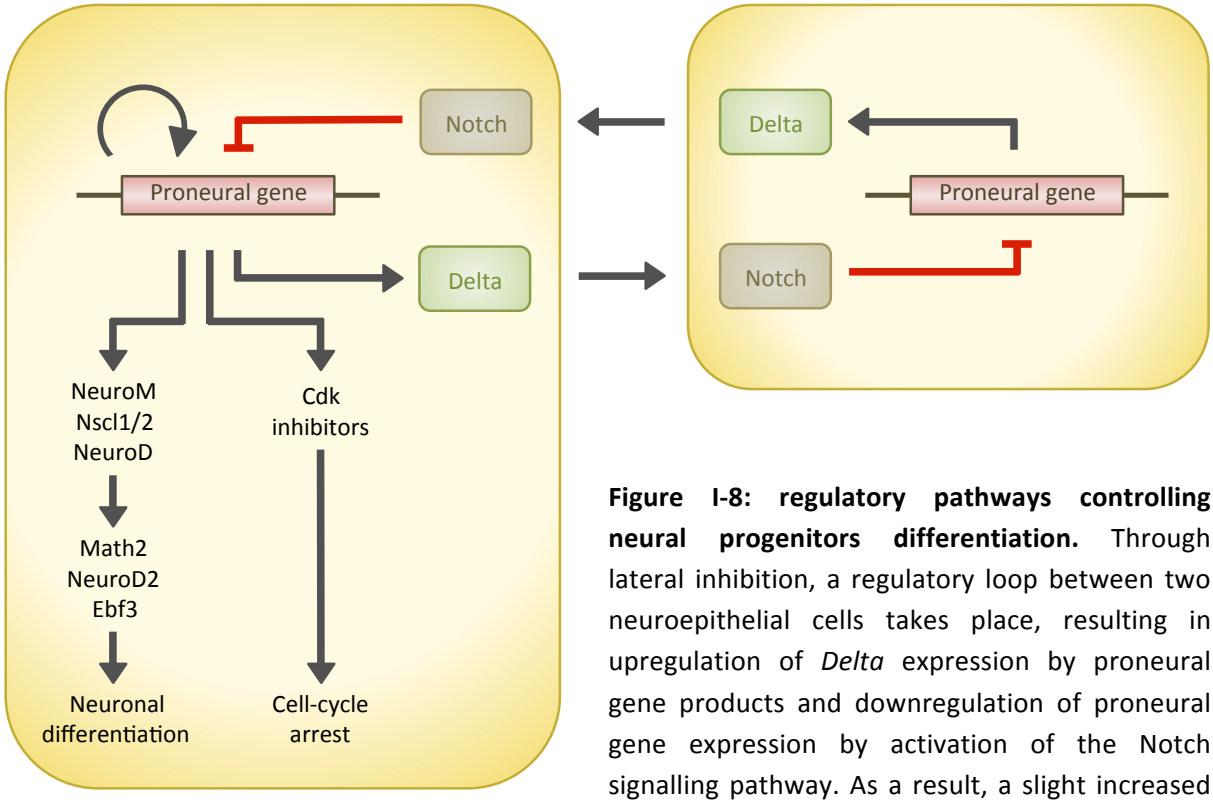

Figure I-8: regulatory pathways controlling neural progenitors differentiation. Through lateral inhibition, a regulatory loop between two neuroepithelial cells takes place, resulting in upregulation of *Delta* expression by proneural gene products and downregulation of proneural gene expression by activation of the Notch signalling pathway. As a result, a slight increased expression of proneural genes in one of the cells, which will further become a neural progenitor, will revert in repression of the proneural function in the neighbouring cell and further increase of proneural gene expression in the future neural progenitor. In neural progenitors, the highly expressed proneural genes ensure the cell-cycle arrest by activation of Cdk (cyclin-dependent kinases) inhibitors and promote the initiation of the neuronal differentiation programme by induction of other bHLH differentiation genes, such as *NeuroD* in vertebrates. Neuronal differentiation continues with the subsequent activation of later differentiation genes like *Math2* or *NeuroD2* and the final establishment of neuronal lineages (adapted from (Bertrand, N *et al.*, 2002)).

Late acting differentiation genes encode bHLH proteins, among others, that have been associated to differentiation of the committed neural progenitors and are expressed in early post-mitotic cells migrating toward the mantle layer, where proneural genes like Ngn no longer maintain appreciable expression levels. These late differentiating bHLH genes are shown to be under the direct control of proneural genes. This way, gain-of-function experiments in chicken embryos have shown how overexpression of Ngn proneural genes cease progenitor division and promote ectopic neuronal differentiation through activation of the differentiation genes *NeuroD* and *NeuroM,* thus placing expression of these genes in a later stage during neuronal differentiation (Figure I-8) (Blader, P *et al.*, 1997; Ma, Q *et al.*,

1996; Mizuguchi, R *et al.*, 2001). *NeuroD* and *NeuroM*, as well as some proneural genes like *Ngn2* and *Mash1*, have been implicated in the specification of neuronal or glial fate of neural progenitors in defined regions from the CNS (Nieto, M *et al.*, 2001; Sun, Y *et al.*, 2001; Tomita, K *et al.*, 2000). Interestingly, the overexpression of late differentiating proteins also induces the ectopic activation of proneural genes, thus suggesting an effect for these proteins in triggering the complete differentiation programme (Garcia-Dominguez, M *et al.*, 2003).

Activation of bHLH genes also occurs in even further stages, thus also accounting for late acting differentiation genes. In this manner, the use of knockout mice has permitted to describe how expression of *NeuroD2* is necessary for the proper development of hippocampus, cortex, dentate gyrus and cerebellum. It expression is described to be regulated by Ngn1 and NeuroD, situating *NeuroD2* in a latter step during neuronal differentiation (Figure I-8) (Lee, JE, 1997; Lin, CH *et al.*, 2004; Olson, JM *et al.*, 2001). Other genes encoding non-bHLH proteins also coordinate differentiation of neural progenitors. Examples of this are Ebf genes, which encode for proteins with an atypical helix-loop-helix (HLH) domain. *Ebf3*, for instance, is expressed in an extended fashion during cell-cycle exit and differentiation of neural progenitors in the chick hindbrain and spinal cord regions from the neural tube (Garcia-Dominguez, M *et al.*, 2003).

Finally, the neuronal-subtype specification is another key step in the differentiation process. Proneural genes have been associated to the establishment of certain populations of neurons, assigning them a role not only in the initial commitment of neural progenitors but also in the final determination of neuron specificity. In this manner, a role for *Mash1* in the specification of noradrenergic neurons has been well established (Goridis, C and Brunet, JF, 1999). Genes encoding for bHLH proteins with no proneural function have also been implicated in the specification of neuronal identity, for example in retina (reviewed in (Cepko, CL, 1999)). An interesting feature of neuron specification is the necessity of interaction between bHLH and homeobox proteins. In this way, it has been described how amacrine cells establishment requires the coexpression of *NeuroD* or *Math3* together with the homeobox gene *Chx10* or how bipolar cells are generated after *NeuroD* or *Math3* coexpression together with *Pax6* (Figure I-5C) ((Hatakeyama, J *et al.*, 2001; Inoue, T *et al.*, 2002) and reviewed in (Bertrand, N *et al.*, 2002)).

3.2 SUMO (Small Ubiquitin-like MOdifier)

SUMO (Small Ubiquitin-like MOdifier) is a small polypeptide of about 100 amino acids that shares a high similarity with ubiquitin in terms of 3D conformation, though only having an 18% identity with its amino acid sequence (Bayer, P *et al.*, 1998). As ubiquitin, SUMO is a post-translational modifier that covalently attaches to its target proteins in a process termed as SUMOylation. It belongs to the family of Ubiquitin-like proteins (Ubl), characterized by the ubiquitin fold (globular β-grasp fold) and a characteristic C-terminal Gly-Gly motif that is exposed after proteolytic maturation. In the years 1996 and 1997 SUMO was firstly identified as an Ubiquitin-like polypeptide, being responsible for the reversible modification of the nucleoporin Ran GTPase-activating protein 1 (RanGAP1) (Mahajan, R *et al.*, 1997; Matunis, MJ *et al.*, 1996). Since then, our knowledge on SUMO has greatly increased and thousands of new targets have been identified, allowing the assignation of a role for SUMOylation in many aspects of the eukaryotic cell life.

SUMO is present in eukaryotes, being SUMOylation an essential process in virtually all of them, and is highly conserved through species. Only one isoform of the gene has been identified in lower eukaryotes like *Saccharomyces cerevisiae*, where SUMO is encoded by *SMT3* (Johnson, ES *et al.*, 1997). On the contrary, more than one gene encoding for SUMO is found in higher eukaryotes. To this point, four isoforms have been identified in mammals (Guo, D *et al.*, 2004; Melchior, F, 2000) and termed *SUMO1* (also known as human *Smt3c*, *PIC1*, *GMP1* and *sentrin*), *SUMO2* (also known as *Smt3a* and *Sentrin3*), *SUMO3* (also known as *Smt3b* and *Sentrin2*) and *SUMO4* (Bohren, KM *et al.*, 2004), though only SUMO1, SUMO2 and SUMO3 have been reported to be functionally conjugatable and ubiquitously expressed in vertebrates (Guo, D *et al.*, 2004). Variations in gene nomenclature are due to SUMO being described in different works at the same period of time.

SUMO2 and SUMO3 share a 97% identity in their amino acid sequence when maturated and they are usually referred to as SUMO2/3, as they cannot be distinguished by antibodies up to date. SUMO1 shares only a 47% sequence identity with SUMO2 (Saitoh, H and Hinchey, J, 2000; Vertegaal, AC *et al.*, 2006). SUMO1 is normally conjugated to proteins regulating many biological processes, but exerting a prominent role in transcription repression (Garcia-Dominguez, M and Reyes, JC, 2009). On the contrary, most SUMO2 and

SUMO3 are free in the cell and rapidly conjugated to proteins in response to a variety of stress conditions (Tempe, D *et al.*, 2008). There are, however, examples of target proteins such as topoisomerase II and CAAT/enhancer-binding protein-beta (C/EBPβ) that are specifically modified by SUMO2/3 under non-stress conditions (Azuma, Y *et al.*, 2003; Eaton, EM and Sealy, L, 2003). SUMO4 is encoded by a sequence located within an intron of the human TAB2 gene and it has been described to be highly expressed in kidney cells (Wei, W *et al.*, 2008). Non-coding SUMO pseudogenes have been also identified, being SUMO1 pseudogene 3 (SUMO1P3) regulated in some types of cancer (Mei, D *et al.*, 2013; Zhan, Y *et al.*, 2016).

SUMOylation shares several similarities with ubiquitylation. Both molecules need to be maturated prior to be completely functional. SUMO is maturated by the action of specific isopeptidases, exposing two glycines at the C-terminus of the protein that will be necessary for its conjugation to the target proteins. So-called SUMOylation takes place when the C-terminus part of SUMO is covalently attached to the ε-amino group of a lysine present in a target protein by a thioester bond. This lysine is usually located within the amino acid consensus Ψ-K-X-E, with Ψ being an aliphatic branched amino acid and X any amino acid (Hay, RT, 2005). A SUMOylation consensus site is located within SUMO2/3 sequence, while this site is not present in SUMO1. Consistent with this observation, SUMO2/3 has been described to form SUMO chains *in vitro* and *in vivo*, while this is not the case for SUMO1 (Bohren, KM *et al.*, 2004; Tatham, MH *et al.*, 2001). Nevertheless, it has to be pointed that not all proteins containing a SUMOylation consensus site are SUMOylated, and not all proteins modified by SUMO contain a SUMOylation consensus site. Indeed, some variants for the canonical consensus have been described, including an inverted consensus motif, a consensus motif with a hydrophobic cluster, a negatively charged amino acid-dependent motif and some extended phosphorylation-dependent motifs (Hietakangas, V *et al.*, 2006; Matic, I *et al.*, 2010; Picard, N *et al.*, 2012; Rodriguez, MS *et al.*, 2001; Yang, SH *et al.*, 2006). These data indicates that other aspects, such as subcellular localization or proper presentation of the SUMOylation site in the 3D structure of the target protein, may be required for the covalent attachment of SUMO to its target.

It has been previously stated that proteins are SUMOylated when SUMO is covalently attached to them. However, SUMO is also capable of interacting with proteins through a SUMO interacting motif (SIM) without the establishment of a covalent bond. Usually, the

SIM consists on short hydrophobic stretches with the sequence (V/I)-X-(V/I)-(V/I) or (V/I)-(V/I)-X-(V/I), N- or C-terminally flanked by serine residues and/or by a stretch of acidic amino acids (Hecker, CM *et al.*, 2006; Song, J *et al.*, 2005). SIMs have been identified in numerous SUMO targets and they have been described to account for SUMOylation of the target and to serve as mediators for downstream events that require the interaction with SUMO (Kerscher, O, 2007), for instance to maintain the architecture of a number of chromatin repressor complexes (Garcia-Dominguez, M and Reyes, JC, 2009).

3.2.1 The SUMOylation pathway

SUMOylation appears to be a highly specific process taking into consideration both the selection of protein targets as well as the timing and dynamics of the modification. Though the mechanisms involved in the SUMO modification pathway start to be elucidated, many aspects of both specificity and dynamics still need to be studied. Among the similarities that SUMO shares with ubiquitin, their modification pathway is one of them. In the SUMOylation pathway (Figure I-9), some of the enzymes that participate in the modification by SUMO, such as E1 and E2, have sequences with similarities to their ubiquitin counterparts and are highly conserved in eukaryotes.

Like ubiquitin, all SUMO paralogs are synthesized as an inactive precursor polypeptide that needs to be maturated and activated, in order to become conjugatable to target proteins. The initial maturation is conducted by SUMO-specific isopeptidases that performs a proteolitic cleavage in the C-terminus part of the molecule, exposing the previously mentioned Gly-Gly (Figure I-9) (reviewed in (Hay, RT, 2005)).

Once maturated, the C-terminus part of SUMO needs to be activated in a reaction that is performed by the E1 enzyme. The SUMO E1 enzyme is a heterodimer comprised by the SUMO-activating enzyme subunit 1 (SAE1, also known as Aos1) and the SUMO-activating enzyme subunit 2 (SAE2, also known as Uba2) (Azuma, Y *et al.*, 2001; Desterro, JM *et al.*, 1999; Johnson, ES *et al.*, 1997; Okuma, T *et al.*, 1999). SAE1 and SAE2 share a high sequence identity with the N- and C-termini, respectively, of the ubiquitin-activating enzyme (Dohmen, RJ *et al.*, 1995). Similar to other Ubl E1 enzymes, the SAE1/SAE2 heterodimer activates the C-terminus part of SUMO in a two-step reaction. In a first step, SAE1 subunit hydrolyses ATP

to covalently link the C-terminal carboxyl group of SUMO to AMP. In a second step, breakage of the SUMO-AMP bond by a conformational change in the SEA2 subunit leads to the formation of an intermediate in which the C-terminal carboxyl group of SUMO forms a thioester bond with the sulphydryl group of a cysteine residue (C173) located in SAE2 (Figure I-9) (Olsen, SK *et al.*, 2010).

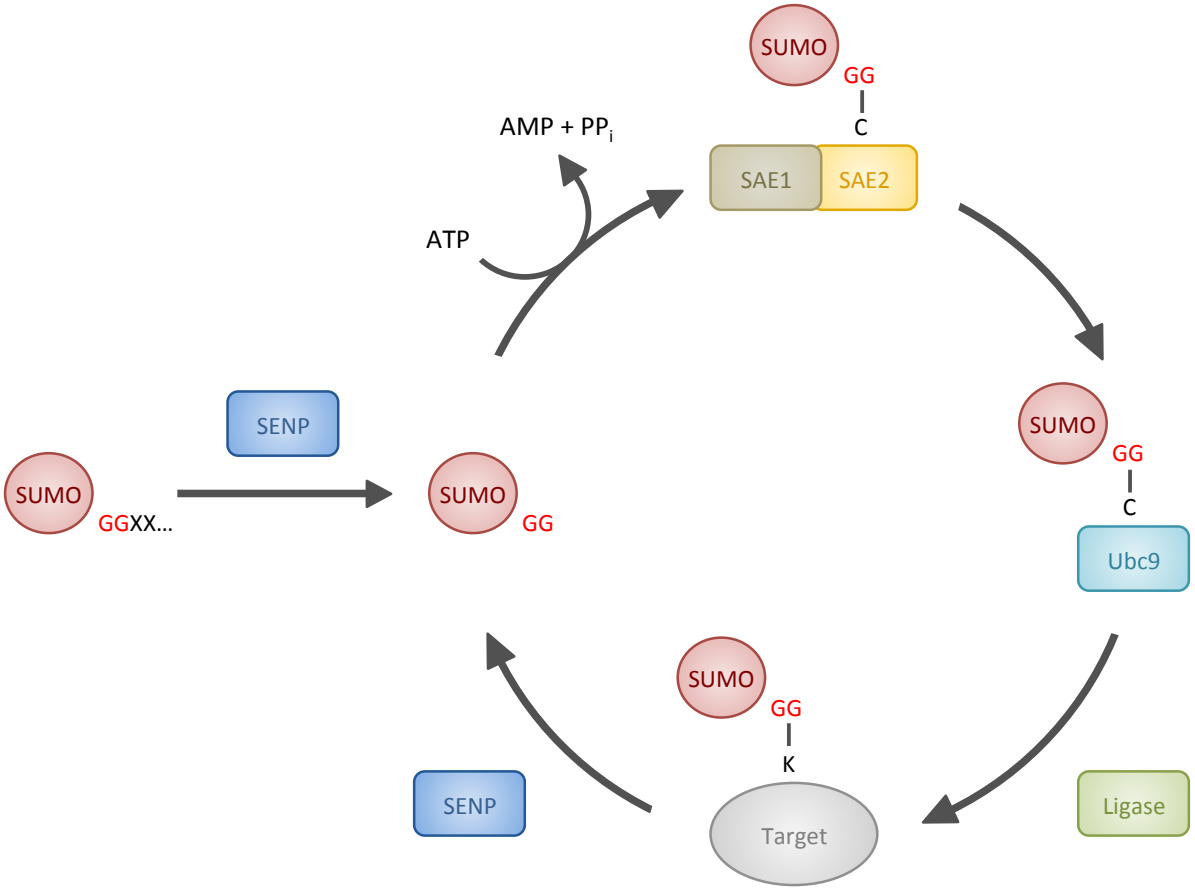

Figure I-9: the SUMOylation pathway. The SUMO modification pathway is similar to ubiquitylation. At the beginning, recently synthesised SUMO needs to be proteolitically maturated by a SUMO-specific protease (SENP) in order to be conjugatable. Maturated SUMO is then activated by the SUMO E1 enzyme (SAE1/SAE2) in an ATP-dependent manner, by formation of a thioester bond between the C-terminal glycine of SUMO and the catalytic cysteine (C) of the SAE2 subunit. SUMO is then transferred to the E2 conjugating enzyme (Ubc9) by the formation of another thioester bond with the enzyme, for finally being conjugated to an acceptor lysine (K) of the target protein, conjugation that is frequently assisted by an E3 ligase. SUMOylation is a highly reversible modification where SENP proteases detach the polypeptide from its target proteins.

The next step in the SUMOylation pathway requires the action of a single SUMO conjugating enzyme, Ubc9. Ubc9 is essential in most of the studied organisms and is highly conserved in eukaryotes, being identical between mouse and human and showing around a 56% identity between the mammalian and *S. cerevisiae* orthologues (review in (Dohmen, RJ, 2004)). The mentioned following step on the SUMOylation pathway consists on a transesterification reaction, in which activated SUMO is transferred from the SAE2 subunit of the activating enzyme to the cysteine 93 of Ubc9, through the formation of a new thioester bond (Desterro, JM *et al.*, 1997; Johnson, ES and Blobel, G, 1997).

In the following step, comprising the final conjugation of SUMO to its target protein, Ubc9-SUMO thioester bond can catalyse the formation of an isopeptide bond between the C-terminal carboxyl group of SUMO and the ε-amino group of an acceptor lysine present in the target protein, though the action of an E3 SUMO ligase is frequently needed (Figure I-9). In spite of this, Ubc9 is capable of performing a function notably distinguishable from the action of ubiquitin conjugating enzymes; Ubc9 is involved in the direct recognition of many SUMO substrates, but the target lysine must be included in the previously mentioned consensus site Ψ-K-X-E, though the affinity of the conjugating enzyme for the SUMO consensus sites is low (reviewed in (Flotho, A and Melchior, F, 2013)). Thus, these targets can be SUMOylated when E1 and high concentrations of Ubc9 are present *in vitro*, without the action of any E3 ligase. However, very few proteins are known to be efficiently SUMOylated *in vivo* without the assistance of an E3 ligase. A well-known exception for this is RanGAP1, whose high affinity binding to Ubc9 permits the establishment of an additional interaction surface (Bernier-Villamor, V *et al.*, 2002). Interestingly, when the acceptor lysine is not included in a consensus site, the presence of an E3 ligase (Yunus, AA and Lima, CD, 2009) or the existence of SIMs (Chang, CC *et al.*, 2011; Meulmeester, E *et al.*, 2008; Zhu, J *et al.*, 2008) in the target protein can facilitate the interaction of the acceptor lysine with the Ubc9-SUMO thioester bond, allowing SUMOylation of the target protein.

3.2.1.1 SUMO ligases

Contrary to the ubiquitylation pathway, where various E2 conjugating enzymes have been described and conduct their function with the assistance of hundreds of known E3

ubiquitin ligases, substrate specificity of the SUMOylation pathway remains as an enigma as there is only one described E2 conjugating enzyme and only a few proteins with E3 SUMO ligase activity have been discovered up to date (Kerscher, O *et al.*, 2006). Interestingly, though all of them increase SUMOylation in a substrate specific manner, it is described how a certain E3 SUMO ligase can target multiple substrates that share only few structural features in common (reviewed in (Melchior, F *et al.*, 2003)). From a general point of view, E3 ligases catalyse the transference of Ubls like SUMO from the E2 conjugating enzyme to the target protein, in a manner that blocks the flexibility of the Ubc9-SUMO thioester bond and changes its orientation to increase its proximity and affinity for the acceptor lysine. As a result, this lysine is capable of performing a nucleophilic attack that results in the formation of an isopeptidic bond with the acceptor lysine, covalently attaching SUMO to its target protein (reviewed in (Flotho, A and Melchior, F, 2013)). The most studied E3 SUMO ligases that have been described to show this last activity could be numbered as an extent group of proteins containing Siz/PIAS-RING (SP-RING) domains and the Ran-binding protein 2 (RanBP2).

The SP-RING domain consists on a type of zinc-finger domain classically associated to DNA binding that is highly conserved among eukaryotes and shares similarities with the RING finger domain present in many E3 ubiquitin ligases. In this manner, some of the SP-RING E3 ligases include Siz1, Siz2, methyl methanesulphonate-sensitivity protein 21 (Mms21) and molecular zipper protein 3 (Zip3) in yeast and the protein inhibitor of activated STAT (PIAS) family of proteins in mammals, that in mouse and human are represented at least by PIAS1, PIASx (PIAS2), PIAS3 and PIASγ (PIAS4). However, two splice variants are described for PIASx; PIASxα and PIASxß ((Chung, CD *et al.*, 1997; Liu, B *et al.*, 1998) and reviewed in (Rytinki, MM *et al.*, 2009)). Proteins that comprise the PIAS family in mammals are highly conserved, regarding the first 430 N-terminal amino acids, though their total length varies from PIAS4 with 510 amino acids to PIAS1 with 651. In all of these ligases, five well established structural domains have been identified: an N-terminal SAP (scaffold attachment factor-A/B, acinus and PIAS) domain, a PINIT motif, the previously mentioned SP-RING, a SIM and a C-terminal region enriched in serine/threonine (S/T) (Figure I-10A). Notably, the SP-RING domain has been described to be necessary for the interaction with Ubc9 (reviewed in (Rytinki, MM *et al.*, 2009)). The target proteins for SUMOylation would interact with the rest of domains present in the PIAS ligases (Hochstrasser, M, 2001). Interestingly, the SIM

located in PIAS ligases has not been related with a SUMO ligase function and, indeed, its deletion on PIASxα has been described to stimulate its ligase activity (Kotaja, N *et al.*, 2002). It is also worth noting that specificity for SUMO paralogs has been poorly described for these ligases. Nevertheless, one example is PIAS4 whose PINIT domain has been related to specificity for SUMO1 (Wong, KA *et al.*, 2004).

A

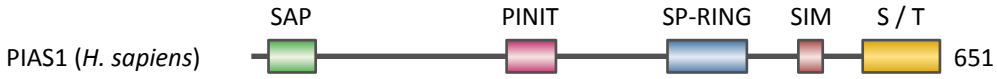

B

PIAS1	Topors
PIAS2 (x)	HDAC II
PIAS3	Pc2
PIAS4 (γ)	PHD domain
RanBP2	

Figure I-10: E3 SUMO ligases and PIAS1 structure domains. (A) Structural domains of human PIAS1 E3 ligase. The SAP domain has been related to sequence-specific DNA binding. A PINIT domain has been associated to the nuclear localization of the protein. The following SP-RING domain is described to be responsible for binding to the E2 conjugating enzyme Ubc9. A SIM and a C-terminal region enriched in serine and threonine residues (S/T) are also represented. **(B)** The listed proteins show SUMO E3 ligase activity and have been deeply characterised.

As previously mentioned, RanBP2 (also known as Nup358) sums to the list of E3 SUMO ligases that have been widely studied (Figure I-10B), but does not resembles to E3 ubiquitin ligases, as it does not contain neither HECT nor RING domains, typical features of many ubiquitin ligases (Pichler, A *et al.*, 2004). RanBP2 is a large protein of 358 kDa located in the Nuclear Pore Complex (NPC). Its *in vitro* activity requires only one of two closely spaced amino acid repeat regions (IR1 and IR2) that, combined with a short spacing region (M), can bind to the Ubc9-SUMO thioester bond (Saitoh, H *et al.*, 2002; Tatham, MH *et al.*, 2005). *In vivo*, together with SUMOylated Ran GTPase-activating protein 1 (RanGAP1) and Ubc9, forms an E3 SUMO ligase complex capable of interacting with multiple proteins that are prone for nucleocytoplasmic transport through the NPC and could be possible SUMOylation targets (Hamada, M *et al.*, 2011; Werner, A *et al.*, 2012).

Other proteins whose E3 SUMO ligase activity has been also studied comprise the human polycomb protein Pc2 (Kagey, MH *et al.*, 2003), the class II histone deacetylases (HDACs II) and the Topors proteins (Gregoire, S and Yang, XJ, 2005; Hammer, E *et al.*, 2007;

Weger, S *et al.*, 2005). In addition, the PHD domains present in some plant and mammal proteins have also been described to exhibit E3 SUMO ligase activity (Figure I-10B) (Garcia-Dominguez, M *et al.*, 2008; Ivanov, AV *et al.*, 2007).

3.2.1.2 SUMO isopeptidases

In eukaryote cells, SUMO-specific peptidases are responsible of three mayor tasks: performing the initial proteolytic cleavage for SUMO maturation, removing single SUMO molecules from modified proteins and depolymerising SUMO chains. Contrary to what is described for ubiquitin, where a large number of specific isopeptidases have been identified and grouped in various classes of proteases (Reyes-Turcu, FE *et al.*, 2009; Wilkinson, KD, 1997), a small number of SUMO proteases have been identified up to date, belonging to the group of cysteine proteases. In this regard, the most well studied SUMO proteases comprise two ubiquitin-like protein-specific proteases (Ulp1 and Ulp2) that have been identified in yeast and six sentrin-specific proteases (SENPs) (SENP1-3 and SENP5-7), identified in humans. The first identified SUMO isopeptidase was yeast Ulp1 (Li, SJ and Hochstrasser, M, 1999). SENP proteins were then identified in other organisms by sequence identity-based studies (reviewed in (Hay, RT, 2007; Hickey, CM *et al.*, 2012)). The structural analysis of Ulp1 (Mossessova, E and Lima, CD, 2000) and further analysis of SENP1 (Reverter, D and Lima, CD, 2006; Shen, L *et al.*, 2006; Shen, LN *et al.*, 2006) revealed that these proteins belong to the family of cysteine proteases, showing a characteristic His-Asp-Cys catalytic triad present in the adenovirus processing protease (AVP) (Li, SJ and Hochstrasser, M, 1999). The active site of Ulp1 is comprised by a ß-sheet in addition to two helixes, creating a central cleft in the protein with the approximate length of a lysine side chain. The cysteine included in the catalytic triad is located at the N-terminus of the central helix, whereas histidine and aspartic acid residues from the active site are both located in the ß-sheet. The C-terminal Gly-Gly motif of SUMO is located to this cleft and orientates in a *cis* configuration, establishing a turn in the C-terminal end of immature SUMO precursors or in the isopeptide bond of SUMOylated proteins. Primary structures of Ulp1, SENP1 and SENP2 show how their catalytic domain, similar between them, is located to their C-terminal end (Figure I-11).

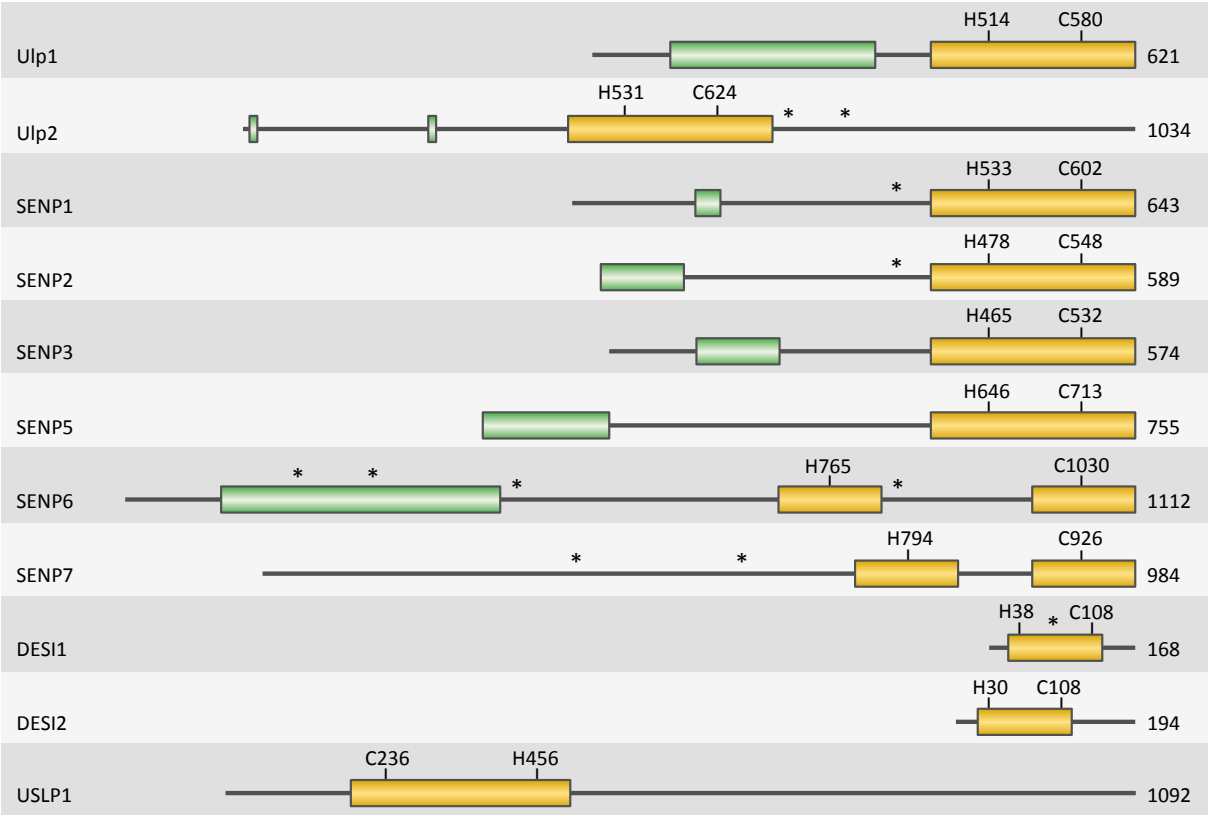

Figure I-11: structure domains in SUMO-specific isopeptidases. Structure domains and length (in amino acids) of SUMO-specific isopeptidases present in yeast and vertebrates, showing the N-terminal domains involved in subcellular localization (green) and the C-terminal catalytic domain (yellow), indicating the key histidine (H) and cysteine (C) residues from the active sites. Putative SIM sequences have been indicated with asterisks. Human SENP1-7 proteins are represented, while for deSUMOylating isopeptidase 1 (DESI1) and DESI2, the mouse proteins are shown. Human Ubiquitin-specific protease-like 1 (USPL1) is also represented.

Catalytic domains of SENP6, SENP7 and Ulp2 have also been described to date and have less than 30% of sequence identity with the previous ones, comprising a new subgroup of SUMO-specific proteases (Li, SJ and Hochstrasser, M, 1999). This last group of proteases present four conserved loop insertions in their catalytic domain that could be related with SUMO paralog specificity, as SUMO2/3 recognition by the loop1 has been described to affect the higher activity that these proteases present towards SUMO2/3 (Alegre, KO and Reverter, D, 2011; Lima, CD and Reverter, D, 2008). Specificity of the C-terminal catalytic domain from these proteins for conjugated SUMO isoforms has been shown not to be strong *in vitro* though some of them, as the previously mentioned SENP6 and SENP7, exhibit increased

activity towards one or another paralog. Interestingly, greater paralogue specificity is sometimes observed *in vivo* but the mechanisms implicated are not completely understood. Nevertheless, high paralog specificity of the C-terminal catalytic domain for immature SUMO precursors has been detailed (Di Bacco, A *et al.*, 2006; Shen, LN *et al.*, 2006; Xu, Z and Au, SW, 2005). On the contrary, the N-terminal part of Ubl and SENP proteases has been shown to regulate the specificity for SUMO substrates *in vivo* by promoting interaction with specific targets and controlling subcellular localization of the proteases. To this point, it is described that SENP1 and SENP2 localize in the nuclear pore, nuclear bodies and nucleoplasm. SENP3 and SENP5 localize to the nucleolus and SENP6 and SENP7 localize to the nucleoplasm (reviewed in (Hickey, CM *et al.*, 2012)). In contrary to the C-terminus, the N-terminal regions are poorly conserved (Figure I-11). The presence of putative SIMs in non-catalytic regions has also been described for Ulp2 and most of SENP proteases. Though SUMO is bound to the catalytic domain by other surfaces, these SIMs could increase the affinity for SUMO or SUMO chains, or could account for a correct orientation of the SUMOylated protein in the protease.

Recently, three new SUMO-specific proteases have been described in humans, deSUMOylating isopeptidase 1 (DESI1), DESI2 (Shin, EJ *et al.*, 2012) and the ubiquitin-specific protease-like 1 (USPL1) (Schulz, S *et al.*, 2012). DESI1 and DESI2 proteins share little sequence identity with Ulp and SENP proteases and belong to the PPPDE (permuted papain fold peptidases of double-stranded RNA viruses and eukaryotes) class of proteases. Interestingly, its catalytic activity is based on their ability to dimerise, thus comprising a surface groove between the two monomers that contains the active sites of the dimeric protease (Suh, HY *et al.*, 2012).

3.2.2 Role of SUMOylation in the cell

Post-translational modification by SUMO has been associated with multiple functions in the eukaryotic cell and this is understandable, taking into consideration the high number of SUMO substrates identified so far and the basis of the modification, in which the addition of a polypeptide to a given protein adds new interacting surfaces or either blocks certain domains present in the target substrate.

SUMOylation has been implicated in the subcellular localization of proteins, with a predominant role in nuclear localization. A paradigmatic example for this function would be RanGAP1 modification by SUMO1, which translocates the target protein from the cytoplasm to the NPC (Mahajan, R *et al.*, 1997; Matunis, MJ *et al.*, 1996). SUMOylation has been shown to be also necessary to target RanGAP1 to the mitotic spindle during mitosis (Joseph, J *et al.*, 2002). Nevertheless, it should be mentioned that, though SUMOylated proteins have been identified in the cell cytoplasm, nuclear targeting is required for most of them to be modified by SUMO *in vivo* (Rodriguez, MS *et al.*, 2001).

Several works also establish an association for SUMO with DNA repair. SUMOylation, together with ubiquitylation, has been shown to orchestrate the cellular responses to a variety of DNA aberrations, due either to exogenous damage or to natural occurring DNA metabolism, such as postreplication repair, base-excision repair and the repair of most cytotoxic double-strand breaks (reviewed in (Jackson, SP and Durocher, D, 2013)). Several works in yeast and higher eukaryotes have established genetic associations with chromosome condensation, cohesion and segregation during mitosis and meiosis for every component of the SUMOylation pathway (reviewed in (Seeler, JS and Dejean, A, 2003)), adding modification by SUMO to the factors that maintain genetic stability in the eukaryotic cell.

SUMOylation has shown to be necessary for regulation and stabilization of some proteins, as it has been studied how the same lysine residues can be modified in certain circumstances either by SUMOylation, ubiquitylation, acetylation or phosphorylation. A well-known example of this competition mechanism is Iκbα, where SUMOylation of lysine 21 is shown to inhibit phosphorylation-induced ubiquitylation and subsequent proteasomal degradation (Desterro, JM *et al.*, 1998).

One of the most important functions attributed to SUMOylation is the modification of transcription factors in order to control gene expression. This way, modification by SUMO1 has been typically related to transcriptional repression. Certain exceptions are known, like the increase in target gene expression mediated by heat shock transcription factors HSF1 and HSF2 when modified by SUMO1 (Goodson, ML *et al.*, 2001; Hong, Y *et al.*, 2001). But as said, many are the examples where repressor domains present in transcription factors display their repressor activity when at least one lysine residue included in the repressor domain is modified by SUMO1 (reviewed in (Garcia-Dominguez, M and Reyes, JC,

2009)). SUMO2/3 though, has been mostly shown not to be conjugated to proteins under normal conditions, but to rapidly modify a variety of proteins during the cellular response to various stresses like hypoxia (Yang, W *et al.*, 2012) or heat stress (Castoralova, M *et al.*, 2012).

Finally, though not being a cellular function *per se*, it is important to mention how evolution has made possible for pathogens to take advantage of the SUMOylation pathway during infection. As the SUMO modification pathway only comprises one single E1 and E2 enzyme, any interference with these enzymes has remarkable effects. In fact, it has been described how certain viruses and bacteria enhance their infection by targeting host E1 or E2 enzymes for proteasome-mediated degradation (reviewed in (Flotho, A and Melchior, F, 2013)).

3.2.2.1 SUMOylation in neurons

A number of functions for SUMO in adult neurons have been encountered (reviewed in (Martin, S *et al.*, 2007)). As an example, SUMOylation of the postsynaptic scaffolding protein gephyrin has been described in neurons and related to GABAergic transmission (Ghosh, H *et al.*, 2016). In addition to this, previous works suggested a role for SUMOylation in synaptic plasticity and trafficking. To this point, a regulatory role has been established for SUMO in the synapse formation of cerebellar granule neurons, where the myocyte enhancer factor 2 (MEF2) turns to be a transcriptional repressor or an activator depending on its SUMOylated or not SUMOylated state, respectively (reviewed in (Beg, AA and Scheiffele, P, 2006)). In addition to this, not only substrates but also enzymes of the SUMO modification pathway like SAE1, Ubc9, SENP1 and SENP6, have been detected in rat synaptosomes (reviewed in (Luo, J *et al.*, 2013)).

The implication of SUMO with neurodegenerative diseases that generate due to the accumulation of aberrant proteins, like Alzheimer and Parkinson diseases, has also been described. In these cases, SUMOylation seems to prevent degradation of these aberrant products by competition with ubiquitylation and proteasome-mediated degradation. In the case of Alzheimer, pathological progression has been related to synaptic failure and later accumulation of insoluble amyloid-ß and microtubule-associated protein tau aggregates.

Both amyloid-ß and tau proteins have been shown to be SUMOylated and alterations in enzymes of the SUMO pathway, like SAE2 or SENP3, have been reported in affected tissues (reviewed in (Lee, L *et al.*, 2013)). Parkinson disease is not defined by a single pathology, but rather comprises a variety of syndromes. Though little is known about the causes of the disease, most of the cases are characterized by the presence of Lewy bodies containing fibrillar α-synuclein. DJ-1 and parkin are proteins also related with the disease. SUMO conjugation has been described for the three proteins and been associated to their solubility and aggregation properties, though no clear relationship with disease progression has been established (reviewed in (Eckermann, K, 2013)).

SUMOylation is associated with transcriptional regulation, a critical feature in neuronal development. Up to date, few reports have linked SUMOylation with the control of this process. Thus, SUMOylation of the transcription factor SoxN has been proposed to repress its transcriptional activity, which is necessary for the proper formation of the CNS in *Drosophila* (Savare, J *et al.*, 2005). On the other hand, SUMOylation of Braf35, a subunit of the LSD1-CoREST histone demethylase complex has been shown to be necessary for the maintenance of the undifferentiated state of neuronal precursors (Ceballos-Chavez, M *et al.*, 2012). Despite these findings, the establishment of clear implication of additional SUMO targets and of components of the SUMOylation pathway in orchestrating different aspects of neural development remains elusive. Thus, it is mandatory to address research in the field through new and complementary approaches.

3.3 Objectives

Taking into consideration the previously mentioned works, enough evidences point to a connection between the SUMO modification pathway and neuronal development. Thus, three main objectives have been projected in this work to study this connection:

1) To analyse the function of the interaction between Krox20 and Ubc9 during hindbrain development.

2) To study the regulation of the SUMOylation pathway and its components in the context of neurogenesis.

3) To identify SUMO targets differentially modified under proliferation and neuronal differentiation conditions.

4 Results

Understanding the mechanisms involved in the neural development is an arduous task since it involves the comprehension of numerous pathways and signalling systems implicated in the tight regulation and control of this process. Many of these mechanisms remain unclear.

A signalling system that is acquiring more relevance regarding transcriptional control is the post-translational modification by SUMO. SUMOylation is essential in vertebrates. Adding this consideration to its relevance in transcriptional control and many other functions in the cell, it is likely to think that this post-translational modification might be implicated in the neuronal differentiation process. In this work, we analyse the role of SUMOylation in three different scenarios of neural development, to shed light on the mechanisms involved in this complex process.

The first scenario focuses on the formation of the hindbrain in vertebrates, where an intricate and highly regulated compartmentalizing process takes place during the development of this region of the embryonic central nervous system. Starting from preliminary results obtained from a two-hybrid experiment, we have described a system where SUMOylation plays a regulatory role during hindbrain formation.

The second scenario turns into the neural tube. The development of this structure is simpler than that of the hindbrain and we have taken advantage of a variety of tools and models to analyse how does the SUMOylation machinery behave during the neuronal differentiation processes that take place during its formation.

Once having investigated the behaviour of the SUMO modification pathway in neurogenesis, the last scenario focuses on determine which target proteins have a role in neuronal differentiation through regulation by SUMO. For this purpose, a Stable Isotope Labelling with Amino acids in Cell culture (SILAC) experiment comparing the SUMO proteome of proliferative and differentiating P19 cells has been done to initially identify proteins that change their SUMOylation state during this process, without changing their expression levels. The results obtained could open new ways on understanding the role of the SUMO modification pathway in neural development.

4.1 Study of the role of SUMO during hindbrain formation.

4.1.1 Krox20 interacts with Ubc9.

From a previous two-hybrid screening based on mouse Krox20 lacking the two transactivation domains present in this transcription factor and an 8.5 dpc mouse embryo cDNA library (Garcia-Dominguez, M *et al.*, 2006), seven positive clones were isolated corresponding to the SUMO-conjugating enzyme Ubc9 from mouse. Validation of one of these clones by two-hybrid experiments assessed that Krox20 interacts with Ubc9 (Figure R-1A), opening a new connection between a neural development-related protein and the SUMO modification pathway.

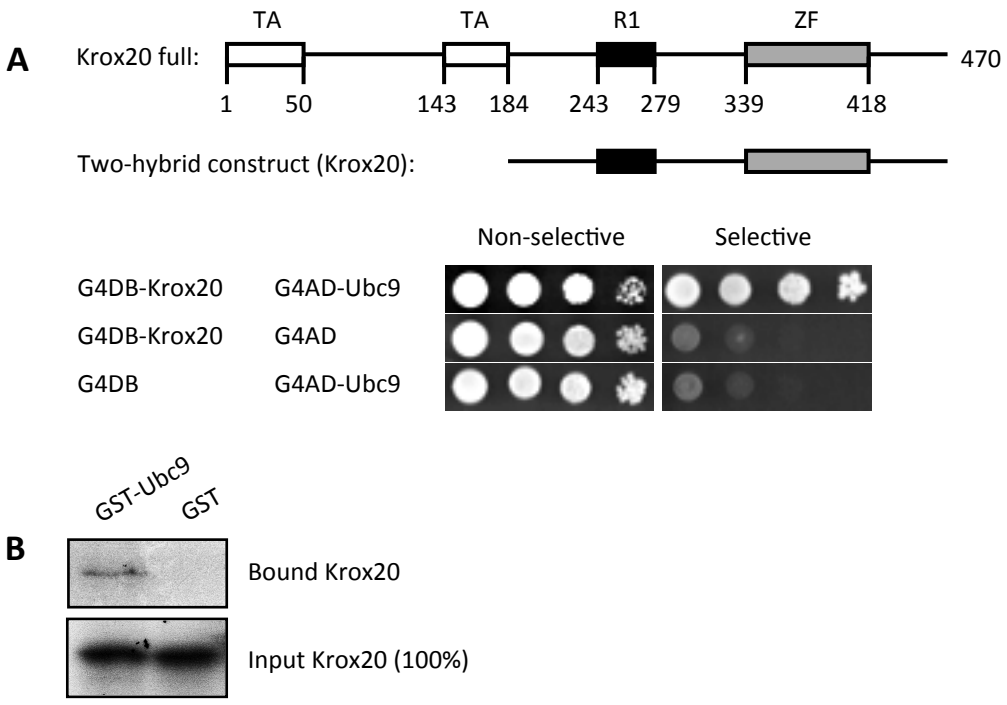

Figure R-1: Two-hybrid validation of the interaction between Krox20 and Ubc9. (A) Yeast was cotransformed with the indicated constructs and grown in selective and non-selective media for two-hybrid experiment. Bait and prey constructs were based on the Gal4 DNA-binding domain (G4BD) and Gal4 activation domain (G4AD) vectors, respectively. **(B)** Pull-down of *in vitro* translated and radioactively labelled Krox20 was performed against 0.5 µg of purified glutathione S-transferase (GST) or a GST-Ubc9 fusion, immobilized to a glutathione sepharose matrix. 100% of input was loaded relative to the precipitated volume. TA: transactivation domain; ZF: zinc-finger domain.

Pull-down experiments with purified glutathione S-transferase (GST) or a GST-Ubc9 fusion and *in vitro* translated Krox20 (see Materials and Methods) demonstrated a direct and specific interaction between Krox20 and Ubc9 (Figure R1-B). We mapped the fragment of Krox20 responsible for Ubc9 interaction by using the yeast two-hybrid assay (see Materials and Methods). Analysis indicated that the zinc-finger domain present in Krox20 (amino acids 339 to 418) was necessary and sufficient for binding to Ubc9 (Figure R-2).

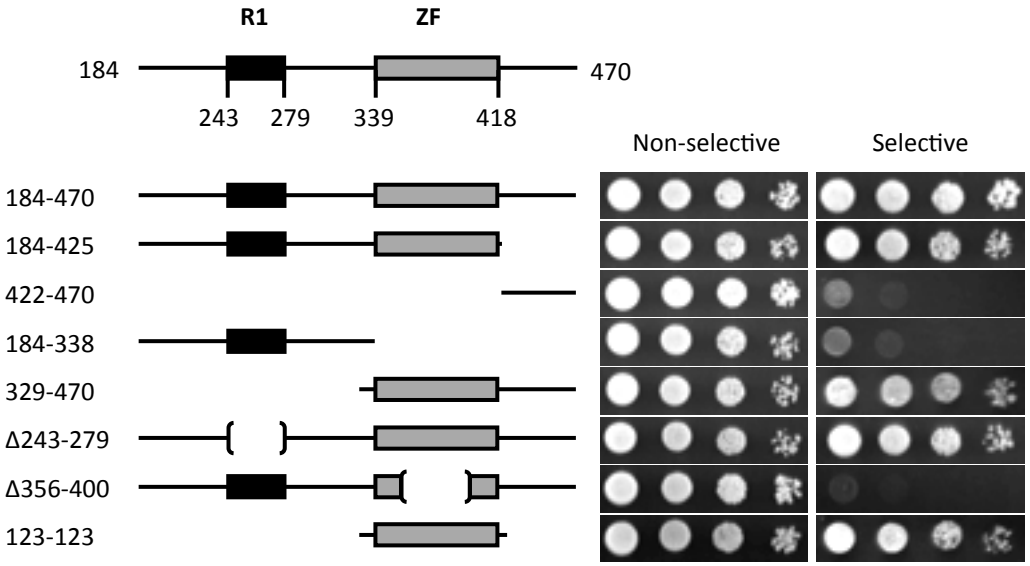

Figure R-2: The zinc-finger domain of Krox20 mediates its interaction with Ubc9. Krox20 deletion constructs were cotransformed in yeast as indicated, following growth in selective and non-selective media, to test interaction of the indicated Krox20 mutants with Ubc9 by two-hybrid experiment. Krox20 bait mutants were based on the G4DB vector and were cotransformed with the G4AD-Ubc9 prey construct.

Protein interaction with Ubc9 often leads to SUMOylation of the interacting protein. However, it has been previously reported that Krox20 is not modified by SUMO (Garcia-Dominguez, M *et al.*, 2006). Ubc9 also interacts with SUMO ligases as these proteins facilitate the transfer of SUMO from Ubc9 to the target protein. We therefore speculated that Krox20 might recruit Ubc9 to function as a ligase in the SUMOylation of other proteins. To this point, Nab1 and Nab2 have been described as Krox20 corepressors (Russo, MW *et al.*, 1995; Svaren, J *et al.*, 1996) that represent good candidates. Indeed, amino acid sequence analysis revealed two SUMOylation consensus sites in mouse Nab2 (K379 and K517) (Figure R-3). A two-hybrid assay did not reveal direct interaction between Nab2 and Ubc9 (Figure R-4).

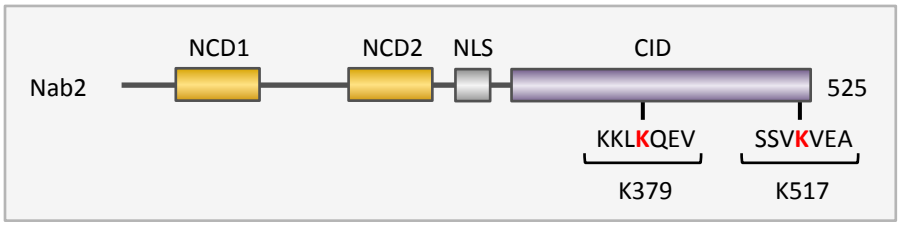

Figure R-3: Nab2 presents two putative SUMOylation consensus sites. Amino acid sequence analysis of Nab2 protein with the GPS SUMO 2.0 software showed two ΨKxE-type SUMOylation sites with scores of 3,597 and 3,431 for K379 and K517, respectively. The analysis was performed using a high threshold.

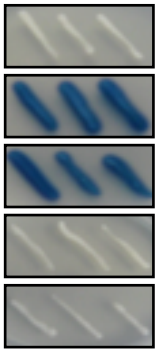

Figure R-4: Nab2 protein does not interact with Ubc9. *In situ* ß-gal activity was analysed to determine interaction (blue) or absence of interaction (white) between Nab2 and Ubc9 by two-hybrid experiment, when cotransformed yeast with the indicated constructs were grown in X-Gal supplied non-selective medium.

4.1.2 Krox20 functions as a SUMO ligase.

To test Nab proteins modification by SUMO, we performed SUMOylation assays in 293T cells transfected with Flag-tagged Nab expression constructs and analysed the cell extracts by Western blot (Figure R-5). The only transfection of Nab2 resulted in detection of a single band of less than 66 kDa, according to its estimated mass of 56,6 kDa. However, when Nab2 and Krox20 expression vectors were cotransfected, two additional bands were observed, consistent with the modification of both predicted SUMOylation sites by a single SUMO molecule. In the cell, SUMO1 is mostly bound to proteins, resulting in a reduced pool of free SUMO1 (Gareau, JR and Lima, CD, 2010). The addition of low amounts of a Histidine-tagged SUMO1 (His-SUMO1) expression vector in cotransfections resulted in increased modification of Nab and the appearance of an additional third upper band corresponding to both SUMOylated sites (Figure R-5A). To assess Nab2 modification by SUMO, two different

tagged SUMO molecules were tested. To this point, a fusion construct consisting on the GFP and SUMO1 (GFP-SUMO1) was also efficiently conjugated to Nab2, showing a size change of SUMOylated Nab2 when compared to His-SUMO1, concordant with the higher mass of the GFP (Figure R-5B).

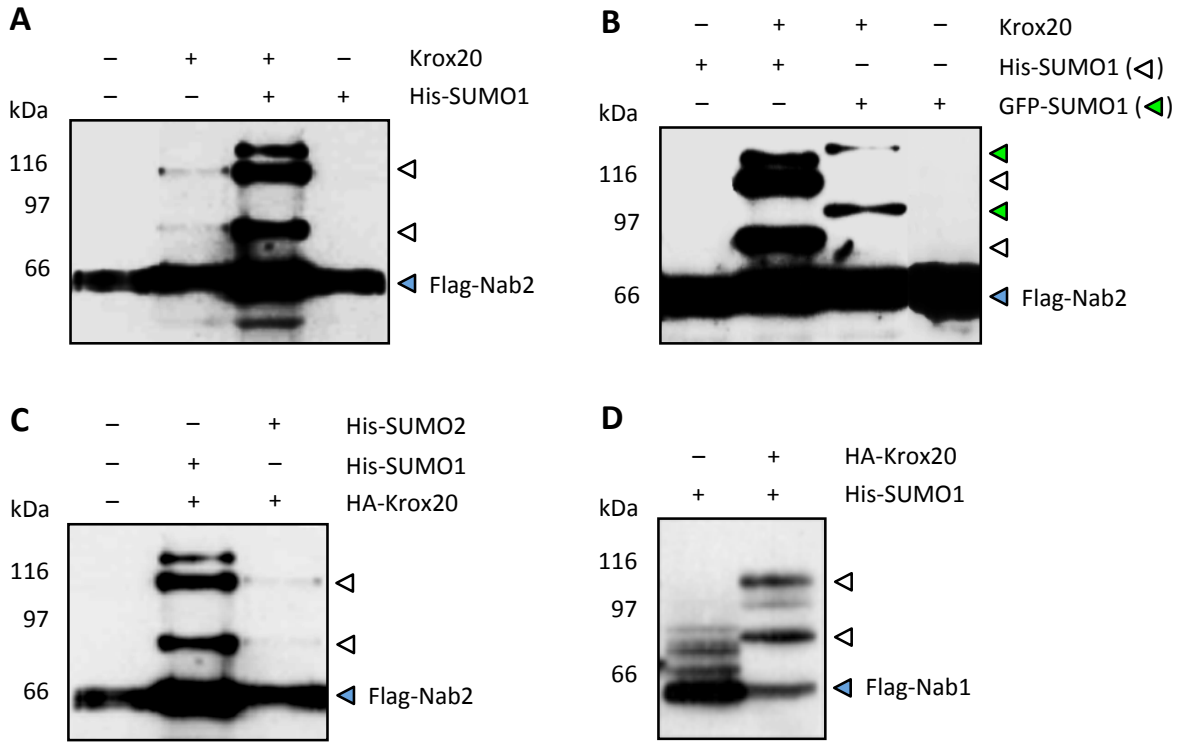

Figure R-5: Nab modification by SUMO1 is enhanced by Krox20. *In vivo* SUMOylation assays were performed transfecting 293T cells with the indicated expression constructs of different versions of Krox20 and SUMO, as well as Flag-tagged Nab. After cell harvesting, denaturing protein extraction was performed to analyse Nab SUMOylation by Western blot using antibodies against the Flag epitope. Blue arrowheads indicate unmodified Nab while white or green arrowheads indicate diverse Nab SUMOylated forms. **(A, D)** Nab1 and Nab2 are modified by SUMO1 when cotransfected with Krox20, and SUMOylation is enhanced by addition of low amounts of SUMO1. Nab2 shows no modification when low amounts of SUMO1 are cotransfected in the absence of Krox20. **(B)** To assess Nab2 modification by SUMO1 in the presence of Krox20, different tagged versions of SUMO1 are transfected. An increase in SUMOylated Nab2 bands is observed when cotransfecting GFP-tagged SUMO1 in comparison to His-tagged SUMO1. **(C)** Specificity of Nab modification by SUMO1 is observed as almost no modification of Nab is observed when cotransfected with SUMO2 and compared to SUMO1 in the presence of Krox20.

Nab2 was not modified by SUMO2 after cotransfection of a His–SUMO2 expression construct (Figure R-5C). Nab1 was also SUMOylated by SUMO1 in the presence of Krox20 (Figure R-5D). As Nab1 and Nab2 are highly homologous and have been shown to display similar functions (Svaren, J *et al.*, 1996), we restricted the following experiments to Nab2, from now referred to as Nab. As a next step, we wanted to assess the specificity of Krox20 SUMO ligase action. In transfection experiments, Nab was specifically modified in the presence of Krox20, as a non-related transcription factor (NeuroM) had no effect. Additionally, we generated an Ubc9 mutant encompassing a single mutation in the catalytic site (Ubc9C93S) responsible for its non-covalent interaction with SUMO. Interestingly, cotransfection of this mutant prevented Nab SUMOylation in the presence of Krox20 (Figure R-6A).

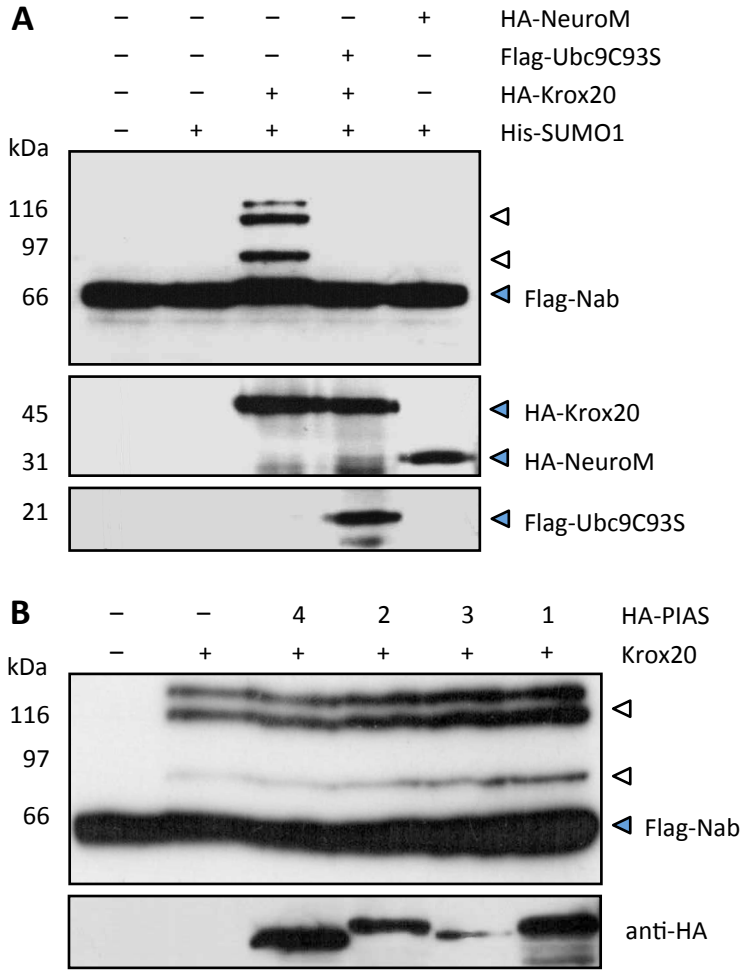

Figure R-6: Specificity of Krox20 SUMO ligase action in Nab SUMOylation. The indicated expression constructs were transfected in 293T cells for SUMO modification assays in the same conditions shown in Figure R-5. **(A)** SUMOylation of Flag-tagged Nab is disrupted when trans-fecting a catalitic Ubc9C93S mutant in the presence of Krox20. Krox20 and no other transcription factor as NeuroM specifically enhances Nab SUMO-ylation by SUMO1. Blots with HA antibodies are shown to check expression of Krox20 or NeuroM. Expression of the Ubc9 C93S mutant is shown using Flag anti-bodies. **(B)** Modification of Flag-tagged Nab is not altered when different ligases of the PIAS family were cotransfected and com-pared to Nab SUMOylation in the only presence of Krox20. His-tagged SUMO1 is included in all tested conditions. Blots using HA antibodies are shown to check PIAS expression.

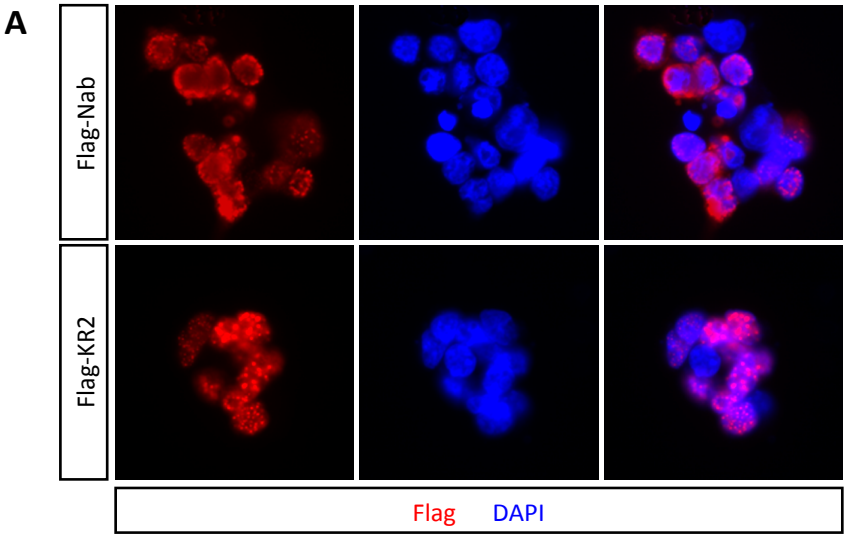

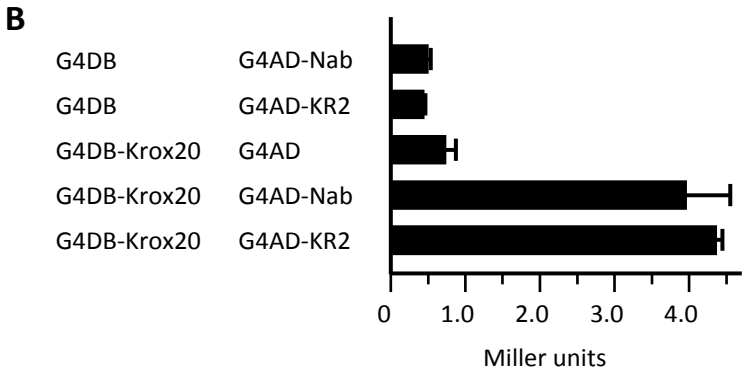

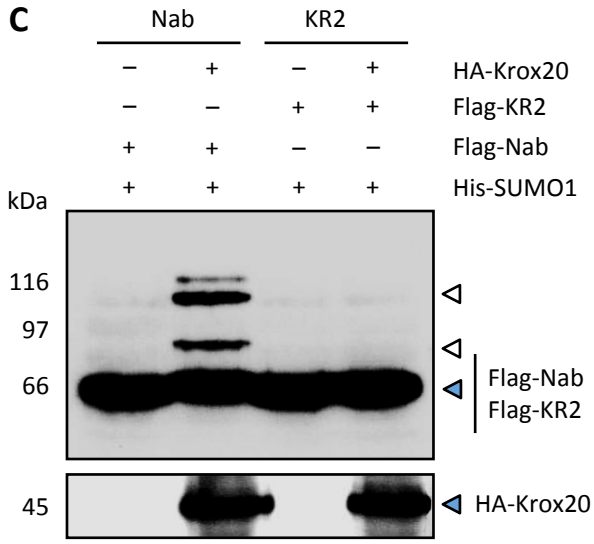

Figure R-7: A K379R and K517R Nab double mutant (KR2) is not modified by SUMO1. **(A)** Localization of Flag-tagged Nab wild type and KR2 mutant was analysed by immuno-fluorescence of 293T cells after transfection of the indicated expression constructs. Flag antibodies were used to reveal Nab localization in the cells (red). Nuclei was visualized by DAPI counterstaining (blue). **(B)** The interaction of both wild type Nab and KR2 mutant with Krox20 was analysed by two-hybrid experiments. For this, the indicated expression constructs were transformed in yeast and ß-galactosidase activity was measured and indicated in Miller units corresponding to means of three independent experiments ± s.d. **(C)** The indicated expression constructs were transfected in 293T cells to test SUMOylation of Nab KR2 mutant. After cell harvesting, denaturing protein extracts were analysed by Western blot using Flag antibodies showing the absence of SUMOylated Nab KR2 mutant in comparison with wild type Nab. HA antibodies were used to check the expression levels of wild type Krox20 and KR2 mutant.

Overexpression of the protein inhibitor of activated STAT (PIAS) proteins was also tested, not significantly modifying Nab SUMOylation in the presence of Krox20 (Figure R-6B). To check whether the two consensus sites identified in Nab were responsible of its SUMOylation, we designed a double mutant of the putative target lysines, K379R and K517R (KR2). To test that Nab cellular properties were not altered by these two mutations, cellular localization was analysed on one hand by immunofluorescence and compared to the wild type Nab, showing in both cases a nuclear localization as revealed by DAPI counterstaining (Figure R-7A). On the other hand, Nab-Krox20 interaction capabilities were not altered by these mutations as shown by quantification of ß-galactosidase activity in two-hybrid experiments (Figure R-7B). As expected, this mutant was not SUMOylated after cotransfection of 293T cells with Krox20 and His-SUMO1 (Figure R-7C).

We next investigated the involvement of Krox20-Nab interaction in Nab SUMOylation, as would be expected for a SUMO E3 ligase, by transfection of 293T cells. The single mutation I268F in Krox20 and the double mutation Q64RH95Q in Nab have been shown to abrogate Krox20-Nab interaction (Svaren, J *et al.*, 1998). We found that both mutations prevented SUMOylation (Figure R-8A). By contrast, neither Krox20 nor the I268F mutant showed any effect in general SUMOylation, as monitored by modification of the carboxyl terminal part of RanGAP1 (RanGAP1-C-ter), a well-known SUMO1 substrate (Figure R-8B).

To shed light on the endogenous mechanisms that involve SUMO ligase action of Krox20 in the cell, we turned to the P19 cell line, as these cells express both Krox20 and Nab. Quantitative PCR analysis of non-treated and serum stimulated cells were carried out to observe that, though Nab presented a basal expression prior to serum stimulation, P19 cells showed an increase in the expression levels of both Nab and Krox20 after serum stimulation (see Materials and Methods) (Figure R-9A). When analysing Nab endogenous SUMOylation at the protein level, we were not able to observe Nab modification by endogenous SUMO1. It has been described how SUMOylation of some proteins is difficult to observe by Western blot, as the amount of modified protein is very limited in comparison with the unmodified form (Hay, RT, 2005). Thus, we decided to transfect P19 cells with low amounts of the His-SUMO1 expression vector to analyse Nab SUMOylation after pull-down of the His-tagged products. As shown by Western blot, although SUMOylated Nab forms could not be detected in the input (1.5% of the total), they were observed in the precipitates. Moreover,

the presence of these bands was strongly reinforced after serum stimulation; that is, upon induction of Krox20 (Figure R-9B). SUMOylation of endogenous Nab was also observed in pull-down experiments after transfection of a Krox20 expression vector without serum stimulation (Figure R-9C). Finally, knockdown of induced Krox20 by a combination of two short interfering RNA (siRNA) molecules that were cotransfected with His-SUMO1 prior to serum stimulation prevented serum-induced SUMOylation of endogenous Nab as shown by Western blot after pull-down (Figure R-9D).

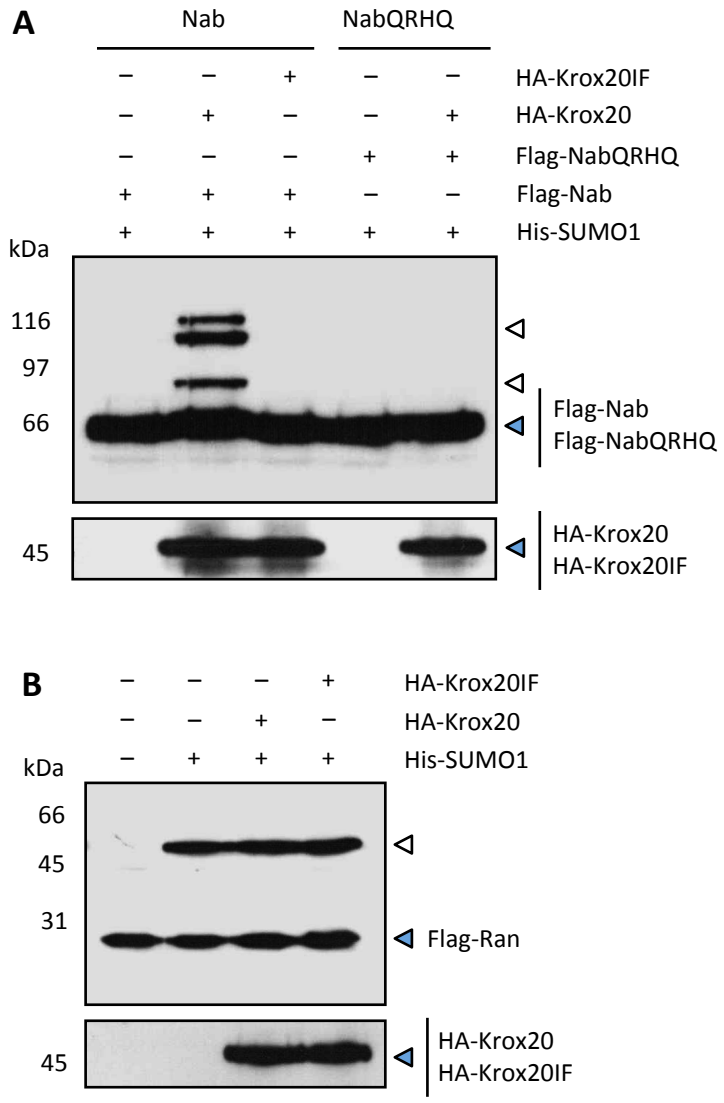

Figure R-8: Physical interaction between Nab and Krox20 is necessary for Nab SUMOylation. SUMOylation assays were performed by transfection of 293T with the indicated expression constructs. Cells were harvested 24h after transfection and denaturing protein extracts were analysed by Western blot. **(A)** SUMOylation of Nab and Krox20 non-interacting mutants was analysed by Western blot using Flag antibodies against the Flag-tagged Nab. The absence of SUMOylated Nab bands in the presence of the mutants shows how Krox20 and Nab need to interact for proper SUMO ligase and target function, respectively. Blots with HA antibodies are shown as controls for the expression of Krox20 constructs. **(B)** Analysis of Flag-tagged RanGAP1-Cter (Ran) SUMOylation was conducted on transfected 293T cells to discard an indirect effect of Krox20IF mutant on overall SUMO modification in the cell. Western blot with Flag antibodies showed how Ran was equally modified by SUMO in the presence of either wild type Krox20 or I268F mutant. HA antibodies were used to check the expression levels of wild type Krox20 and I268F mutant.

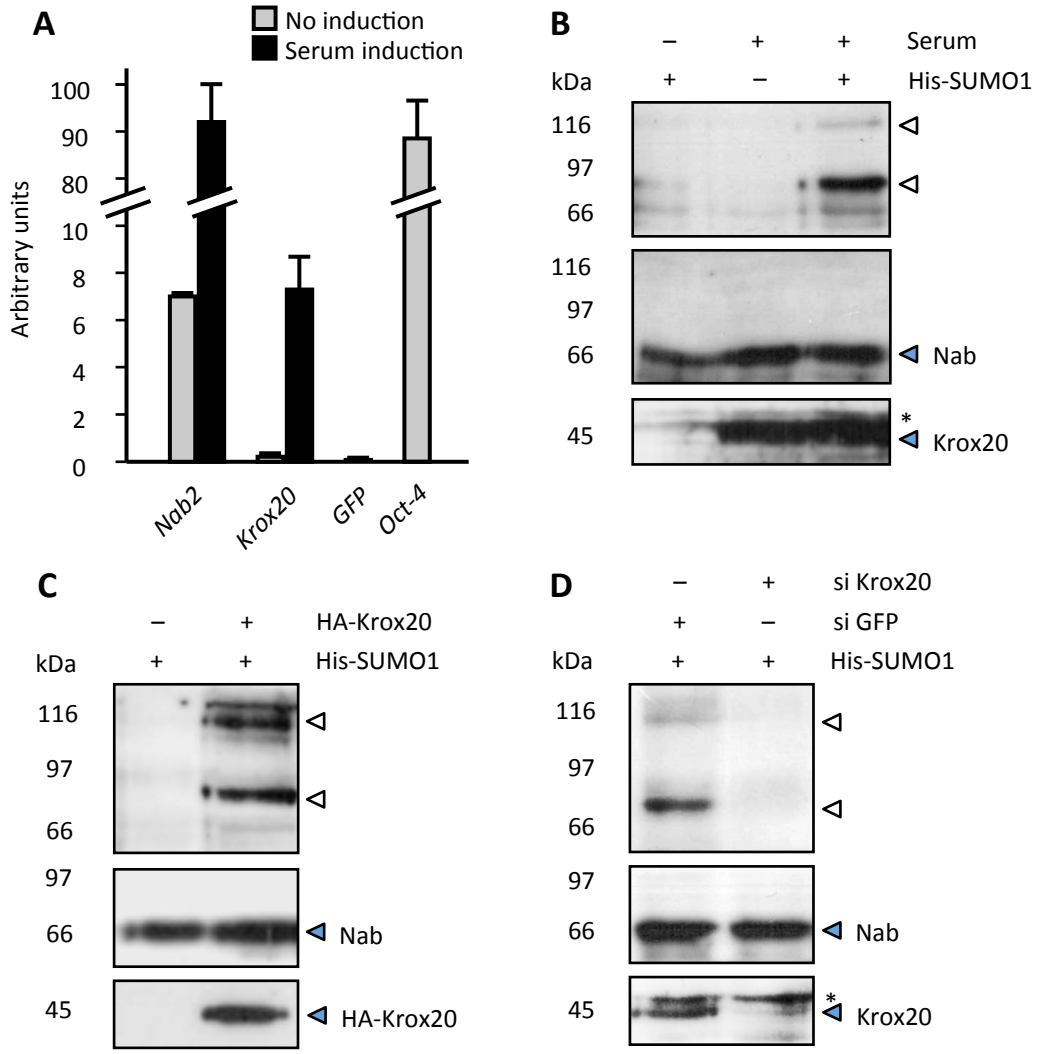

Figure R-9: Endogenous Nab is SUMOylated in P19 cells after serum-induced Krox20 expression. (A) Expression levels of *Nab2* and *Krox20* were analysed by quantitative PCR in proliferating P19 cells after RNA isolation (grey bars). Expression levels of absent (*GFP*) and well-expressed genes (*Oct4*) in this condition are also shown as controls. *Nab2* and *Krox20* expression was also analysed after serum stimulation (black bars). Means of arbitrary units of three independent experiments ± s.d. are represented. **(B-D)** SUMOylation of endogenous Nab was analysed by pull-down experiments against the polyhistidine tag of SUMO1 and Western blot using the indicated antibodies. Upper blots show pull-down of SUMOylated endogenous Nab revealed with Nab antibodies while the two lower blots show 1.5% input of the indicated proteins. Note that Krox20 antibodies also reveal a non-specific upper band (*). **(B)** Endogenous Nab SUMOylation was visualized after transfection of His-SUMO1 and induction of Krox20 expression by serum stimulation. Blot using antibodies against endogenous Krox20 is shown as a control of Krox20 expression induction. Endogenous Nab expression is also shown. **(C)** SUMOylation of endogenous Nab was also observed when P19 cells were transfected with HA-tagged Krox20 under normal growth conditions. **(D)** Knock-down experiments show how SUMOylation of endogenous Nab was impaired when transfecting a small interfering RNA (siRNA; si) against Krox20 prior to serum induction, but not with a control siRNA against the GFP.

To definitively demonstrate that Krox20 functions as a SUMO ligase for Nab, we performed *in vitro* SUMOylation assays with proteins purified from *E. coli* (Figure R-10A and R-10B). As illustrated in Figure R-10C, SUMOylation of Nab took place in vitro and was indeed dependent on the presence of Krox20. Furthermore, chemiluminescence measurement from the bands detected by Western blot and comparison with the amount of loaded protein revealed that $0.3x10^{-12}$ mol of Krox20 were sufficient to modify at least $2.78x10^{-12}$ mol of Nab. These results suggest a catalytic and not stoichiometric function of Krox20, as would be expected for a SUMO ligase.

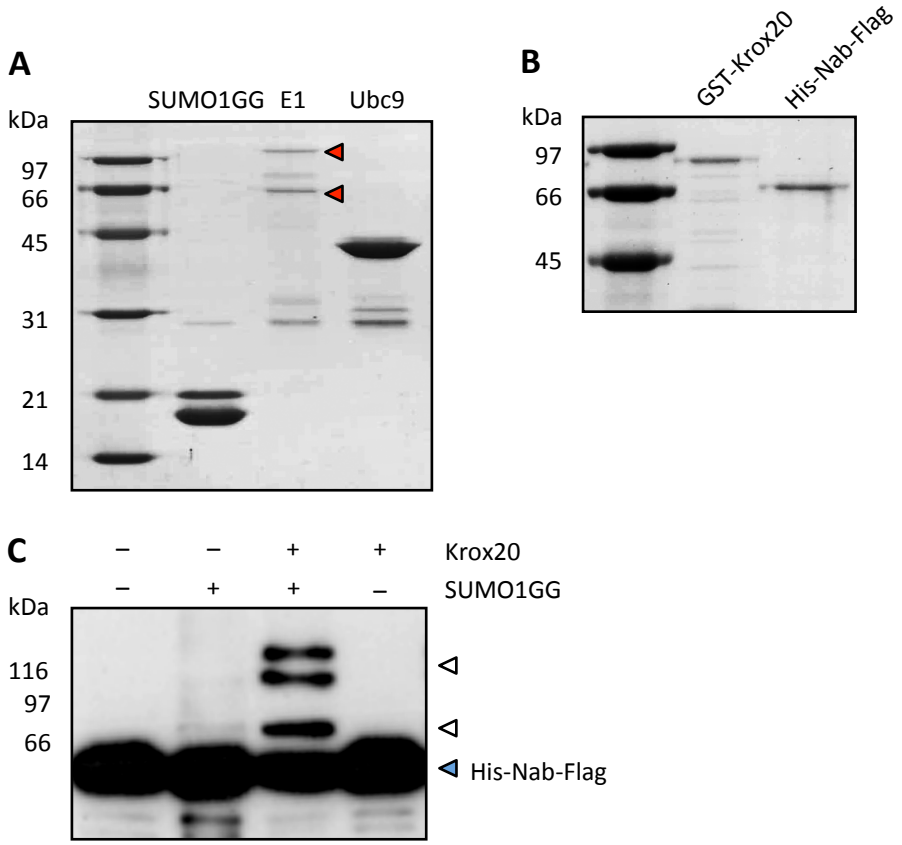

Figure R-10: *In vitro* SUMOylation assay to assess the SUMO ligase role of Krox20 in Nab modification by SUMO1. (A, B) Coomassie blue staining of recombinant fusion proteins purified from *E. coli*. Mouse E1 monomers (red arrows), Ubc9, Krox20 and human matured SUMO1 (SUMO1GG) were purified as GST-fusion proteins and SUMO1GG was later excised from GST. Nab-Flag was purified as a His-tagged version using a nickel affinity matrix. **(C)** *In vitro* SUMOylation assay with the previously shown purified proteins to test modification by SUMO1GG of 300 ng of Nab in the presence of 15 ng of Krox20 by Western blot using Flag antibodies. SUMOylated products correspond to 52.96% ± 2.74% (means ± s.d.) of total loaded protein when chemiluminescence of three independent experiments was measured.

4.1.3 Nab mediates SUMO recruitment to the chromatin.

SUMOylation has been related to many roles in the cell, being modification by SUMO1 mostly connected to transcriptional regulation (Seeler, JS and Dejean, A, 2003). As Nab SUMOylation by Krox20 has been shown to be specific for SUMO1 (Figure R-5C), we next investigated whether SUMO1 can be recruited to a Nab regulated sequence in the context of chromatin. We chose to examine the *Id4* promoter because it has been previously shown to be regulated by the Krox20–Nab complex (Mager, GM *et al.*, 2008). In P19 cells growing under serum deprivation, chromatin immunoprecipitation (ChIP) experiments analysing SUMO1 incorporation revealed that serum addition led to a threefold increase in SUMO levels associated to the *Id4* promoter (Figure R-11). To investigate whether Nab SUMOylation was involved, cells were transfected with wild type Nab or the KR2 mutant immediately after serum deprivation. Whereas in the presence of wild type Nab the increase of SUMO levels was similar to those observed in the absence of transfection, serum-mediated accumulation of SUMO on the *Id4* promoter was impaired with the KR2 mutant, presumably due to competition with the endogenous Nab (Figure R-11).

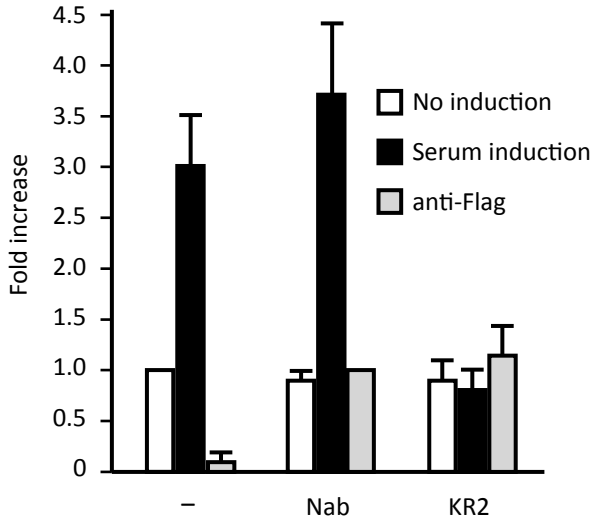

Figure R-11: Serum induction triggers SUMO1 accumulation to a Nab-Krox20 regulated DNA sequence. SUMO1 incorporation levels to the *Id4* promoter, analysed by chromatin immunoprecipitation (ChIP) assays and quantitative PCR of P19 cells transfected with Flag-tagged wild type Nab or with the KR2 mutant. Untransfected P19 were also included in the experiments (–). SUMO1 incorporation was measured under normal growth conditions (white bars) or after serum stimulation (black bars). Levels of SUMO1 incorporation were normalized to the values of untransfected and untreated cells. Flag incorporation was also measured as a control (grey bars) and values were normalized to untreated cells transfected with wild type Nab.

It has been reported that CHD4 interacts with Nab proteins and participates in, but does not account for, full repression activity associated with Nab (Srinivasan, R *et al.*, 2006), which indicates the existence of additional mechanisms involved in the repressive function of Nab. To this point, it is worth nothing to mention that, among the numerous roles attributed to SUMO in the eukaryotic cell, SUMOylation has been mostly linked to transcriptional repression (Garcia-Dominguez, M and Reyes, JC, 2009). Thus, we wanted to analyse how Nab SUMOylation correlates with its interaction with CHD4. After cotransfection of P19 cells with CHD4 and the wild type Nab or the KR2 mutant, immunoprecipitation experiments showed how CHD4 is equally bound to both wild type Nab and KR2 (Figure 12), suggesting that SUMOylation is not involved in CHD4 recruitment.

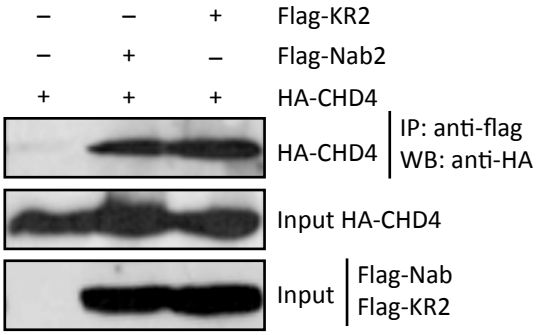

Figure R-12: Nab interaction with CHD4 is not altered by mutation of Nab SUMOylation sites. 293T cells were transfected with expression vectors of a HA-tagged version of the Nab-interacting domain from CHD4 and with Flag-tagged versions of Nab and the KR2 mutant. Cell extracts were subjected to immunoprecipitation with Flag antibodies and the precipitates were analysed by Western blot with HA antibodies. 10% of input proteins are also shown.

4.1.4 Nab SUMOylation modulates Krox20 activity in vivo.

To evaluate whether Nab SUMOylation has an impact on Krox20 transcriptional control, we took advantage of a *lacZ*-based reporter under the control of an *EphA4* element (Garcia-Dominguez, M *et al.*, 2006), known to be under the positive control of Krox20 (Theil, T *et al.*, 1998). This reporter was transfected in P19 cells together with Krox20, SUMO1 and Nab expression constructs. The results showed how the reporter was activated when transfecting the Krox20 expression construct but downregulated when also cotransfecting Nab, which could be modified by the endogenous SUMO1. A more severe downregulation is observed when SUMO1 is also cotransfected, as a high amount of free SUMO1 would be available in this condition. The sole transfection of Krox20 with SUMO1 showed no effect, as

the amount of Nab to be SUMOylated was not changed. Interestingly, the cotransfection of the KR2 mutant with Krox20 resulted in an increased reporter activity, suggesting a dominant-negative effect of the KR2 mutant (Figure R-13).

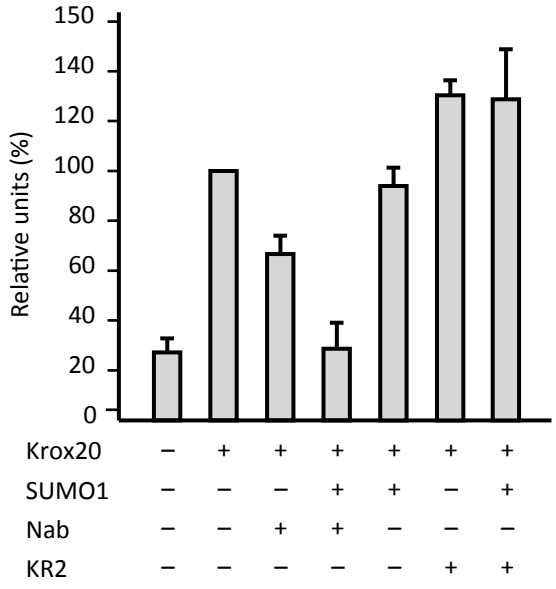

Figure R-13: Nab SUMOylation represses Krox20 transcriptional activity in P19 cells. A *LacZ* reporter under the control of an *EphA4* element, responsive to Krox20, was cotransfected with the indicated expression constructs to analyse the transcriptional activity of Krox20 in P19 cells. Relative units of ß-galactosidase activity were normalized to the values obtained in cells only cotransfected with Krox20. Values represent means ± s.d. of three independent experiments.

To shed light on how SUMOylated Nab modulates Krox20 activity *in vivo*, we decided to perform a functional analysis in the hindbrain. In this embryonic structure, Krox20 regulates various genes during the formation of rhombomeres 3 and 5 (r3 and r5), including itself and Nab genes (Chomette, D *et al.*, 2006; Desmazieres, A *et al.*, 2009; Giudicelli, F *et al.*, 2001; Mechta-Grigoriou, F *et al.*, 2000). Prior to the functional analysis, we thought appropriate to check the expression of Ubc9 in the same territories where Krox20 and Nab express during hindbrain development. In fact, it has been described that Ubc9 expression is regulated during nervous system development in rats (Watanabe, M *et al.*, 2008). To analyse the expression pattern of Ubc9 we turned to the chick embryo and performed *in* situ hybridization experiments using specific riboprobes (see Materials and Methods). As shown in Figure R-14A, *Ubc9* is widely expressed in the whole hindbrain, but higher expression can be observed in the intersections between rhombomeres. Double *in situ* hybridizations were also performed including riboprobes against *Krox20*, which expression is restricted to r3 and r5. Coexpression of both markers can be observed in Figure R-14B. To conform this pattern, immunofluorescence experiments were conducted to analyse the expression of Ubc9

together with EphA4 (Figure R-14C), expressed in r3 and r5 and under the direct control of Krox20 (Theil, T *et al.*, 1998), and the neuron specific marker ßIII-tubulin (Figure R-14D). This last marker reveals progenitors that have differentiated into neurons and that, in the studied developmental stages, mostly appear in even numbered rhombomeres. These results confirmed that Ubc9 is expressed in rhombomeres 3 and 5. A detailed analysis of Ubc9 expression revealed that, as shown in the previous *in situ* hybridization experiments, a higher accumulation of the protein was observed in the frontiers between rhombomeres (Figure R-14E).

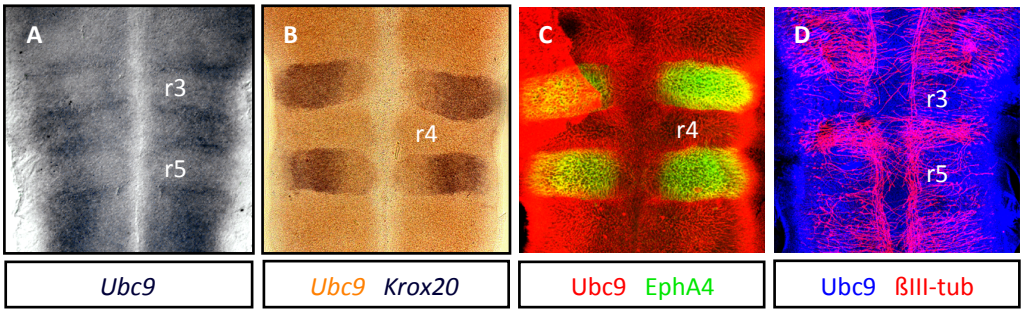

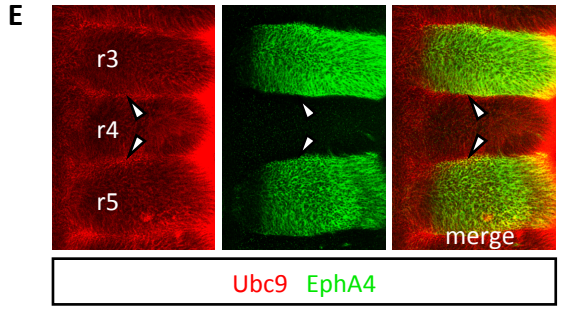

Figure R-14: Expression of Ubc9 in the hindbrain. Flat mounts from the hindbrain of HH13-14 chick embryos processed to analyse the expression of various markers in rhombomeres 3 to 5. **(A, B)** *In situ* hybridization using antisense RNA probes against *Ubc9* (purple) or against Ubc9 (orange) and Krox20 (purple). **(C, D)** Immunofluorescence using antibodies against Ubc9 (red) and EphA4 (green) **(C)** or against Ubc9 (blue) and the neural marker ßIII-tubulin (red) **(D)**. **(E)** Detail of an immuno-fluorescence experiment as described in (C). Rhombomere 4 (r4) marks the limits of EphA4 expression (green) in r3 and r5. Higher expression levels of Ubc9 (red) can be observed in the intersections between rhombomeres (white arrows).

Electroporation of chick embryos allows gain-of-function analysis in the hindbrain (see Materials and Methods). This technic allows the transfection of the neural progenitors from one side of the hindbrain, so that the other side can be used as a control (Itasaki, N *et al.*, 1999). Using this technic, we analysed the effect of Nab and SUMO1 ectopic expression over the expression levels of the marker EphA4 (Figure R-15). Limited repression of EphA4

after electroporation of Nab expression vectors has been previously reported (Desmazieres, A *et al.*, 2009) and was confirmed in our experiments (Figure R-15A, 15B and 15I). Interestingly, we observed that coelectroporation of Nab expression vectors with SUMO expression vectors led to more severe repression (Figure R-15C, 15D and 15I) while the sole electroporation of SUMO1 had no effect (Figure R-15E, 15F and 15I).

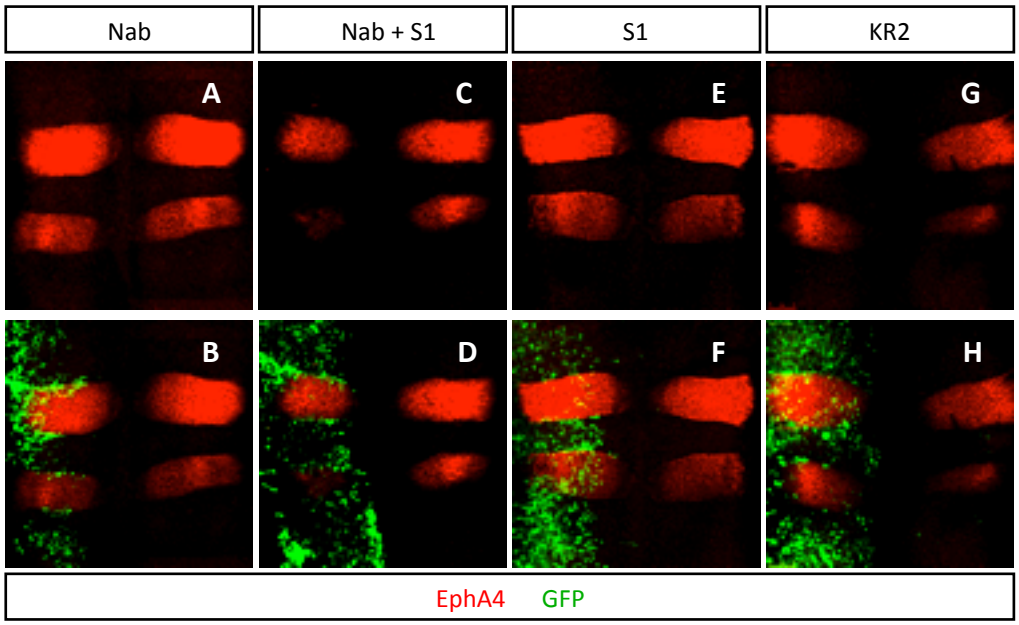

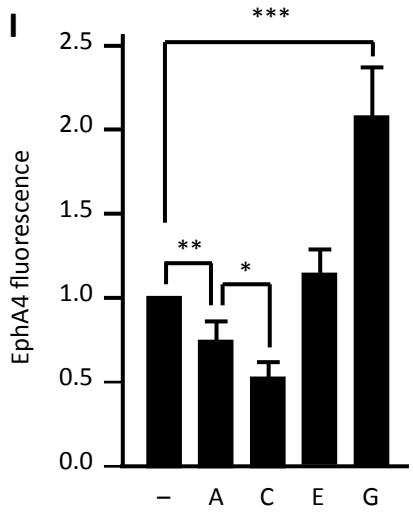

Figure R-15: Nab SUMOylation represses Krox20 transcriptional activity in the chick hindbrain. (A-H) Flat mount of the hindbrain from HH13-14 chick embryos electroporated on the left side with the indicated expression constructs. 24h later, embryos were harvested and immunofluorescence experiments were conducted to analyse the transcriptional activity of Krox20 using EphA4 antibodies (red). To monitor the electroporated side of the hindbrain, a GFP expression vector was included in all the experiments (green). **(I)** Fluorescence intensities of EphA4 were measured in A, C, E and G with MetaMorph software (see Materials and Methods). For this, regions of the same area in r3 and r5 were defined on both electroporated and control sides and intensity values were normalized to the control side (–). Values are means ± s.d. of 5-8 samples from three independent experiments. Statistical significance was analysed using the Student's *t*-test.

To check that these results were due to Nab SUMOylation and not to simultaneous overexpression of Nab and SUMO1, the SUMOylation defective mutant KR2 was tested, showing a very interesting result as EphA4 expression was not reduced but increased in the electroporated side (Figure R-15G, 15H and 15I). This result supports a dominant-negative effect of the KR2 mutant that would compete with wild type Nab for interacting with Krox20. Taking these results into consideration, we decided to further investigate the effects of electroporating the KR2 mutant. Expression analysis of the r4 marker *Hoxb1* together with *EphA4* by double *in situ* hybridization showed that electroporation of the KR2 mutant also resulted in reduced r4 size (Figure R-16A and 16B), possibly associated with aberrant expansion of r3 and/or r5. Finally, we analysed the effects of electroporating the KR2 mutant over *Krox20* expression, as it is described to be self-regulated in a positive way (Chomette, D *et al.*, 2006; Schneider-Maunoury, S *et al.*, 1993). Expression of *Krox20* itself appeared upregulated after KR2 electroporation, similarly to *EphA4* (Figure R-16A and 16B). Together, these data support an involvement of Nab SUMOylation in the repression of Krox20 activity during hindbrain development.

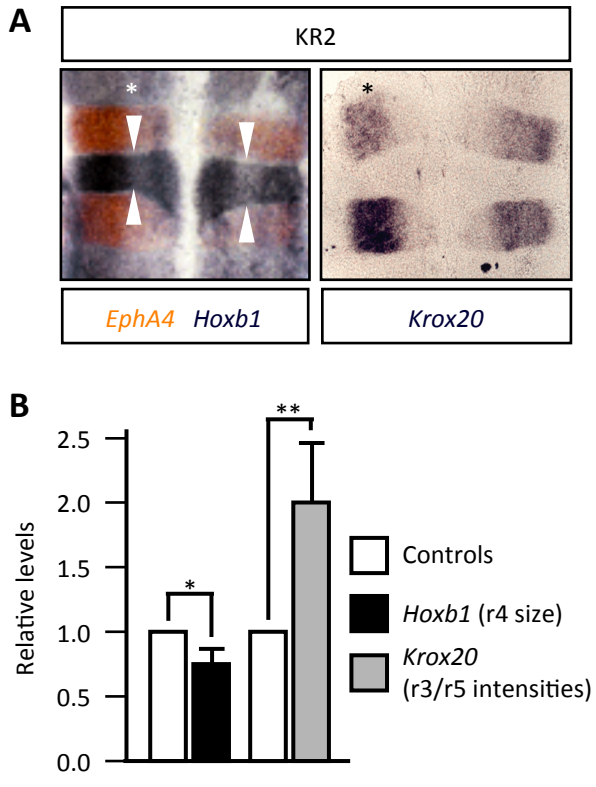

Figure R-16: Nab modification by SUMO1 affects the expansion of r3 and r5. (A) Flat mounts from the hindbrain of HH13-14 chick embryos electroporated on the left side (*) with the Nab KR2 expression construct. Embryos were harvested 24h after electroporation and processed for *in situ* hybridization. Specific antisense RNA probes against *EphA4* (orange), *Hoxb1* and *Krox20* (purple) were utilised to analyse these genes expression and determine the extension of r4 territory (white arrows). **(B)** The size of r4 was measured as the extension of *Hoxb1* expression with ImageJ software and the intensity of *Krox20* expression was measured with MetaMorph software (see materials and Methods). In both cases, signal values of the electroporated sides were normalized to their control sides. Values are means ± s.d. of 5-8 samples from three independent experiments. Statistical significance was analysed using the Student's *t*-test.

4.2 Study of the components of the SUMOylation pathway in the process of neuronal differentiation.

With the aim of studying whether the SUMO modification pathway is implicated in neuronal development, we decided to analyse global SUMOylation and the expression profile of the different pathway components, comparing proliferating and differentiating cells through different approaches.

4.2.1 Retinoic acid-mediated neuronal differentiation results in free SUMO pool changes.

As a first attempt to investigate the involvement of SUMOylation in neuronal differentiation we focused on studying whether the process involves changes in the levels of SUMO conjugation. Thus, we evaluated SUMO conjugation under proliferation and neuronal differentiation conditions. We took advantage of the pluripotent P19 cell line, a mouse teratocarcinoma cell line easy to differentiate into neurons by treating the cells with retinoic acid (RA) (MacPherson, PA *et al.*, 1997) (see Materials and Methods). After four days of treatment, although cells have not achieved terminal differentiation, they have reached an interesting differentiating state, as the pluripotency marker Oct4 is completely downregulated while the neuronal marker ßIII-tubulin starts to be abundantly expressed (Figure R-17A). In immunoblots, together with unconjugated (free) SUMO, SUMO1 and SUMO2/3 antibodies detected a smear of bands of high molecular mass (>70 kDa) corresponding to SUMOylated proteins (Figure R-17A). In addition, Western blots with SUMO1 antibodies showed that SUMOylated RanGAP1 is clearly identified as a band of about 80 kDa. To estimate SUMO conjugation we decided to compare the amount of the unconjugated form in cell extracts prepared under denaturing conditions with the unconjugated form in cell extracts prepared under non denaturing conditions as described in (Sharma, P *et al.*, 2013). Denaturing conditions preserve conjugated SUMO from the action of the endogenous specific proteases. Thus, measured free SUMO in this case corresponds to the naturally existing free SUMO pool. On the other hand, non-denaturing conditions enable SUMO deconjugation from targets. In this case, measured free SUMO corresponds to the total amount present in the cell.

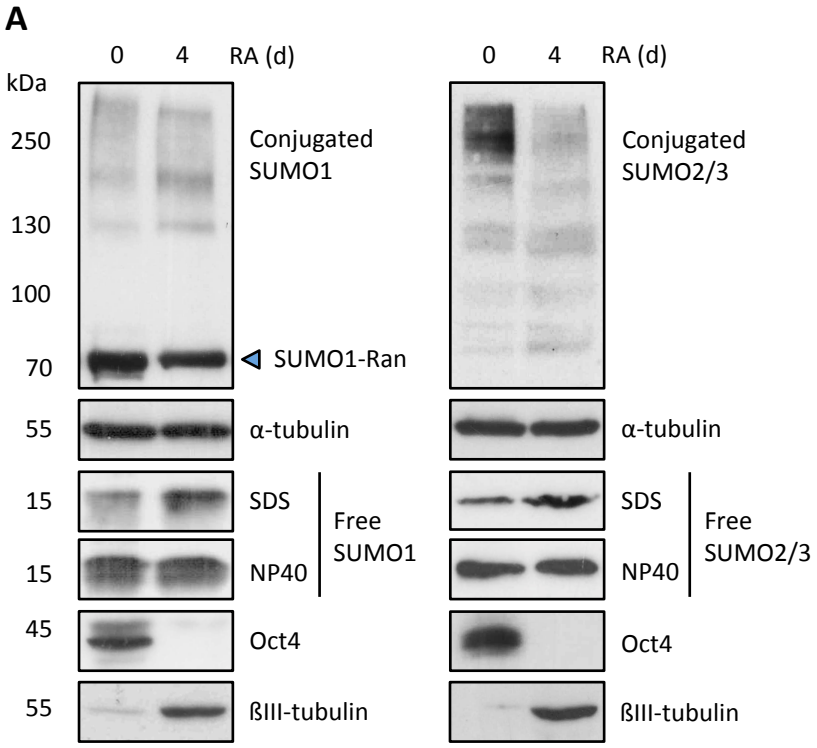

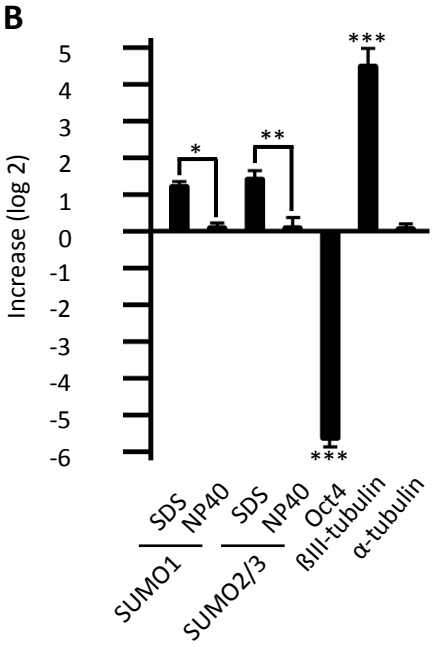

Figure R-17: Neuronal differentiation increases the free SUMO pool available in P19 cells treated with RA. (A) Western blot to analyse the expression of the indicated proteins in P19 cells under proliferative conditions or after 4 days (d) of treatment with retinoic acid (RA). Protein extractions were performed under denaturing conditions to analyse SUMO conjugated products. For analysis of free SUMO, denaturing (SDS) and non-denaturing (NP40) protein extractions were performed (see Materials and Methods). SUMOylated RanGAP1 can be observed in SUMO1 blots (arrowhead). Oct4 and ßIII-tubulin were visualized as controls of the differentiation process, while α-tubulin was visualized as a loading control. 20 µg of total protein were loaded per lane. **(B)** Quantification of the increase in expression levels of the indicated proteins from proliferation to 4d of RA treatment. Values are means from three independent experiments ± s.d. Statistical analysis of the changes in free SUMO pools between denaturing and non-denaturing conditions, as well as Oct4 and ßIII-tubulin changes, were analysed by the Student's *t*-test.

Interestingly, RA-treated cells exhibited a 2-fold increase in both free SUMO1 and SUMO2/3 pools as detected under denaturing conditions, while no changes were observed in total SUMO as measured under non-denaturing conditions (Figure R-17). Increase in free SUMO1 mostly correlated with reduced levels of SUMOylated RanGAP1. By contrast, increase in free SUMO2/3 correlated with a decrease in SUMO2/3 high molecular mass bands. Thus, our results indicate that although global levels of SUMO1 and SUMO2/3 seem not to be altered by RA treatment, differentiation correlates with appreciable net deconjugation of both molecules.

4.2.2 SUMO overexpression impairs neuronal differentiation.

As a next step in assigning a role to SUMO modification in neuronal differentiation, we decided to analyse how neurogenesis proceeds when globally altering SUMOylation. For that purpose, we chose to investigate the effect of SUMO overexpression on the process. We first checked by Western blot that SUMO1 and SUMO2 overexpression resulted in enhanced SUMOylation in P19 cells, as can be observed in Figure R-18.

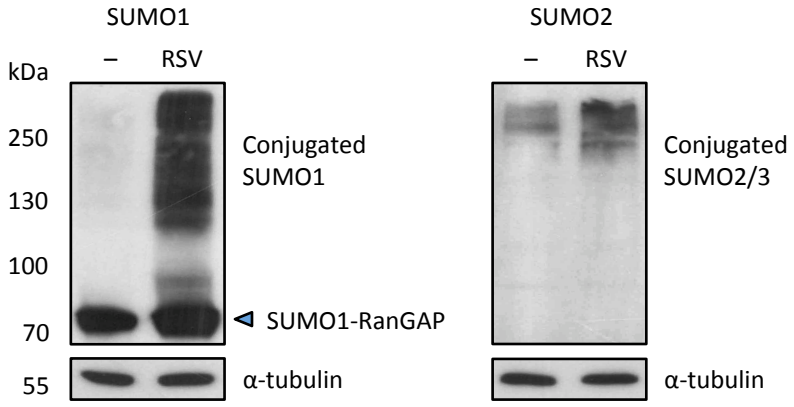

Figure R-18: Increase of SUMOylated proteins after transfection of SUMO expression constructs in P19 cells. P19 cells were transfected with the indicated expression constructs for SUMO1 and SUMO2 and, after cell harvesting, denaturing protein extracts were analysed by western blot with SUMO1 and SUMO2/3 antibodies. An increase in SUMOylated products was detected when cells transfected with SUMO (RSV) were compared to control cells transfected with empty vector (–). Western blot with SUMO1 antibody also shows an increase in SUMOylated RanGAP. Blots using α-tubulin antibody are shown as loading controls. 20 μg of total protein were loaded per lane.

A well-established model for quantification of neurogenesis in P19 cells consists on estimating the proportion of cells expressing the neuronal marker ßIII-tubulin among cells transfected with expression constructs for the neurogenic factor NeuroD2 and its cofactor E12 that lead to their differentiation (Farah, MH *et al.*, 2000; Garcia-Gutierrez, P *et al.*, 2012). To monitor transfected cells, a GFP expression vector was routinely included in transfections. With this approach and as shown in Figure R-19, we could observe that about 61% of transfected cells expressed the neural specific marker ßIII-tubulin 72 h after transfection, in agreement with previous reports (Garcia-Gutierrez, P *et al.*, 2014; Garcia-Gutierrez, P *et al.*, 2012).

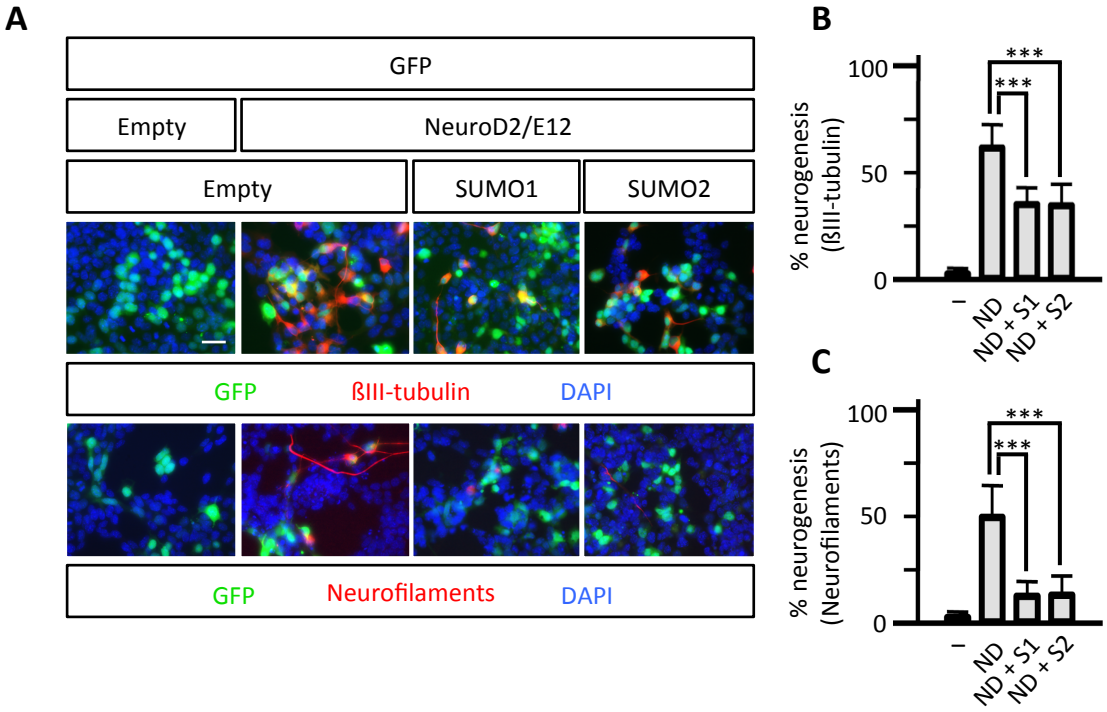

Figure R-19: SUMO overexpression interferes with P19 neuronal differentiation. (A) Immunofluorescence experiments on P19 cells transfected with expression constructs for NeuroD2 and its cofactor E12, to induce neuronal differentiation, or with empty vector. SUMO1 or SUMO2 expression constructs or their corresponding empty vector were also cotransfected when indicated. A GFP expression vector was also included to monitorize transfected cells (green). ßIII-tubulin or Neurofilaments antibodies were used to analyse neuronal differentiation (red) and DNA was counterstained with DAPI (blue). Scale bar 20 µm. **(B)** Quantification of neuronal differentiation in transfected cells was obtained as the percentage of transfected cells that expressed GFP (green) that also expressed the analysed neuron specific marker (red). Values are means of quantifications from 30 areas in total from three independent experiments. Statistical analysis was performed by the Student's *t*-test.

However, when also including SUMO1 or SUMO2 expression constructs in transfections, the proportion of ßIII-tubulin positive cells fell to 34% (Figures R-19A and 19B), indicating that overexpressing SUMO impaired neuronal differentiation. Similar results were obtained when analysing Neurofilaments, another neuronal marker (Figures R-19A and 19C). To confirm these observations in a more physiological context, we turned to the developing neural tube of vertebrate embryos, where neural progenitors exiting the cell cycle undergo migration from the proliferative compartment or ventricular zone (VZ) to the differentiation compartment or mantle layer (ML), coupled to the onset of neuronal markers expression.

Electroporation of the chick neural tube enables transfection of progenitors close to the lumen in one side of the tube to perform gain- and loss-of-function experiments. As Figure R-20 shows, the percentage of neurogenesis can also be estimated in this model by electroporating the progenitors with a reporter construct and quantifying cells that, after migrating to the ML, coexpress the reporter and neuron specific markers, over the total amount of cells expressing the reporter.

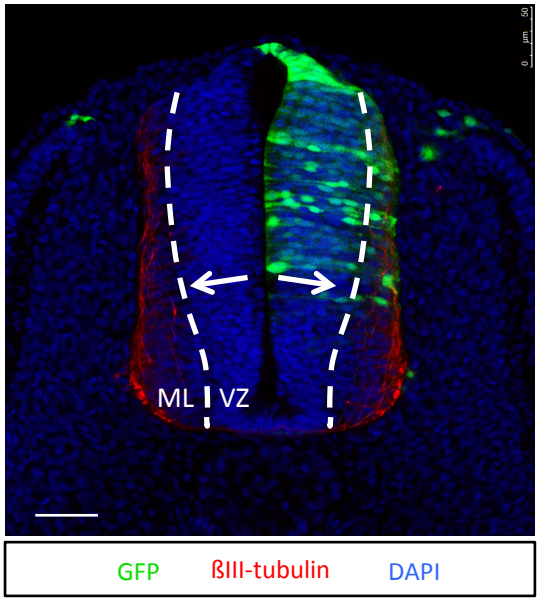

Figure R-20: Quantification of neuronal differentiation in the chick neural tube. Neural progenitors are electro-porated with a GFP expression vector (green). The neural progenitors eventually start to migrate from the ventricular zone (VZ) to the mantle layer (ML) as indicated by the white arrows, while they get differentiated and start ex-pressing the neural marker ßIII-tubulin (red). GFP positive cells that coexpress the neural marker and localize to the ML are quantified and relativized to the total amount of cells that express GFP in both compartments separated by a dashed line (VZ and ML). Scale bar 50 µm. DNA is counterstained with DAPI (blue).

In our case, electroporation of a GFP expression construct at the thoracic level indicated that 30 h after electroporation, about 23% of transfected progenitors migrated from the VZ to the ML and expressed the neuronal marker ßIII-tubulin (Figures R-21A and 21B). Thus, 23% of cells electroporated with the reporter naturally differentiated into neurons after 30 h. However, when an expression construct for a neurogenic factor, for

instance Neurogenin2, was incorporated in the electroporation experiment, up to 87% of reporter-positive cells got differentiated. We then analysed the effect of also incorporating SUMO1 or SUMO2 expression constructs, and observed that in the presence of Neurogenin2, SUMO1 and SUMO2 reduced neurogenesis from 87 to 33 and 42%, respectively (Figures R-21A and 21B).

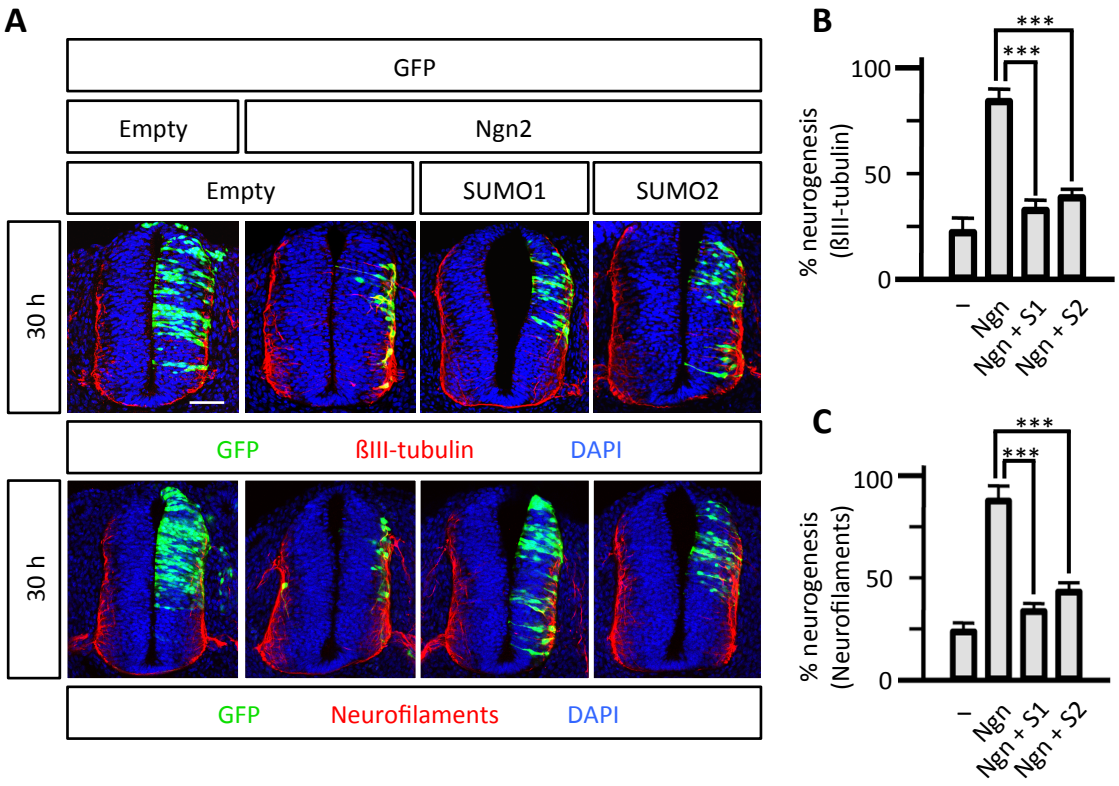

Figure R-21: SUMO overexpression interferes with neuronal differentiation in the chick neural tube. (A) The neural tube of chick embryos at stage HH17 was electroporated on the right side with empty vector or an expression construct for Neurogenin2 (Ngn2) to induce neurogenesis. SUMO1 or SUMO2 expression constructs or their corresponding empty vector were coelectroporated when indicated and a GFP expression vector was also included to monitorize the electroporated side of the neural tube (green). Neurogenesis was analysed 30h after electroporation by immunofluorescence on transverse sections of the neural tube using antibodies for neuron specific markers ßIII-tubulin or Neurofilaments (red). DNA was counterstained with DAPI (blue). Electroporated cells that expressed GFP and were differentiating into neurons were identified by localization to the mantle layer (ML) and expression of the neuron specific markers. Scale bar 50 µm. **(B, C)** Quantification of neurogenesis in (A) obtained as the percentage of GFP positive cells (green) that have migrated from the proliferative compartment or ventricular zone (VZ) to the differentiated compartment (ML) and that express ßIII-tubulin **(B)** or Neurofilaments **(C)**. Values are means ± s.d. obtained by quantifying cells of a total of 6 sections from 2 independent experiments. Statistical analysis was performed using the Student's *t*-test.

Analysis of Neurofilaments also confirmed these results (Figures R-21A and 21C). To investigate whether SUMO overexpression in fact interferes with neuronal differentiation rather than simply delaying it, we also analysed effects of SUMO overexpression 40 h after electroporation. Results were similar to those obtained at 30 h (Figure R-22), supporting an impairment of the process rather than a delay. These results confirm in an animal model that overexpressing SUMO interferes with neuronal differentiation.

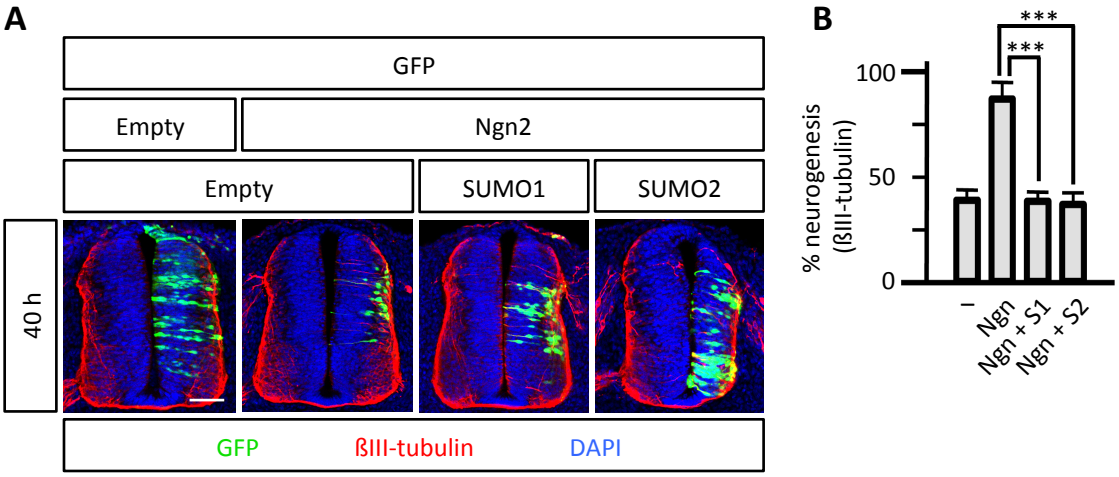

Figure R-22: SUMO overexpression impairs neuronal differentiation rather than delaying it. (A) The neural tube of chick embryos at stage HH17 was electroporated on the right side as previously shown in Figure R-21. Neurogenesis was analysed 40h after electroporation by immunofluorescence on transverse sections of the neural tube using ßIII-tubulin antibodies (red). DNA was counterstained with DAPI (blue). Electroporated cells that expressed GFP and were differentiating into neurons were identified by localization to the mantle layer (ML) and expression of the neuron specific marker ßIII-tubulin. Scale bar 50 µm. **(B)** Quantification of neurogenesis in (A) obtained as the percentage of GFP positive cells (green) that have migrated from the proliferative compartment or ventricular zone (VZ) to the differentiated compartment (ML) and that express ßIII-tubulin. Values are means ± s.d. obtained by quantifying cells of a total of 6 sections from 2 independent experiments. Statistical analysis was performed using the Student's *t*-test.

4.2.3 Neuronal differentiation proceeds without significant changes in gene expression of SUMO ligases and basic pathway components.

As the previous results showed that SUMOylation is altered during neuronal differentiation, it seemed appropriate to investigate the components of its modification pathway during this process. For this purpose, we undertook a gene expression analysis of the basic components of the SUMOylation pathway and SUMO ligases of the PIAS family.

The RA differentiation protocol of P19 cells involves two periods of two days in which cells are treated with RA in non-adherent dishes, where they form embryonic bodies, plus a period of three days in which cells are disaggregated and cultured in adherence without RA. At this point, cells have reached an advanced differentiation state and have extended dendrite and axon-like processes. Thus, 0, 2, 4 and 7 days appeared as relevant points for the analysis of neuronal differentiation (Figure R-23).

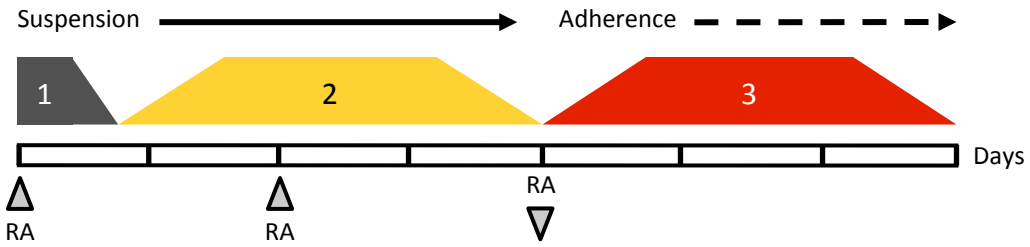

Figure R-23: RA treatment to induce neural differentiation of P19 cells. P19 cells are cultured in suspension with low serum and RA supplemented medium to induce the initial response (1). Cells are grown in these conditions during four days (with RA replacement at day 2) in which they form embryoid bodies and the initial differentiation takes place (2). Finally, P19 cells are disaggregated and plated in adherence and grown in complete medium without RA to reach the terminal differentiation, in which axon and dendrite like processes start to extend (3).

After designing oligonucleotides coding regions of genes corresponding to different components of the SUMO modification pathway from mouse (see Table M-6) real-time PCR analysis showed in Figure R-24 (see Materials and Methods) indicated that genes coding for *Sumo1*, *Sumo2* and *Sumo3* were not significantly altered along the differentiation protocol. Those coding for other basic components of the SUMOylation pathway, notably monomers

of the E1 heterodimer *Sae1/Uba2* and the conjugating enzyme *Ubc9* similarly did not show significant differences (Figure R-24). Regarding genes coding for PIAS ligases, some of them showed a progressive increase along differentiation, with maximum levels at 7 days, and not exceeding a 3-fold increase in any case. As a control of the cellular differentiation process, the pluripotency gene *Oct4* appeared drastically downregulated at day 2, while high expression levels of the neuronal ßIII-tubulin gene (*Tubb3*) were detected from day 4 (Figure R-24). Hence, gene expression analysis indicates that genes coding for SUMO molecules and basic components of the SUMOylation pathway are not significantly subjected to regulation along the neuronal differentiation protocol in P19 cells, while some PIAS ligases genes are moderately upregulated.

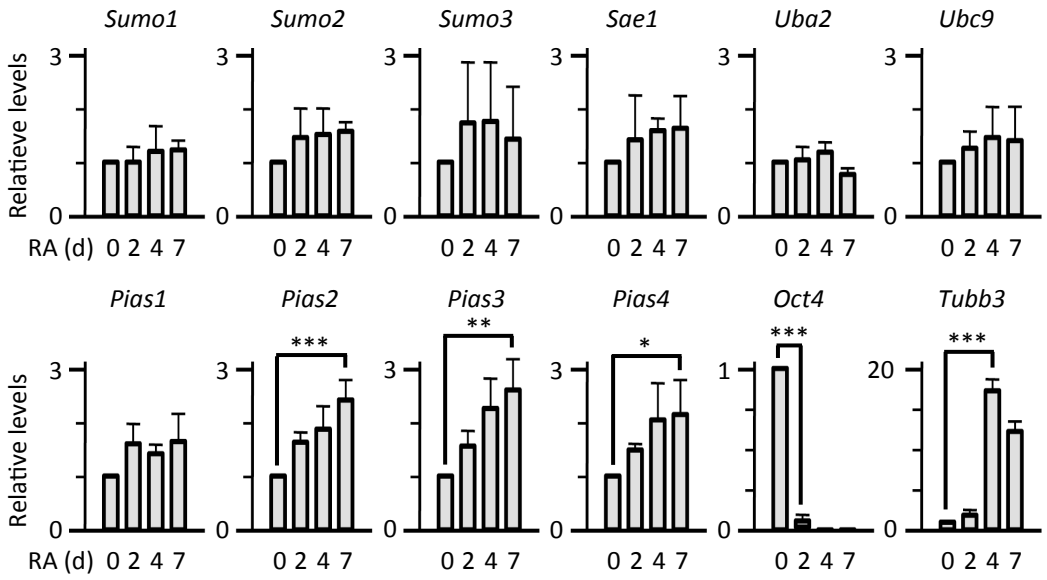

Figure R-24: Expression analysis of PIAS ligases and basic components of the SUMOylation machinery during P19 neuronal differentiation with RA treatment. Real-Time PCR determined relative expression levels of the indicated genes. P19 cells were harvested after the following conditions: 2 or 4 days (d) of RA treatment in suspension, and 4 days of RA treatment in suspension following growth on adherent dishes for 3 more days (7). Proliferative cells grown in adherence were also harvested as t = 0 (0). Expression levels were normalized to the levels at 0 days. Values are means ± s.d. of three independent experiments in duplicate. Note that Y-axis for *Oct4* and *Tubb3* are different from the rest of genes. Statistical significance of changes in gene expression was analysed by the Student's *t*-test, and P-values for *Pias2*, *Pias3*, *Pias4* and *Tubb3* upregulation, as well as for *Oct4* downregulation, were indicated.

4.2.4 The SUMO proteases Senp5 and Senp7 are upregulated during neuronal differentiation.

We continued our gene expression analysis by looking at genes coding for SUMO proteases. For that purpose, we investigated the six members of the SENP family (*Senp1-3*, *5-7*) and one member of the more recently described DeSI family of proteases, *Desi1* (Shin, EJ *et al.*, 2012). Results indicated that expression levels of most of the analysed genes remained quite unaltered along the differentiation protocol, with the surprising exception of *Senp5* and *Senp7*. *Senp5* expression progressively augmented to reach a 9-fold increase at day 7 (Figure R-25A). In contrast, Senp7 levels picked at day 4, displaying a 16-fold increase if compared with day 0, and dropping slightly at day 7 (Figure R-25A). As *Senp7* gene expression displayed the highest variation following induction of neuronal differentiation, we chose to further investigate it.

We first studied whether increased gene expression correlated with increased protein levels. Western blot experiments demonstrated a 4.3- fold increase in protein levels at day 4, which decreased to 2.8-fold by day 7 (Figures R-25B and 25C). As controls, we confirmed downregulation of Oct4, upregulation of ßIII-tubulin and no changes in α-tubulin (Figures R-25B and 25C). To exclude that the obtained results were due to a direct effect of RA rather than the process of neuronal differentiation, we confirmed upregulation of Senp7 also when applying the neuronal differentiation protocol involving transfection of the neurogenic factor NeuroD2 and its cofactor E12 (Figure R-26). As an additional control, Senp3 levels were also checked and no differences were observed between days 0 and 4 (Figure R-26). Altogether, these results show that both mRNA and protein levels of Senp7 are upregulated following induction of neuronal differentiation in P19 cells.

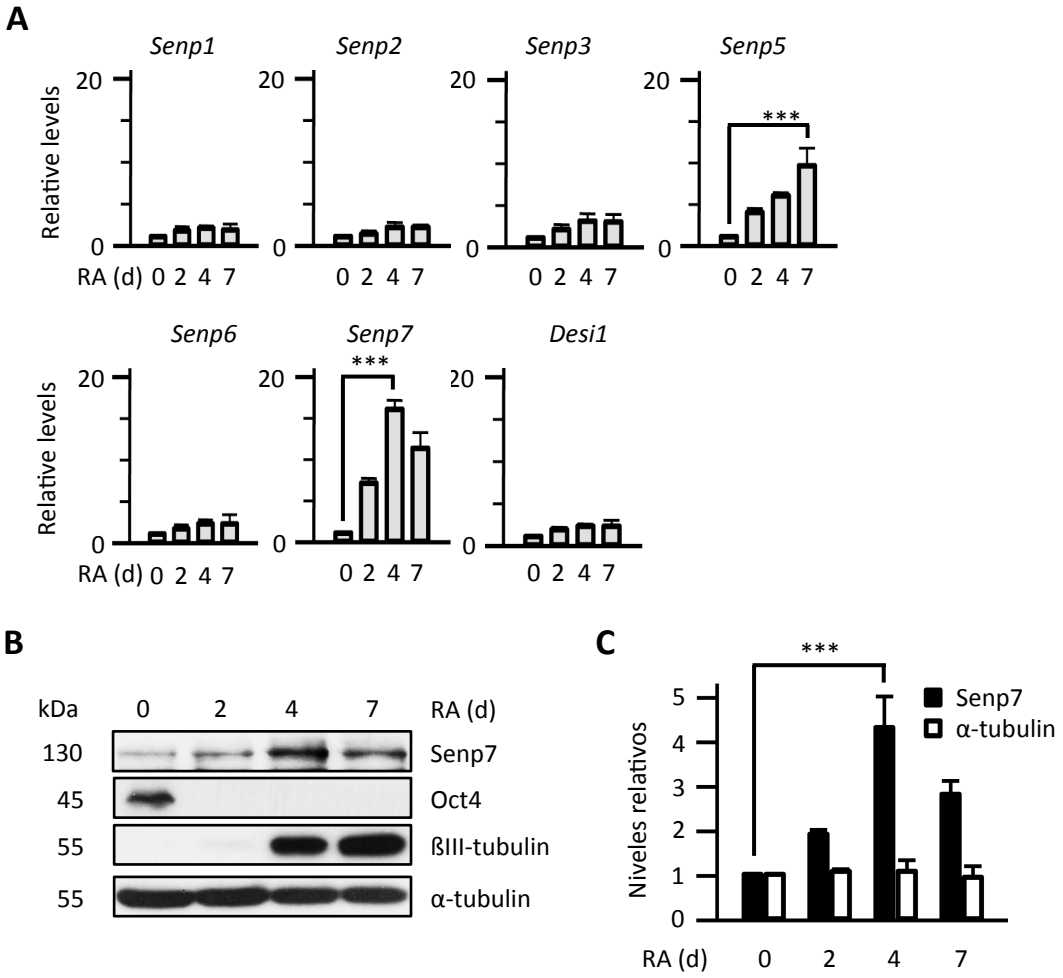

Figure R-25: Senp5 and Senp7 are upregulated during P19 neuronal differentiation by RA treatment. (A) Real-Time PCR determined relative expression levels of the indicated SUMO proteases genes. P19 cells were treated as previously indicated in Figure R-24. Expression levels were normalized to the levels at 0 days. Values are means ± s.d. of three independent experiments in duplicate. Statistical significance of changes in gene expression was analysed by the Student's *t*-test, and P-values for *Senp5* and *Senp7* upregulation were indicated. **(B)** Protein levels of Senp7 were analysed by Western blot along the differentiation protocol applied in (A). Levels of Oct4 and ßIII-tubulin were determined as controls for neurogenesis. Blots for α-tubulin are also included as a loading control. 20 µg of total protein were loaded per lane. **(C)** Relative levels of Senp7 protein as quantified in (B). Protein levels were normalized to the level at 0 days. Values are means ± s.d. from four independent experiments. Statistical significance of this experiment was analysed by the Student's *t*-test and P-value for the increase at day 4 with respect to day 0 was indicated.

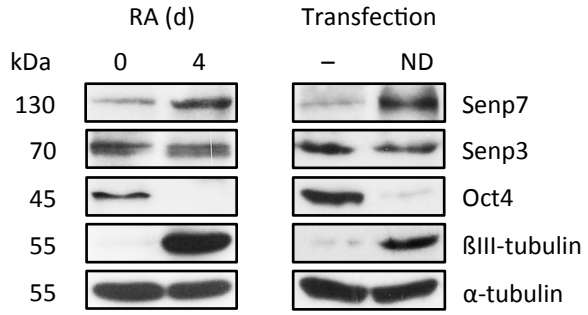

Figure R-26: Both RA treatment and over-expression of neurogenic factor NeuroD2 upregulate Senp7. Senp7, Senp3, Oct4, ßIII-tubulin and α-tubulin protein levels were analysed by Western blot in P19 cells treated with RA for 0 or 4 days (d) (left), or in P19 cells transfected with empty vector (−) or expression constructs for NeuroD2 and E12 (ND) for 3 days (right). 20 µg of total protein were loaded per lane.

4.2.5 Senp7 is required for proper neuronal differentiation.

To functionally investigate the role of Senp7 in neuronal differentiation, we opted for a loss of-function approach. Thus, we generated expression constructs for short hairpin RNA (shRNA) molecules in order to knockdown *Senp7* by RNA interference in P19 cells. We generated two different molecules targeting *Senp7* and both performed equally in knocking down the SUMO protease and in the first experiments of the functional characterization, so results presented correspond to one of these molecules (shRNA mouse *Senp7*#1) (see Table M-4). In P19 cells under proliferation, *Senp7* showed basal expression levels that were lessened to a 33% in cells transfected with the shRNA molecule against *Senp7*, compared to a control shRNA (Figures R-27A and 27C). As *Senp7* upregulation was detected after induction of neuronal differentiation, we decided to also check *Senp7* knocking down by cotransfection of the shRNA against *Senp7* in addition to NeuroD2 and E12. It was under these neuronal differentiation conditions that a 10-fold reduction in the SUMO protease expression was observed when compared to cotransfection of a Control shRNA construct and the neurogenic factors (Figures R-27B and 27D). We then turned to analyse the possible effects that *Senp7* knocking down could have over SUMOylated products accumulation under neuronal differentiation conditions. While no appreciable differences were observed in free and conjugated SUMO1 levels when comparing effects of Control and *Senp7* shRNA molecules under neuronal differentiation conditions, a clear effect on SUMO2/3 conjugation

was observed. Thus, under neuronal differentiation conditions, *Senp7* shRNA preserved high molecular mass products from deconjugation in comparison with Control shRNA, which correlated with no increase in free SUMO2/3 (Figure R-28).

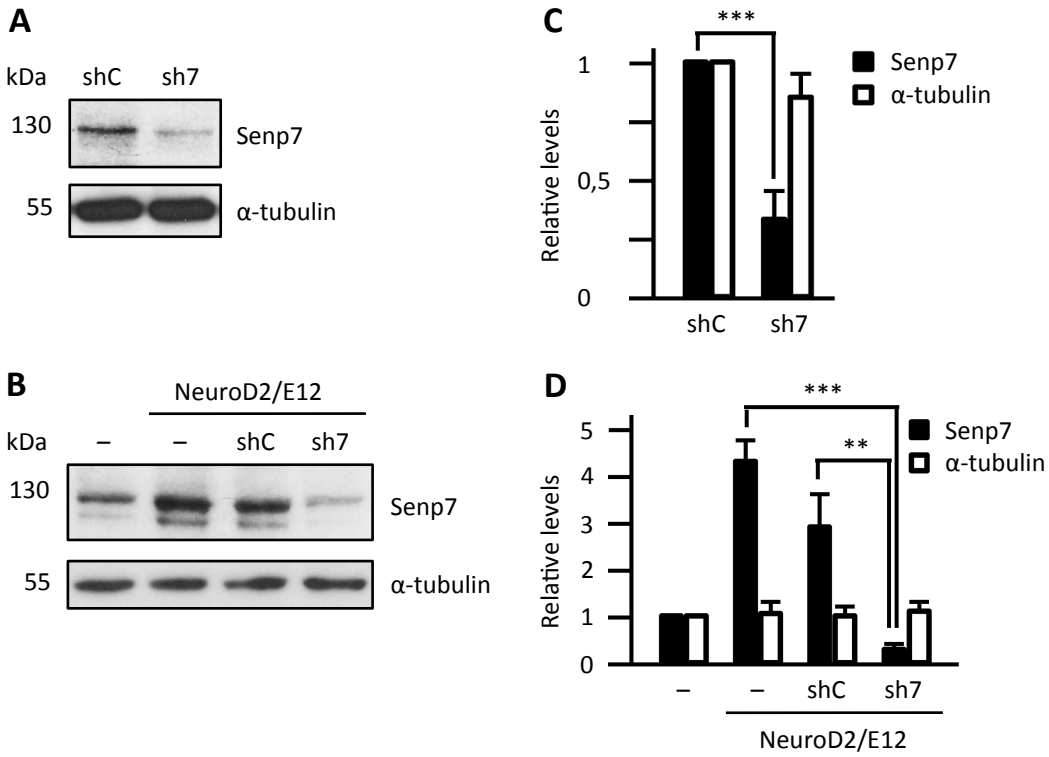

Figure R-27: Senp7 knockdown during P19 neuronal differentiation. (A) P19 cells growing under proliferative conditions were transfected with either control shRNA (shC) or Senp7 shRNA (sh7) expression constructs, and Senp7 protein levels were analysed 72h after transfection by western blot. **(B)** P19 cells were transfected with NeuroD2 and E12 expression constructs or with the corresponding empty vector (–). Cells transfected with NeuroD2 and E12 expression constructs were cotransfected with either control shRNA (shC) or Senp7 shRNA (sh7) expression constructs, or with the corresponding empty vector (–). Senp7 levels were analysed 72h after transfection by Western blot. **(A, B)** α-tubulin was revealed as a loading control. 20 µg of total protein were loaded per lane. **(C, D)** Quantification of relative protein levels determined in (A) and (B), respectively. Protein levels in (C) were normalized to the levels of cells transfected with the control shRNA construct. Protein levels in (D) were normalized to the levels of cells transfected with empty vectors. Values are means ± s.d. of two independent experiments. Statistical significance of Senp7 knockdown by the Senp7 shRNA with respect to control shRNA in (C) and with respect to Control shRNA or empty vector in (D) was analysed by the Student's *t*-test.

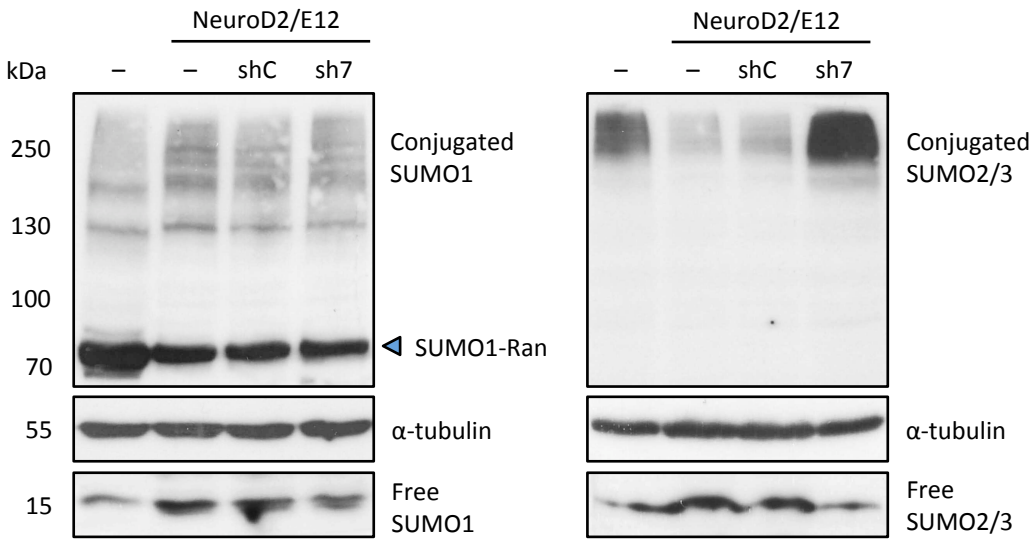

Figure R-28: Senp7 knockdown prevents deconjugation of SUMO2/3 during P19 neuronal differentiation. Effect of *Senp7* shRNA compared to control shRNA on SUMO1 (left) and SUMO2/3 (right) conjugation was verified by Western blot of denaturing protein extracts from P19 cells transfected as indicated in Figure R-27B. α-tubulin was revealed as a loading control. Arrowhead indicates SUMOylated RanGAP1 (Ran) on SUMO1 blot. 30 µg of total protein were loaded per lane.

We then performed a neurogenesis analysis similar to the one previously described (Figures R-19 and R-21). Thus, NeuroD2/E12-induced neurogenesis in P19 cells corresponded to 61% of transfected cells and interestingly dropped to 27% when cotransfecting an expression construct for *Senp7* shRNA, while no significant effects were observed when using a Control shRNA expression construct (58% of neurogenesis) (Figures R-29A and 29B). We also developed two different molecules targeting the chick *Senp7* sequence. Both molecules also performed equally in the loss-of-function analysis so results presented correspond to one of these molecules (shRNA chick *Senp7*#1) (see Table M-4). The obtained results indicated that when electroporating chick *Senp7* shRNA, Neurogenin2-promoted differentiation was significantly impaired, while a Control shRNA molecule had no effect. The use of *Senp7* shRNA lessened neurogenesis to 40%, while almost 80% was observed in the presence of Control shRNA (Figures R-29C and 29D). Thus, induced neurogenesis by overexpression of neurogenic factors, both in P19 cells and in chick embryos, is severely compromised by *Senp7* knock-down.

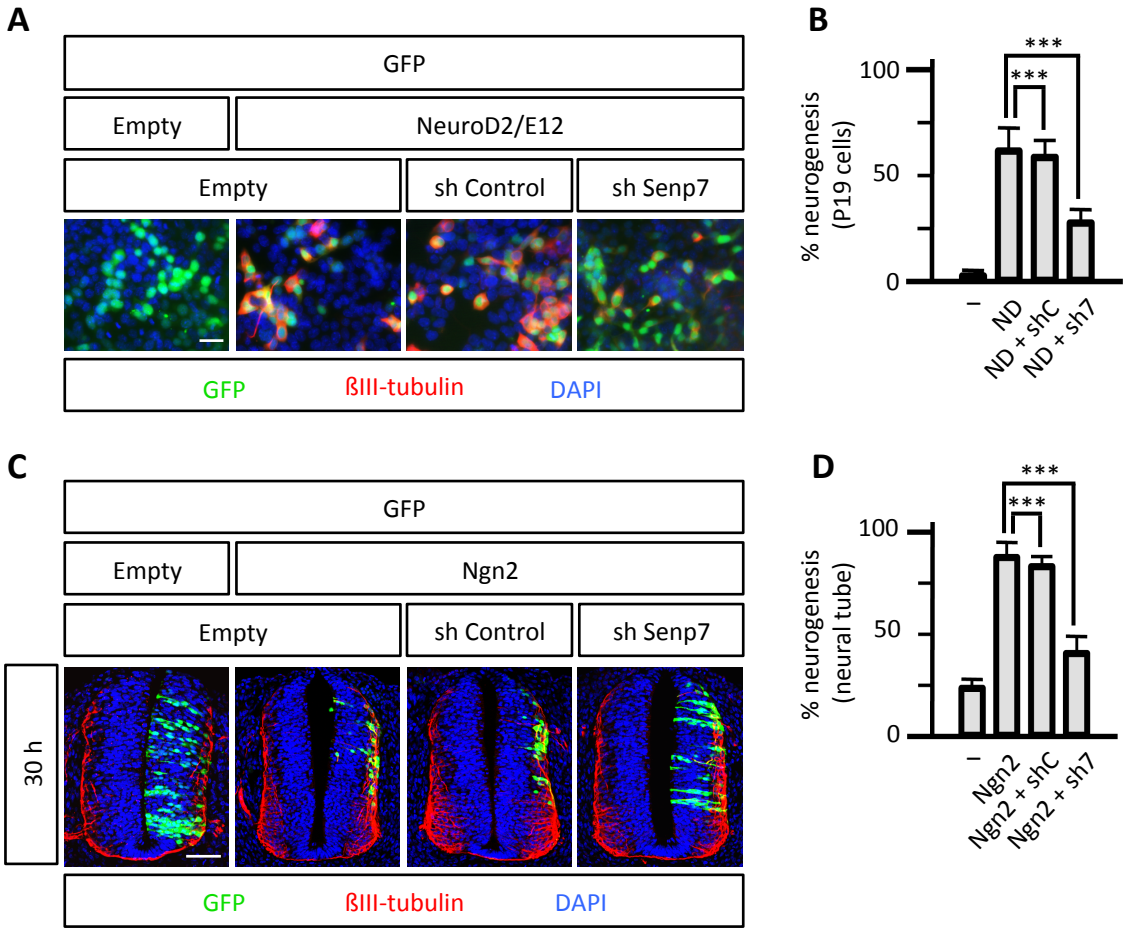

Figure R-29: Senp7 knockdown impairs neuronal differentiation in both P19 cells and chick neural tube. (A) P19 cells were transfected with empty vector or expression vectors for NeuroD2 and E12 to induce neuronal differentiation, together with expression constructs for Senp7 shRNA (sh Senp7) or control shRNA (sh Control) molecules, or the corresponding empty vector. Transfected cells were monitored by expression of a GFP expression vector (green) and those differentiating into neurons were revealed by expression of the neuron specific marker ßIII-tubulin (red). DNA was counterstained with DAPI (blue). Scale bar 20 µm. **(B)** Quantification of the % of neurogenesis of the analysis in (A) as the proportion of GFP positive cells (green) expressing the ßIII-tubulin marker (red). Values are means± s.d. obtained by counting cells from a total of 30 areas of 3 independent experiments. Statistical significance of the effect of the Senp7 shRNA construct on neuronal differentiation with respect to Control shRNA or empty vector was analysed by the Student's t-test. **(C)** The neural tube of chick embryos at stage HH17 was electroporated on the right side with empty vector or an expression vector for Neurogenin2 (Ngn2) to induce neuronal differentiation, together with expression constructs for Senp7 shRNA, control shRNA or the corresponding empty vector. Neurogenesis was evaluated by immunofluorescence after 30h on transverse sections of the spinal cord. Electroporated cells were monitored by expression of a GFP reporter (green) and those differentiating into neurons were identified by localization to the ML and expression of the neuronal

marker ßIII-tubulin (red). DNA was counterstained with DAPI (blue). Scale bar 50 µm. **(D)** Quantification of the % of neurogenesis of the analysis in (C) as the percentage of the GFP positive cells (green) that have migrated to the ML and express the neuronal marker ßIII-tubulin (red). Values are means ± s.d. obtained by counting cells in a total of 6 sections from 2 independent experiments. Statistical significance of the effect of the Senp7 shRNA construct on neuronal differentiation with respect to Control shRNA was analysed by the Student's *t*-test.

4.2.6 The Senp7 promoter is transiently activated following induction of neuronal differentiation.

To get insights into the way Senp7 responds to induction of neuronal differentiation, we performed an *in vivo* reporter analysis in the developing neural tube. Thus, we decided to analyse reporter activation of a GFP construct driven by the 5' upstream region of the *Senp7* gene, encompassing the *Senp7* promoter (S7p). To this end, we compared expression of this construct (S7p-GFP) with that of a GFP driven by the constitutive promoter CMV (CMV-GFP) in electroporation experiments on the chick neural tube. We initially used the human S7p sequence, as it was available in our laboratory. In all the experiments, transfected cells were monitored by expression of the mCherry protein driven by a CMV promoter (CMV-mCherry). This expression construct was coelectroporated with the GFP constructs (Figure R-30) and analysed 10-20 h after electroporation.

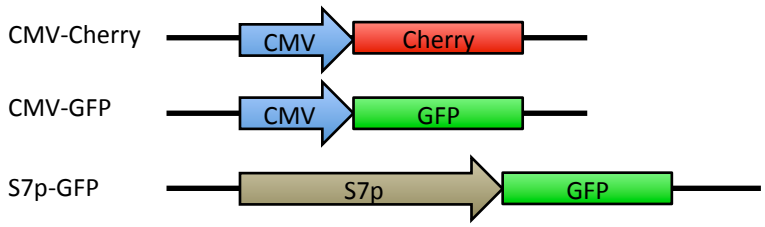

Figure R-30: Schematic representation of the reporter constructs used to analyse the activation of *Senp7* expression during neurogenesis. GFP or monomer Cherry reporters were placed under the control of the constitutive CMV promoter (CMV) and GFP reporter was also placed under the control of the promoter region of the human *Senp7* gene (S7p).

As illustrated in Figure R-31A, while virtually all cells expressing mCherry also expressed GFP when expression of this last was driven by the CMV promoter, very few of the mCherry positive cells displayed GFP when its expression was driven by the S7p sequence. In addition, these GFP positive cells seemed to localize to the ML, as revealed by detection of the ML-associated marker ßIII-tubulin (Figure R-31B). These results may indicate that the *Senp7* promoter is activated in a subset of differentiating neurons. However, these results may also indicate that the *Senp7* promoter is early and transiently activated in differentiating neurons so that at the time of the analysis the reporter starts to be downregulated. To shed light on the way that *Senp7* promoter is activated, we analysed reporter activation following induction of neurogenesis. We tested Neurogenin2 as well as NeuroM, as both are early neurogenic factors (Bertrand, N *et al.*, 2002; Roztocil, T *et al.*, 1997). Twenty hours after coelectroporation of the GFP reporter and the indicated constructs in Figure R-31C, very few of the mCherry positive cells displayed GFP even in the presence of neurogenic factors. However, 10 h after electroporation, a high number of mCherry positive cells were also GFP positive (Figure R-31C) when expression constructs for neurogenic factors were coelectroporated, confirming neurogenesis-mediated activation of the reporter and pointing to its early and transient expression in differentiating neurons. Although most mCherry positive cells did not exhibit GFP 20 h after electroporation, they massively localized to the pial surface, indicative of neuronal differentiation driven by the neurogenic factors. We confirmed former results using the chick Senp7 promoter (Figure R-32). Hence, under naturally occurring neurogenesis, a reduced number of electroporated neuronal progenitors activate the S7P-GFP reporter 10 or 20 h after electroporation. However, when inducing neurogenesis, very early (10 h after electroporation) and massive activation of the reporter was observed, to be switched off soon after (20 h after electroporation), indicating transient activation of the reporter in differentiating neurons.

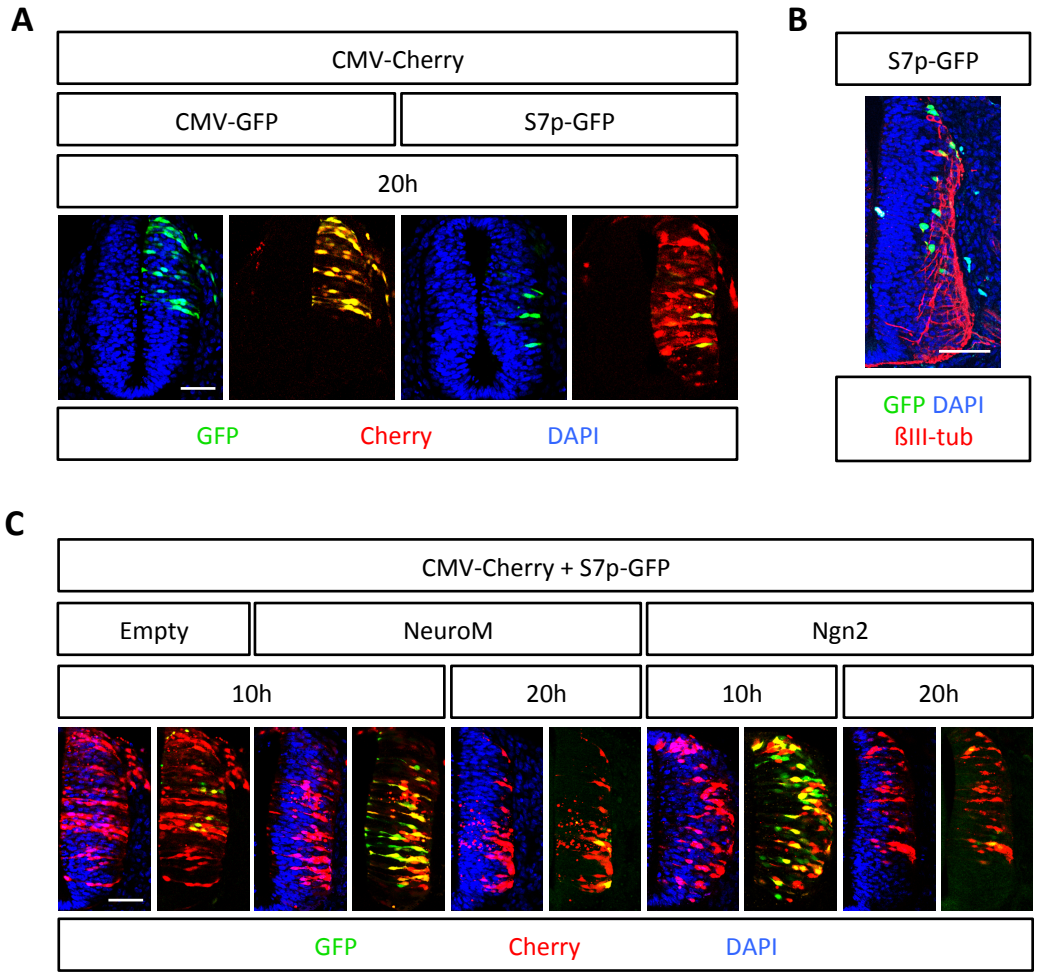

Figure R-31: human *Senp7* promoter is early and transiently activated in neurogenesis. (A) The neural tube of chick embryos at stage HH17 was electroporated on the right side with the indicated reporter constructs, and reporter activation of CMV-GFP or S7p-GFP (green) constructs was compared 20h after electroporation by immunofluorescence. A CMV-Cherry (red) expression vector was also included in both experiments to monitor electroporated cells. **(B)** Analysis of the localization of cells in which the S7p-GFP reporter (green) was active and expressed the neuron specific marker ßIII-tubulin (red). **(C)** Activation of the S7p-GFP reporter construct (green) was analysed under induced neurogenesis, 10 and 20h after coelectroporation with expression constructs for the neurogenic factors NeuroM or Neurogenin2 (Ngn2), as indicated. The corresponding empty vectors were electroporated as a control of natural-occurring neurogenesis and analysed 10 h after electroporation. A CMV-Cherry expression vector was included in all the experiments to monitor the electroporated cells (red). **(A-C)** DNA was counterstained with DAPI (blue). Two different merged combinations of the different channels are shown for each experiment in (C): DAPI and Cherry (left) or GFP reporter and Cherry (right). Scale bars 50 µm.

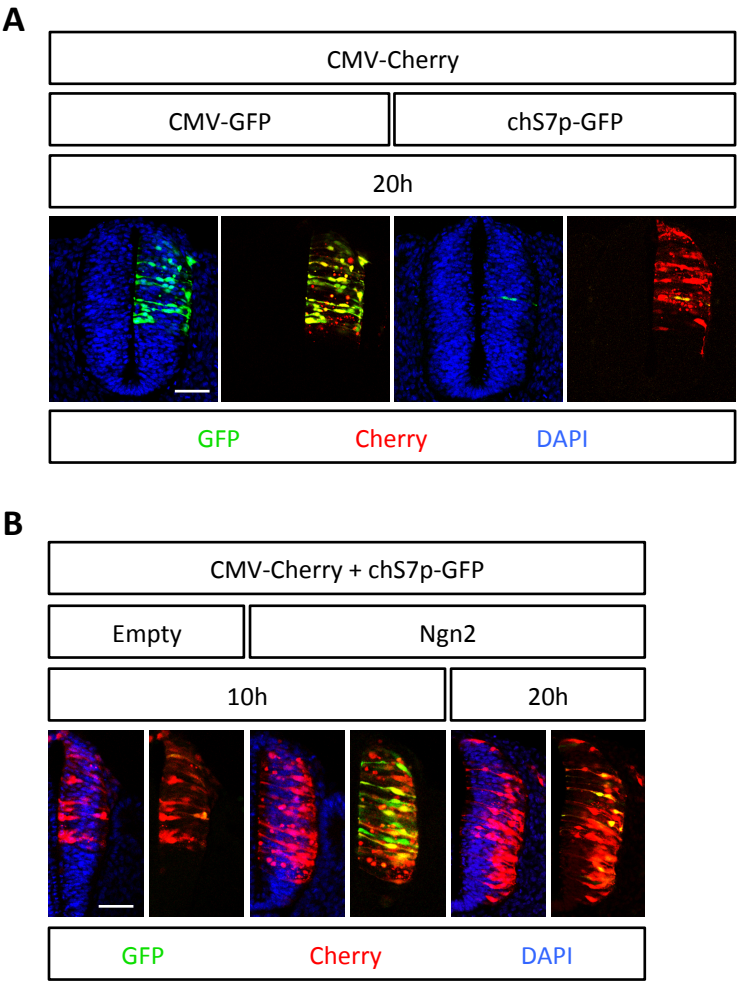

Figure R-32: *Senp7* chick promoter shows the same activation pattern than the human promoter in the chick neural tube. (A) The neural tube of chick embryos at stage HH17 was electroporated as previously shown in Figure R-31A. A GFP reporter under the control of the promoter region of chicken *Senp7* gene (chS7p-GFP) was used in this experiment instead of the human *Senp7* reporter. Reporter activation was compared 20h after electroporation by immunofluores-cence, as previously indicated. A CMV-Cherry expression vector was included in both experiments to monitor the electroporated cells (red). DNA was counterstained with DAPI (blue). **(B)** Activation of the chS7p-GFP reporter construct (green) was analysed under induced neurogenesis, 10 and 20h after coelectroporation with an expression construct for the neurogenic factor Neurogenin2 (Ngn2) or its empty vector, as previously shown in Figure R-31C. A CMV-Cherry expression vector was included in all the experiments to monitor the electroporated cells (red). DNA was counterstained with DAPI (blue). Scale bar 50 µm.

4.3 Identification of proteins that exhibit changes in their SUMOylation state during P19 neuronal differentiation.

The previous data and evidences support a role or connection between SUMOylation and neuronal differentiation. Tanking into consideration these results and the fact that in this work we have already focused on the implication of the SUMO modification pathway itself in the process of neuronal differentiation, we wanted to take a further step studying target proteins that change their SUMOylation state during this process. For this purpose, a SILAC based proteomic analysis comparing the SUMO proteome of proliferative and differentiating P19 cells was envisaged, establishing a collaboration with the group of Prof. Frauke Melchior in the Center for Molecular Biology of the University of Heidelberg (ZMBH), that has developed a purification protocol of endogenously SUMOylated proteins. Thus, this system lacks of the inconveniences of other systems based on the expression of labelled SUMO molecules.

4.3.1 P19 cells undergo neuronal differentiation when grown under SILAC conditions.

A SILAC experiment requires very specialized conditions of cell culture, including special medium without Arginine and Lysine, the use of dialyzed serum and the culture of cells with labelled Arg and Lys. The classic medium (minimum essential medium Eagle with alpha modification (αMEM)) used to routinely culture P19 cells in our hands is not commercially available without Arg and Lys for SILAC, so we were forced to use new growing conditions with Dulbecco's modified Eagle medium (DMEM), which is easily disposable in its SILAC format. Then, P19 cells were tested for normal growth in DMEM, as this medium was going to be used in the further SILAC experiment. For this purpose, the cells were initially cultured in three different growing media with supplemented newborn calf serum (NCS) and fetal bovine serum (FBS) as follows:

- Condition 1: αMEM + 7.5% NCS + 2.5% FBS (classic conditions).
- Condition 2: DMEM + 7.5% NCS + 2.5% FBS
- Condition 3: DMEM + 10% FBS

After a number of cell passages, cells exhibited a normal shape and morphology in the three tested conditions and only a slightly higher growing ratio was observed in the condition 3 when compared to condition 1.

As this work is based in the comparison of the SUMO proteome in proliferating and differentiating conditions, it was mandatory to test whether P19 cells cultured in the new growing conditions with DMEM were able to undergo proper neuronal differentiation. For this purpose, we compared the expression of different markers in proliferation and at distinct times during the differentiation protocol with RA using the new culturing media.

As shown in Figure R-33, by western-blot we could see how the pluripotency marker Oct4 was downregulated after 2d of RA treatment, while the expression of the neural specific marker ßIII-tubulin was increased throughout the protocol, obtaining satisfactory results with the new tested conditions.

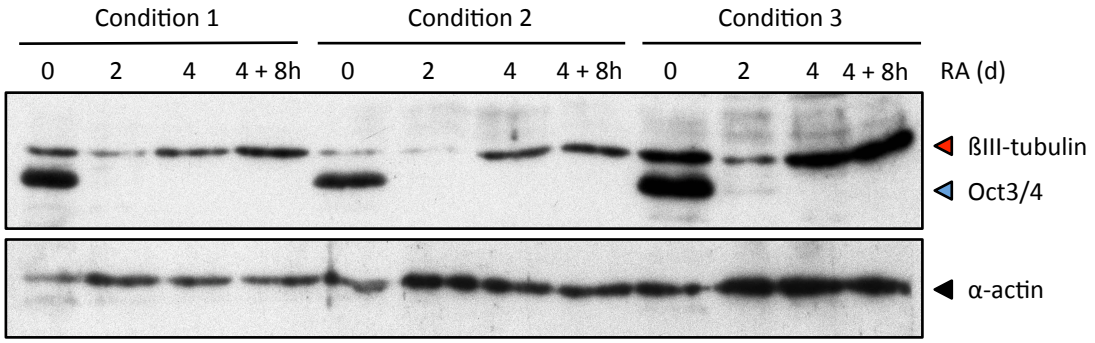

Figure R-33: P19 cells differentiate into neurons when treated with RA in culture media appropriate for SILAC experiments. Analysis by Western blot of P19 cells neural differentiation when cultured in three different growing conditions as indicated on top of each blot (see Materials and Methods). P19 cells were then differentiated with RA and harvested after 2 or 4 days (d) of RA treatment, and 4 days of RA treatment following growth on adherent dishes for 8h (4 + 8h) Proliferative cells were also harvested as t = 0 (0). Protein levels of Oct4 (blue arrow) and ßIII-tubulin (red arrow) were determined as a control of neurogenesis by Western blot. Blots for α-actin are also included as a loading control (black arrow). 5 µg of total protein were loaded per lane.

An additional assay was performed to assess the correct differentiation of these cells by induction of differentiation upon cotransfection of the neurogenic factor NeuroD2 and its cofactor E12. By immunofluorescence experiments (Figure R-34), we could monitorize the expression of ßIII-tubulin in properly differentiated P19 cells.

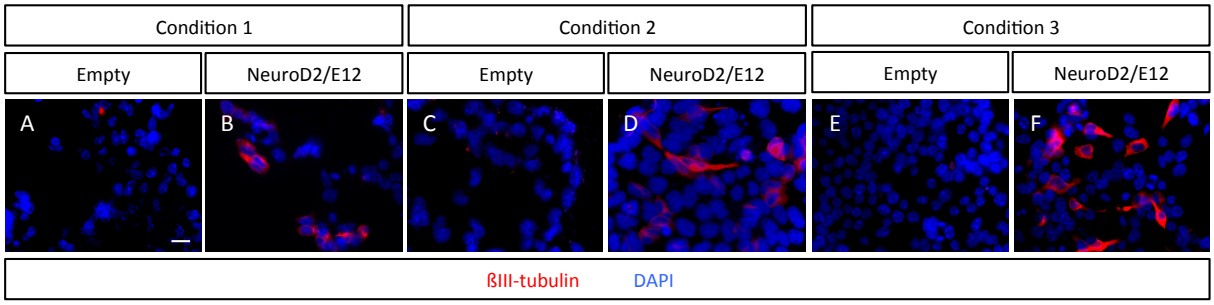

Figure R-34: immunofluorescence of proliferating and differentiating P19 cells. P19 cells grown in condition 1, condition 2 or condition 3 media were transfected with empty vector or with expression constructs for NeuroD2 and its cofactor E12, to induce neuronal differentiation. ßIII-tubulin antibodies were used to analyse neuronal differentiation (red) and DNA was counterstained with DAPI (blue). Scale bar 20 µm.

For a proper mass spectrometry (MS) analysis by SILAC, the incorporation efficiency of labelled amino acid in the cells must be tested, as well as the conversion ratio of Arginine into Proline, which can affect the incorporation efficiency in a negative way. For these tests, P19 cells were cultured in SILAC conditions (see Materials and Methods) during 4 days under proliferation and splitted when necessary, according to approximately six division rounds, and then harvested and lysated. The samples were sent for analysis to the Core Facility for Mass Spectrometry and Proteomics (CFMP) at the ZMBH. Labelled amino acids incorporation to P19 cells was tested and determined to be around 98% for each amino acid, being >95% the recommended threshold value by the CFMP for a proper SILAC experiment. In addition, Arginine to Proline conversion was analysed and determined to be negligible in labelled P19 cells.

The results obtained showed that P19 cells behave normally in SILAC conditions and they can undergo neuronal differentiation in a similar way of that obtained in our previous experiments. Some of our previous results (e.g. *Senp7* upregulation) indicated that 4 days of differentiation is an interesting point to analyse the SUMO proteome in comparison to the proliferative state in P19 cells. Due to the necessity to perform immunoprecipitation of SUMO conjugates, the amount of cell mass needed was high, in order to obtain a sufficient amount of protein. In addition to this, it is also recommended to do a reverse SILAC labelling when performing an accurate MS analysis, in order to discard false positive results that could

be obtained in a single experiment comparing two different labelled conditions. These considerations made us to work with a high number of cells in the final large-scale experiment (see Materials and Methods), detailed in the workflow chart shown in Figure R-35.

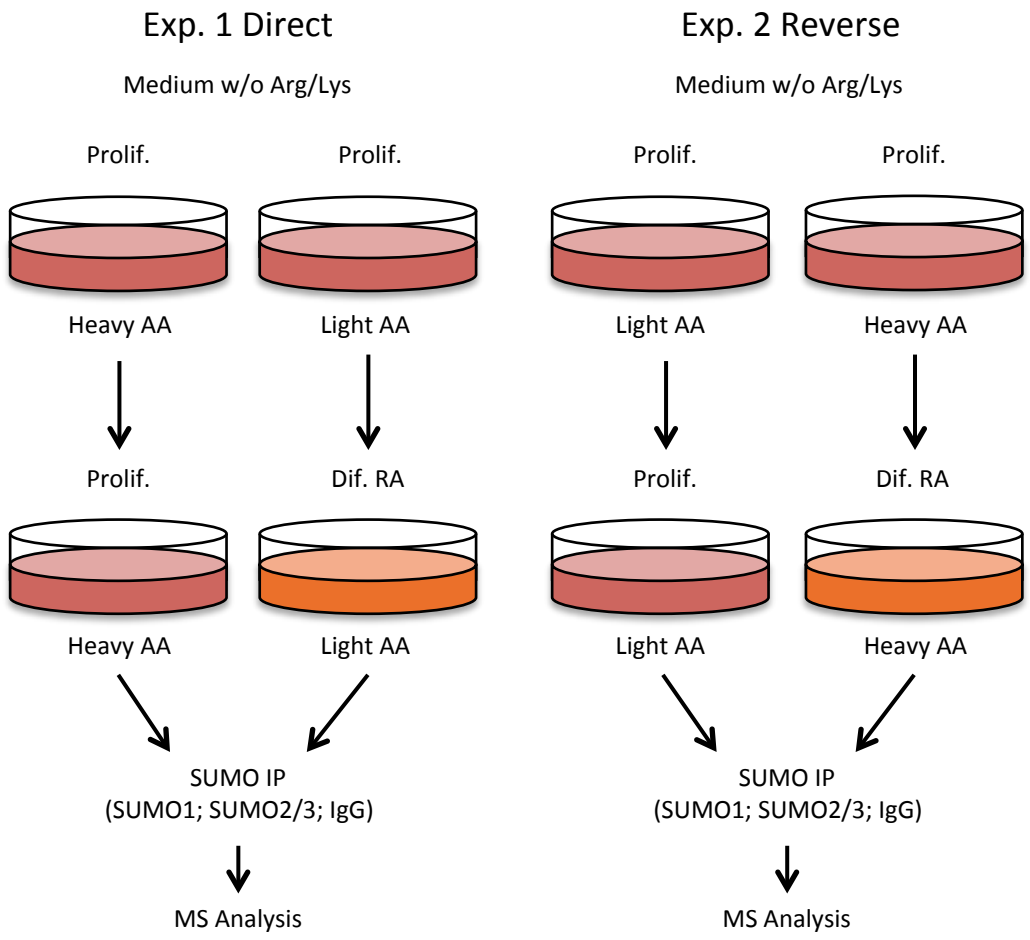

Figure R-35: Large-scale workflow for SILAC experiment and further SUMO immunoprecipitation (IP) of proliferating and differentiating P19 cells. The cells for both direct and reverse SILAC sets of experiments were cultured in SILAC Lys and Arg-free media and harvested as represented: the first set (Exp. 1) was cultured with D4 Lysine and ^{13}C Arginine heavy labelled amino acids (heavy AA) and non-labelled amino acids (light AA) in proliferating (Prolif.) and differentiating (Dif. RA) conditions, respectively. In the second set (Exp. 2), light AA and heavy labelled AA were employed in proliferation and differentiation conditions, respectively. After harvesting, lysing and mixing proliferative and differentiating cells from each experiment as indicated, three SUMO IPs per experiment were performed using specific antibodies against SUMO1, SUMO2/3 and control IgG. Inputs and eluates from the SUMO IP were sent for mass spectrometry (MS) analysis.

4.3.2 SUMO immunoprecipitation and peptide elution effectively enriches P19 cell extracts with endogenously SUMOylated proteins.

To immunoprecipitate SUMO conjugates, the use of an affinity matrix coupled to SUMO antibodies is needed. In this work, SUMO1 and two different batches of SUMO2 antibodies were obtained from hybridoma 21C7 and 8A2 cells (The Developmental Studies Hybridoma Bank at the University of Iowa), respectively, to be coupled to the agarose beads that form the affinity matrix. Control beads were also prepared with commercial normal mouse IgG. We checked the coupling efficiency comparing the release of heavy and light chains of the antibodies prior and after crosslink treatment to the agarose beads by SDS-PAGE (Figure R-36).

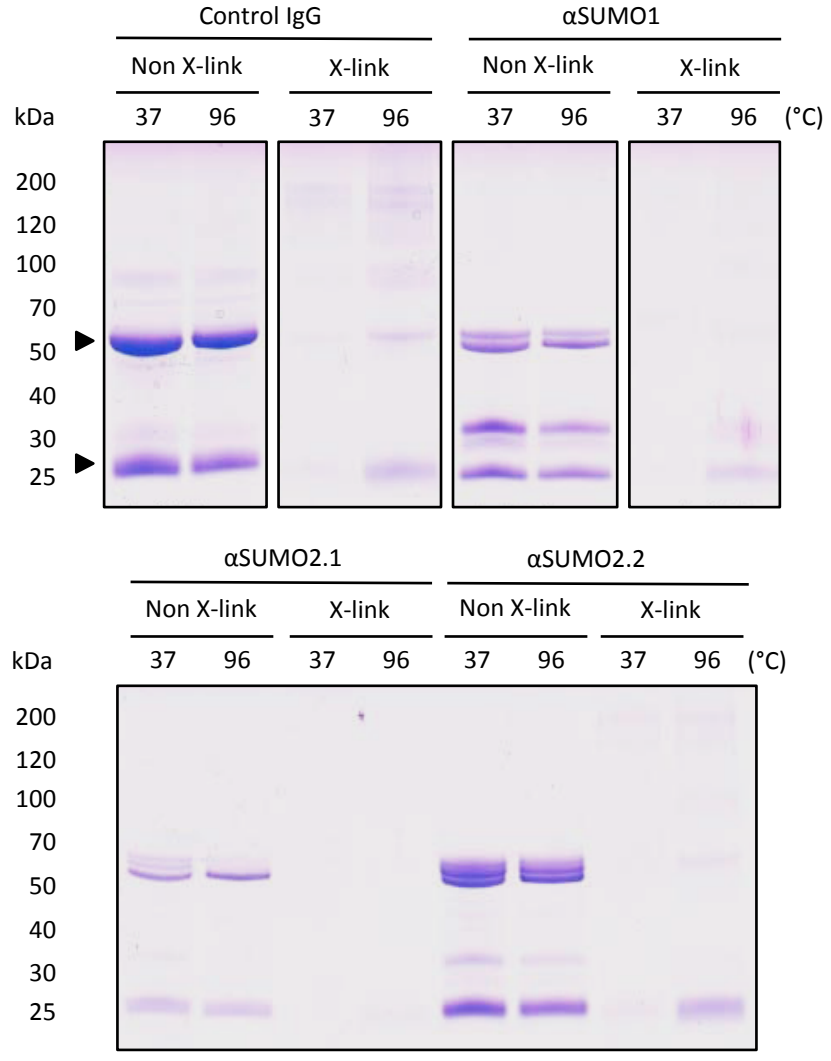

Figure R-36: Coomassie staining of agarose beads coupled to SUMO1 and two batches of SUMO2 antibodies as well as control IgG. The beads incubated with each SUMO antibody or IgG were crosslinked, taking control samples before (Non X-link) and after (X-link) the crosslink treatment. To test crosslinking efficiency, bead supernatants from the control samples were subsequently incubated in the presence of SDS at 37° C or boiled with SDS + DTT at 96° C and separated by SDS-PAGE. Coomassie staining shows how denatured light and heavy chains from the antibodies are almost absent from supernatants of the crosslinked fractions while they are strongly present (arrows) in supernatants of the non-crosslinked fractions.

As expected, when analysing bead pellets and supernatants, non-crosslinked samples showed a high amount of heavy and light chains from the antibodies, both in bead pellets and supernatants, indicating the successful binding of antibodies to the beads. When analysing the crosslinked samples, no antibody chains were observed in the supernatants and only a small fraction appeared in the beads, indicating that, though being incubated with DTT, crosslinking was efficient and most of the antibodies remained attached to the beads. These satisfactory results were obtained for control and SUMO1 beads, as well as for the second batch of SUMO2 beads.

After harvesting all cellular samples of both sets of SILAC experiments according to the workflow chart in Figure R-35 (see Materials and Methods), cell lysates were made in radioimmunoprecipitation assay (RIPA) conditions according to the protocol detailed in (Barysch et al. 2014). For each set of experiments the protein concentration was determined for proliferative and differentiating samples, both samples of each set were mixed to the same protein amount and inputs were taken. Once again, amino acid incorporation efficiency was determined to be 98% and the Arg to Pro conversion was minimum. Then, immunoprecipitation (IP) of SUMO1, SUMO2 and control IgG was performed for each set of lysates using the previously synthesized beads and, after elution with specific peptides corresponding to the epitopes recognized by the antibodies, SUMO conjugates were efficiently purified as shown by Western blot (Figure R-37). Finally, for each set of experiments, inputs and eluted IgG, SUMO1 and SUMO2 samples were sent to the Core Facility for Mass Spectrometry and Proteomics (CFMP) at the ZMBH for MS analysis and identification of proteins that appear to be SUMOylated in one of the proliferating or differentiating conditions and get deSUMOylated in the contrary condition.

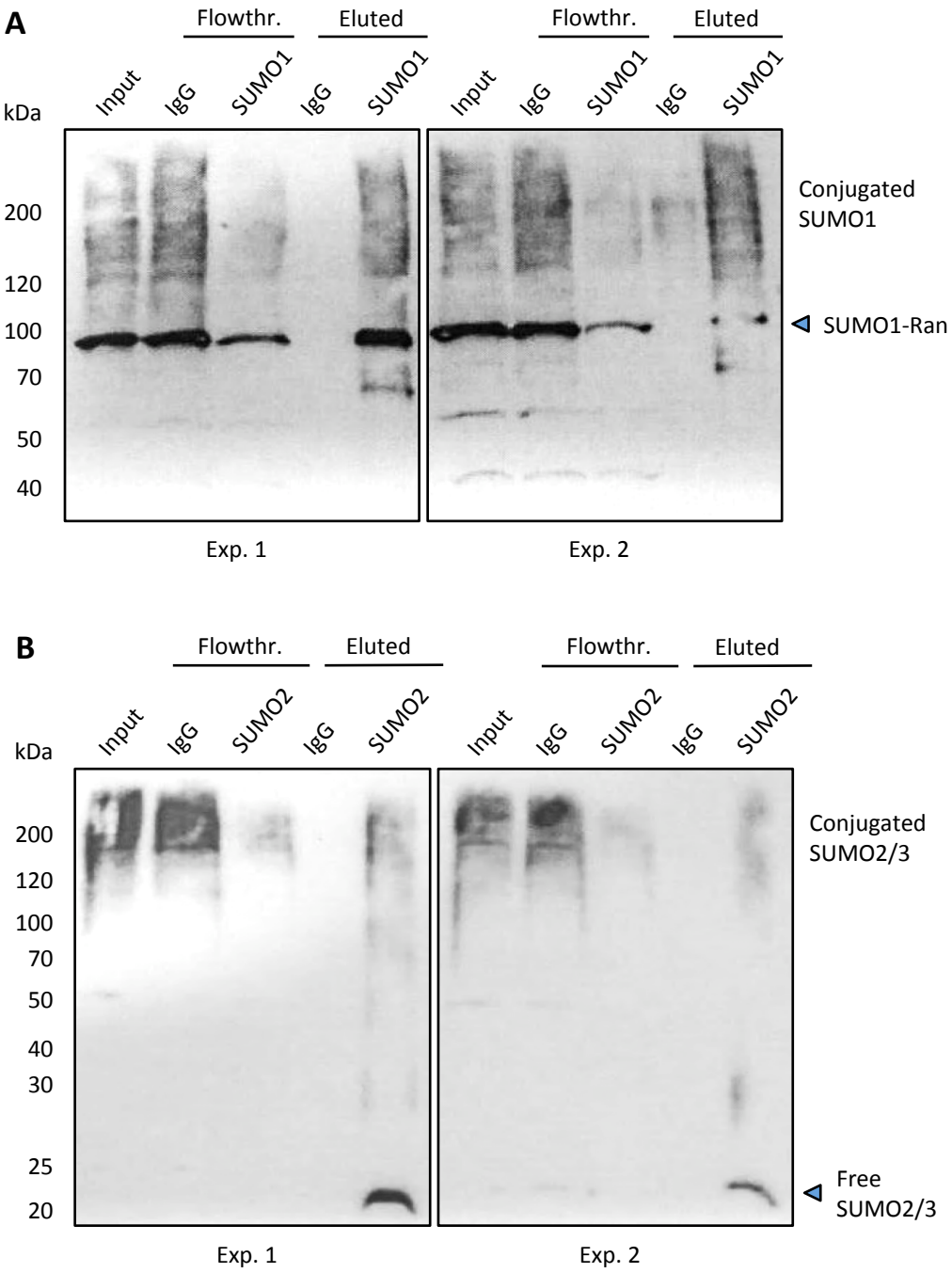

Figure R-37: Purification of endogenously SUMOylated products in proliferative and differentiating P19 cells. P19 cells cultured for SILAC under proliferation and differentiation (see figure R-35) were harvested and lysated in denaturing conditions. After SUMO IP (see Materials and Methods), Western blot analysis showed purified endogenously SUMOylated products when comparing IgG and SUMO1 or SUMO2 eluted proteins. 0.05% of the eluates (Eluted) and flow-throughs (Flowthr.) were loaded and revealed with SUMO1 **(A)** and SUMO2 **(B)** antibodies for each set of SILAC experiments. 0.02% of inputs relative to the lysates volume were also loaded. Flow-through lanes show how SUMOylated proteins are efficiently bound to the matrix when comparing SUMO1 and SUMO2 with the control IgG.

4.3.3 Several proteins are identified as differentially SUMOylated targets between proliferative and differentiating P19 cells.

Mass spectrometry data analysis was conducted in the group of Prof. Frauke Melchior, at the ZMBH in Heidelberg. For this, data of identified Razor and unique peptides, as well as intensities, were considered from inputs and from IgG-IP, SUMO1-IP and SUMO2-IP in both sets of experiments.

After a first statistical analysis of the data, only 2240 proteins from the total identified were considered as true SUMO targets (see Apendix). Then, ratios for each light/heavy labelling intensities from SUMO1-IP and SUMO2-IP fractions were considered. Targets that showed inverse ratios between both experiments for at least one of the SUMO-IP fractions (either SUMO1-IP or SUMO2-IP) were considered as SILAC candidates, including in this category a total of 318 proteins (Figure R-38). These ratio changes could be essentially due to a remarkable change in the SUMOylation state of target proteins, but changes could also be due to a significant alteration of the target expression levels during the differentiation process. To look for proteins that adjust to this first option, a further selection step was necessary, following these criteria:

- Proteins were only considered if they showed an intensity ratio for SUMO1-IP or SUMO2-IP in both sets of experiments and these ratios were ≥2 in one experiment and ≤0.5 in the reverse.

- SUMO1-IP or SUMO2-IP ratios from both sets of experiments needed to have at least a 2-fold difference with the control ratios (either inputs or IgG-IP), according to the following statements:

  - When both input ratios were present, they were compared to the ratios of SUMO1-IP or SUMO2-IP. In the absence of one of the inputs data, both IgG-IP ratios were considered to compare with the IP fractions. Proteins were also included if they presented input ratios from a set of experiments and IgG-IP ratios from the reverse.

- When proteins only showed control ratios from one set of experiments, they were considered only if there was at least a 2-fold difference with the ratios from SUMO1-IP or SUMO2-IP in the same experiment.

- A final consideration included proteins without any control ratio that showed at least a 2-fold difference between their SUMO1-IP and SUMO2-IP ratios since this indicates that, at least, one of the ratios is due to real changes in their SUMOylation levels, assuming that the other SUMO-IP may be considered as a control.

Figure R-38 shows the number of identified proteins that, in accordance to the previously mentioned criteria, are finally considered as targets that presumably change their SUMO1-IP or SUMO2-IP ratios due to relevant changes in their SUMOylation state (relative) without relevant changes in their expression levels. It is important to remark that selection criteria do not exclude proteins moderately changing their expression levels.

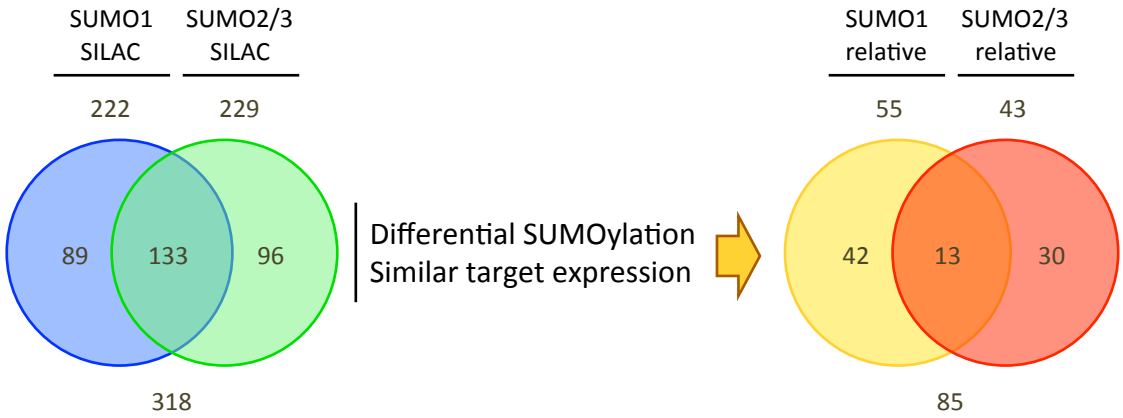

Figure R-38: Venn diagram of SUMO targets identified by MS from the SILAC experiment. Target proteins that changed their SILAC signal when P19 cells got differentiated, due to differential SUMO modification or to great differences in their expression levels, are represented (SUMO SILAC; left). Numbers of proteins modified by SUMO1, SUMO2/3 or both paralogs, are indicated above. The total amount of proteins considered in this case is indicated below. Target proteins whose SILAC signal only changed due to differential SUMO modification but are similarly expressed in both conditions are also represented (SUMO relative; right). Again, numbers of proteins modified by SUMO1, SUMO2/3 or both paralogs, are indicated above. The total amount of proteins considered is indicated below.

For a first work, some of these proteins were selected due to outstanding changes in their SUMO1-IP or SUMO2-IP ratios or to previously described roles showing a potential implication in the neuronal differentiation process (Tables R-1, R-2 and R-3). At this point, it is worth noting that many of these selected proteins correspond to transcription factors and that some of them show to be preferentially modified by SUMO1 or SUMO2/3, though some others do not show this paralog specificity.

Table R-1: Selection of targets differentially modified by SUMO1. Relative SILAC labelling shows proteins that get SUMOylated in proliferation (green) or neuronal differentiation (red) of P19 cells in the first experiment (Exp.1). The reverse labelling is shown for the second experiment (Exp. 2).

SUMO1 SILAC relative																	
Gene	Protein	Razor + unique peptides								Heavy/Light labelling ratios							
		Exp. 1				Exp. 2				Exp. 1 (Prolif/Dif)				Exp. 2 (Dif/Prolif)			
		IgG	Input	S1	S2	IgG	Input	S1	S2	IgG	Input	S1	S2	IgG	Input	S1	S2
Ftl1	Ferritin light chain 1 and 2	3	4	16	3	6	8	15	2	4,33	3,00	9,49	1,93	0,13	0,12	0,05	NaN
Tet1	Methylcytosine dioxygenase TET1	0	0	11	11	0	0	19	5	NaN	NaN	8,12	3,10	NaN	NaN	0,14	0,22
Pml	Protein PML	0	3	22	27	4	1	19	25	NaN	2,68	7,95	6,38	0,34	NaN	0,22	0,27
Morc3	Microrchidia family CW-type zinc-finger 3	10	5	43	50	9	3	41	45	3,04	1,82	4,71	3,35	0,65	0,61	0,25	0,45
Sall2	Sal-like protein 2	0	5	8	7	1	5	5	5	NaN	1,52	3,32	2,59	NaN	0,62	0,26	0,46
Zfp518b	Zinc finger protein 518B	1	0	7	12	0	0	9	8	NaN	NaN	3,01	11,22	NaN	NaN	0,38	0,14
Nacc1	Nucleus accumbens-associated protein 1	0	4	10	9	1	1	6	8	NaN	0,93	1,92	1,04	1,59	NaN	0,47	1,12
Gon4l	GON-4-like protein	0	0	10	13	0	1	17	8	NaN	NaN	1,05	0,40	NaN	NaN	1,38	5,67
Kctd1	BTB/POZ domain-containing protein KCTD1	0	1	8	11	1	0	9	16	NaN	NaN	0,57	0,27	NaN	NaN	1,84	4,30
Kctd15	BTB/POZ domain-containing protein KCTD15	0	2	3	8	2	0	5	11	NaN	NaN	0,48	0,08	NaN	NaN	4,06	17,65
Trim24	Transcription intermediary factor 1-alpha	2	3	25	30	4	1	24	29	NaN	NaN	0,47	0,20	9,23	NaN	2,24	5,68
Ncbp2	Nuclear cap-binding protein subunit 2	0	2	4	0	1	3	3	1	NaN	1,49	0,42	NaN	NaN	0,69	2,48	NaN
Cotl1	Coactosin-like protein	0	4	7	0	1	7	3	0	NaN	0,60	0,19	NaN	NaN	2,01	4,53	NaN
Nrip1	Nuclear receptor-interacting protein 1	0	0	12	21	1	0	9	25	NaN	NaN	0,18	0,16	NaN	NaN	2,83	9,44

IgG: elution from control immunoprecipitation (IP); S1: elution from SUMO1 IP; S2: elution from SUMO2 IP; NaN: not a number.

Table R-2: Selection of targets differentially modified by SUMO2/3. As in the previous table, modified proteins in proliferation (green) or differentiation (red) of P19 cells are shown for the first experiment (Exp. 1). The reverse labelling is shown for the second experiment (Exp. 2).

SUMO2 SILAC relative																	
Gene	Protein	Razor + unique peptides								Heavy/Light labelling ratios							
		Exp. 1				Exp. 2				Exp. 1 (Prolif/Dif)				Exp. 2 (Dif/Prolif)			
		IgG	Input	S1	S2	IgG	Input	S1	S2	IgG	Input	S1	S2	IgG	Input	S1	S2
Utf1	Undifferentiated embryonic cell transcription factor 1	1	11	9	12	8	14	6	10	NaN	13,92	7,84	94,62	0,11	0,13	0,15	0,05
Tcof1	Treacle protein	3	12	14	17	8	17	13	20	8,77	3,83	5,19	7,94	0,27	0,29	0,14	0,11
Nolc1	Nucleolar and coiled- body phosphoprotein 1	1	16	7	7	8	17	9	8	NaN	1,86	3,42	4,05	0,52	0,54	0,30	0,28
Utp3	Something about silencing protein 10	0	0	5	6	1	5	5	6	NaN	NaN	2,61	3,99	NaN	0,78	0,43	0,27
Krr1	KRR1 small subunit processome component homolog	0	6	1	4	0	5	1	4	NaN	1,52	NaN	3,90	NaN	0,79	0,36	0,31
Nop58	Nucleolar protein 58	8	19	26	33	14	25	26	27	1,53	1,38	2,15	3,78	0,69	1,00	0,49	0,30
Cdca8	Borealin	0	2	7	14	2	0	5	12	NaN	1,17	2,04	3,09	0,34	NaN	0,35	0,19
Bptf	Bromodomain PHD-finger Transcription Factor	0	3	13	17	0	2	13	8	NaN	0,85	1,16	1,78	NaN	NaN	0,95	0,47
H2afz	Histone H2A, V and Z	1	4	4	4	3	4	4	4	NaN	0,45	0,59	0,91	1,86	2,08	1,67	1,01
Nup214	Nuclear pore complex protein Nup214	0	20	17	17	1	22	17	19	NaN	1,17	0,92	0,41	NaN	0,86	1,93	3,60
Trim33	E3 ubiquitin-protein ligase TRIM33	2	7	25	26	2	4	25	24	NaN	0,92	0,85	0,28	NaN	1,24	1,29	4,17
Dnajc9	DnaJ homolog subfamily C member 9	1	11	0	3	1	2	3	5	NaN	0,43	NaN	0,20	NaN	1,83	1,87	17,43
Sec22b	Vesicle-trafficking protein SEC22b	1	6	5	9	4	1	5	7	NaN	0,35	0,54	0,17	1,56	NaN	1,60	13,02
Etv6	Transcription factor ETV6	0	2	2	7	0	0	1	8	NaN	0,45	NaN	0,15	NaN	NaN	NaN	10,25
Nxn	Nucleoredoxin	3	14	12	7	6	6	12	10	NaN	0,08	0,21	0,09	7,11	6,43	4,20	49,20

IgG: elution from control immunoprecipitation (IP); S1: elution from SUMO1 IP; S2: elution from SUMO2 IP; NaN: not a number.

Table R-3: Selection of targets indistinctly modified by SUMO1 and SUMO2/3 during P19 cells neuronal differentiation. Modified proteins in proli-feration (green) or differentiation (red) are shown for the first experiment (Exp. 1). The reverse labelling is shown for the second experiment (Exp. 2).

SUMO1/SUMO2 SILAC relative																	
Gene	Protein	Razor + unique peptides								Heavy/Light labelling ratios							
		Exp. 1				Exp. 2				Exp. 1 (Prolif/Dif)				Exp. 2 (Dif/Prolif)			
		IgG	Input	S1	S2	IgG	Input	S1	S2	IgG	Input	S1	S2	IgG	Input	S1	S2
Sall4	Sal-like protein 4	1	12	31	26	5	9	27	27	NaN	6,60	###	19,35	NaN	0,24	0,05	0,07
Utp14a	U3 small nucleolar RNA-associated protein 14 homolog A	0	9	15	8	3	5	13	12	NaN	1,73	4,53	6,31	0,46	0,59	0,22	0,19
Dnttip2	Deoxynucleotidyltransferase terminal-interacting protein 2	0	5	23	6	2	6	20	11	NaN	1,14	4,03	3,67	0,70	0,87	0,25	0,30
Mphosph10	U3 small nucleolar ribonucleoprotein protein MPP10	0	0	8	7	0	2	7	12	NaN	NaN	3,83	3,70	NaN	0,71	0,33	0,22
Atrx	Transcriptional regulator ATRX	15	15	48	55	3	11	45	36	3,54	0,83	2,93	2,77	0,67	1,09	0,32	0,39
Incenp	Inner centromere protein	0	2	3	3	0	2	4	4	NaN	0,85	2,51	5,66	NaN	0,84	0,27	0,20
Suz12	Polycomb protein Suz12	1	1	8	12	0	7	10	17	NaN	NaN	1,61	1,78	NaN	1,38	0,69	0,51
Gtf2i	General transcription factor II-I	2	39	48	73	21	35	43	60	NaN	0,60	0,33	0,15	3,50	1,65	3,79	6,93
Prox1	Prospero homeobox protein 1	0	0	16	14	5	0	9	20	NaN	NaN	0,31	0,58	1,10	NaN	6,02	12,52
Ranbp2	E3 SUMO-protein ligase RanBP2	52	40	121	160	28	39	123	115	0,10	1,16	0,23	0,05	11,37	0,75	6,37	6,05

IgG: elution from control immunoprecipitation (IP); S1: elution from SUMO1 IP; S2: elution from SUMO2 IP; NaN: not a number.

4.3.4 SUMOylation analysis by SDS-PAGE of identified proteins validates the SILAC protocol on proliferating and differentiating P19 cells.

For validation of the MS analysis we wanted to monitorize SUMOylation levels from some of the identified targets using specific antibodies by Western blot. For this purpose, we turned to some relevant proteins which antibodies were available.

P19 cells were grown under the same proliferative and differentiating conditions used in the previous large-scale experiment but without SILAC labelling, and SUMO1 IPs following specific peptide elution was performed. Western blot analyses were initially restricted to samples from SUMO1 IPs as SUMO1 has been mostly related to transcriptional regulation. The results showed how, when looking at the inputs, Morc3, Atrx and Trim24 expression levels remain steady during the differentiation process but, when analysing the elution fractions from the IPs, high molecular bands corresponding to Morc3 and Atrx modified by SUMO1 appear in proliferative P19 cells while higher levels of Trim24 modified by SUMO1 appear after four days of differentiation with RA (Figure R-39A). These results are in agreement with the data obtained in the MS analysis and correspond to proteins existing in both studied conditions that change their net SUMOylation.

By contrast, when analysing SUMOylation of the ferritin light chain (FLC), we could not observe higher molecular mass bands corresponding to SUMO modified FLC, and only a protein band of about 21 kDa was detected, either in both inputs and the IP of the proliferative condition. These bands correspond to the unmodified FLC and indicate a false positive case of a protein that is recognized in an unspecific way by the SUMO antibodies. We also wanted to analyse Irf2bp1 since, although it did not mathematically fit to the restrictive criteria established to be considered as a relative SILAC candidate, MS data suggested differential SUMOylation between the analysed conditions. Thus, we could see by Western blot how Irf2bp1 is more efficiently modified by SUMO1 in differentiating P19 cells, indicating that some proteins excluded from the group of relative SILAC candidates are indeed differentially SUMOylated and expressed in both analysed conditions (Figure R-39A). Protein levels of Ubc9 were also analysed as a negative control of the experiment, as almost no modification by SUMO1 was observed. Blots in Figure R-39B are shown to assess the correct neuronal differentiation of the cells used in these validating experiments.

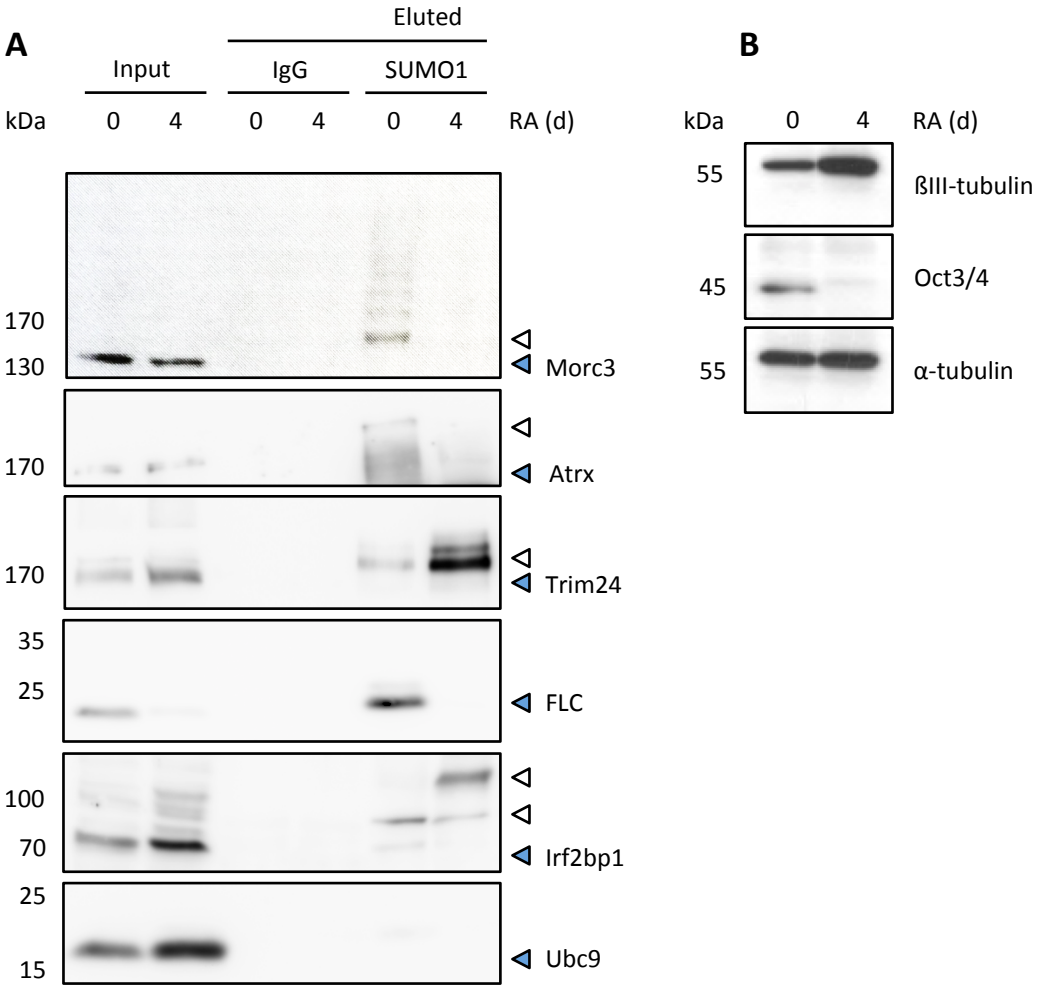

Figure R-39: SUMOylation of targets identified by MS and validated in proliferative and differentiating P19 cells. (A) P19 cells grown in DMEM + FBS (see Materials and Methods) were harvested in proliferative conditions (0) and after 4d of RA treatment (4). After denaturing protein extraction and SUMO1 IP, SUMOylation of Morc3, Atrx, Trim24 and Irf2bp1 was revealed with specific antibodies as indicated. 100% of eluates (Eluted) and 0.02% of inputs relative to the lysate volume were loaded. Blots show non-modified (blue arrows) and SUMO modified (white arrows) forms of the analysed proteins. FLC (Ferritin light chain) **(B)** Whole protein extraction was also performed to monitorize neurogenesis of the cells. Protein levels of Oct4 and ßIII-tubulin were determined by Western blot, loading 15 µg of total protein per lane. Blots for α-tubulin loading 5 µg of total protein are also included as a loading control.

Taking all these data into consideration, we can assume the existence of an interplay between SUMOylation and the process of neuronal differentiation from the large number of proteins that change their SUMOylation state during this process in P19 cells.

5 Discussion

During this work, we have taken advantage of various models and conducted a series of approaches to establish a connection between SUMOylation and neuronal development. Indeed, the presented results show how modification by SUMO has an impact at distinct levels in the process of neuronal differentiation and morphogenesis of the nervous system. The work here described has shed some light into this impact and connections, but further research and interpretation of the obtained results is needed to fully understand the involvement of SUMOylation in the studied processes.

5.1 The transcription factor Krox20 as an E3 SUMO ligase.

Taking into consideration the results obtained in this work, we have established a role for the transcription factor Krox20 as an E3 ligase during SUMOylation of its coregulators, the Nab proteins. Ligase activity of Krox20 is based on a number of observations that also account for the establishment of a regulatory role for SUMO during hindbrain formation. In this way, overexpression of Krox20 under limiting SUMO availability leads to SUMOylation of transfected Nab (Figure R-5), which is in accordance with Krox20 being able to interact with Nab and Ubc9 through different domains; the mentioned repressor domain R1 and the zinc finger domains, respectively (Figures I-5 and R-2). In this regard, physical interaction between the ligase and the target through the previously mentioned domains is critical for the modification of Nab proteins, as demonstrated by the use of interaction mutants (Figure R-8), and also adds to the evidences supporting a role for Krox20 as a SUMO ligase. Additionally, serum-dependent stimulation of P19 cells has proven to be a helpful feature to analyse physiological induction of Krox20 expression, showing that SUMOylation of endogenous Nab can also be observed in cultured cells and is dependent on Krox20 expression (Figure R-9). Finally, to support that a protein acts as an E3 SUMO ligase, *in vitro* experiments with the sole components of the SUMOylation machinery and the target proteins are usually required. In this case, we have provided evidence showing SUMOylation

of Nab2 *in vitro*, in the presence of purified E1, Ubc9, mature SUMO and Krox20 (Figure R-10). Furthermore, this type of assay has allowed us to quantify the amount of SUMOylated Nab2 in respect to input Krox20, showing a ratio of approximately nine fold and suggesting that Krox20 acts in a catalytic rather than stoichiometric manner, as would be expected from an E3 ligase. To our knowledge, this constitutes the first example of a transcription factor functioning as a ligase for the SUMOylation of its own coregulators.

Our results support a role of Krox20 in the local recruitment of Ubc9 in its transcriptional complex for the SUMOylation of other components, as has been shown for Nab proteins, contributing to our understanding of how the specificity of target SUMOylation might be achieved. The possibility that Krox20 could also act as an E3 ligase for the SUMOylation of other factors is an exciting hypothesis, considering the role of Krox20 in various developmental systems (Schneider-Maunoury, S *et al.*, 1993; Topilko, P *et al.*, 1994). Our findings also represent a stimulus for the identification of new ligases. Different types of ligases do not share significant homology. Similarly, no structural domains seem to be shared between Krox20 and previously described ligases, like PIAS proteins or RanBP2. These ligases share the ability to interact with Ubc9, in many cases through apparently unrelated domains. The zinc-finger domain of Krox20 binds to Ubc9. In the same direction, other zinc-based structures like PHD domains have been reported to be involved in Ubc9 binding and ligase function (Garcia-Dominguez, M *et al.*, 2008; Zeng, L *et al.*, 2008).

5.2 Regulation of the hindbrain development by SUMO.

Despite the numerous roles attributed to SUMO in eukaryotic cells, a function in transcriptional repression stands out (Garcia-Dominguez, M and Reyes, JC, 2009). Accordingly, the results presented in this work support that Nab SUMOylation accounts for transcriptional repression. Regarding to this, it has been previously mentioned that the repressive activity of Nab is partly due to its interaction with CHD4 through the CID domain present in the C-terminus part of the protein (Srinivasan, R *et al.*, 2006). In the same direction, the authors have reported that CHD4 participates in the repressor activity associated to Nab2, though full repression activity is not explained by the interaction with CHD4 and additional mechanisms might be involved. Interestingly, the results here

presented arise the possibility that SUMOylation is accounting for this repression activity. Indeed, the fact that both wild type Nab2 and the KR2 mutant have the same interaction capabilities with CHD4 (Figure R-12) suggests that SUMOylation is not involved in CHD4 recruitment, but constitutes an independent mechanism for repression.

It has been proposed that Krox20 mediates expansion of r3 and r5 territories by the non-autonomous recruitment of cells from adjacent even-numbered territories (Giudicelli, F *et al.*, 2001). Thus, it is likely to think that other mechanisms should limit Krox20 activity to restrict expansion of r3 and r5 for proper hindbrain development and induction by Krox20 of its own corepressors, the Nab proteins, has been proposed as a negative feedback regulatory loop that would account for the control of this process (Mechta-Grigoriou, F *et al.*, 2000). Supporting this hypothesis, interference with the interaction between Krox20 and Nab proteins by mutation of the R1 domain in Krox20 and the NCD1 domain in Nab proteins leads to delayed repression of Krox20 target genes (Desmazieres, A *et al.*, 2009; Desmazieres, A *et al.*, 2008). Our gain-of-function experiments with the Nab2 KR2 mutant show that interfering with Nab SUMOylation also leads to altered expression of Krox20 target genes (Figure R-13 and R-15) and to aberrant size of the implicated rhombomeres (Figure R-16). In this direction, the KR2 mutant has proven to be really useful in these gain-of-function experiments, as it shows a dominant-negative effect that is consistent with Nab SUMOylation limiting Krox20 activity and the extension of rhombomeres where Krox20 is expressed, in agreement with the proposed role for Nab proteins (Figure D-1). However, experiments conducted in mice have shown that double Nab knockout or knock-in of the I268F mutation in Krox20 do not lead to major defects in proper patterning of the hindbrain (Desmazieres, A *et al.*, 2008; Le, N *et al.*, 2005), pointing to the presence of redundant mechanisms during hindbrain development that limit the expansion of territories mediated by krox20 expression and transcriptional regulation.

In conclusion, we have revealed an intriguing novel activity of the Krox20 transcription factor, as a SUMO ligase for its coregulators, the Nab proteins. Nab SUMOylation affects Krox20 transcriptional activity, establishing an additional loop in the complex control that Krox20 performs over Nab activity and expression, and over the transcription factor itself.

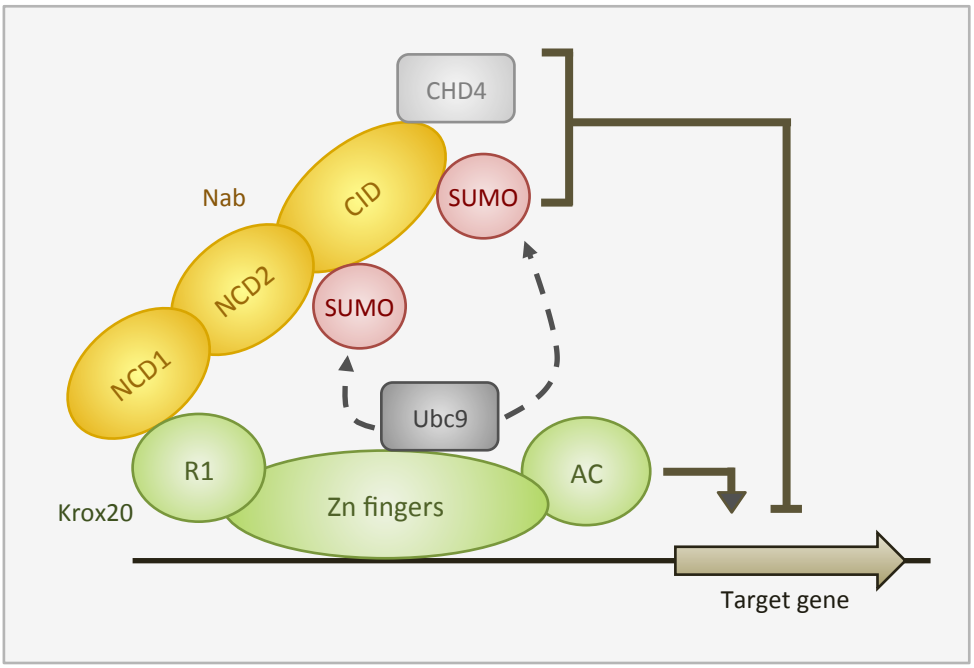

Figure D-1: General model for the regulation of Krox20 in the hindbrain. These schematics show the repressor effect that SUMOylation of Nab mediated by Krox20, together with Nab interaction with CHD4, displays over the transcriptional activity of Krox20. Domains in yellow correspond to Nab and domains in green correspond to Krox20. The black arrow indicates transcriptional activation and the flat-end arrow indicates corepressor activity. Discontinuous arrows correspond to enzymatic conjugation.

5.3 SUMOylation as a regulated process during neurogenesis.

The results previously shown in this work support a role for SUMO in regulating neural development. In further experiments we have investigated, though, whether SUMOylation is regulated during neurogenesis and, if so, which mechanisms are regulating it. Interestingly, we have observed that net SUMO deconjugation is detected during neurogenesis. To this point, in addition to this decrease in the levels of SUMOylated proteins, we have observed that the free-SUMO pool in P19 cells doubles following induction of neuronal differentiation with RA, while protein analysis under non-denaturing conditions reveals no changes in the total SUMO-pool along the process (Figure R-17). These results indicate that neuronal differentiation is linked to a net SUMO deconjugation balance

and are in agreement with previous works reporting that overall SUMOylation decreases during brain development in rodents (Hasegawa, Y *et al.*, 2014; Loriol, C *et al.*, 2012; Watanabe, M *et al.*, 2008). Also in this sense, deSUMOy-lation of the chromatin associated factor Braf35, which is linked to neuronal differentiation, has been reported (Ceballos-Chavez, M *et al.*, 2012).

The results in this work also show how SUMO overexpression leads to the impairment of neurogenesis in P19 cells and chicken neural tube, also pointing to the association of enhanced SUMOylation with an undifferentiated state. Interestingly, overexpression of both SUMO1 and SUMO2 showed the same effect on neurogenesis (Figures R-19 and R-21), raising the question of whether they work independently or share overlapping sets of targets during the differentiation process. In this regard, though SUMOylation has been proven to be an essential mechanism in almost all eukaryotes, SUMO1 has been reported not to be essential in mouse, suggesting that most functions could be fulfilled by SUMO2/3. However, its deletion can lead to severe phenotypes that seem to be background-dependent (Wang, L *et al.*, 2014; Zhang, FP *et al.*, 2008). We have not investigated this aspect, but even if SUMO1 and SUMO2/3 work independently, we cannot discard that when overexpressed, specificity of target modification by the different SUMO paralogs is lost. Although these evidences point to a net SUMO deconjugation during neurogenesis, we should not exclude that de novo SUMOylation of specific targets could be required for this process.

The analysis of the expression levels from different components of the SUMOylation pathway during P19 neuronal differentiation with RA has delivered interesting results. Through this approach, we have observed how upregulation of Senp proteases expression agrees with net SUMO deconjugation. Our results also indicate that several Pias ligases genes are upregulated during this process, suggesting de novo SUMOylation of certain targets (Figure R-24). This possibility has to be taken into account, given that these ligases have been described to regulate the Wnt signalling pathway, related to embryogenesis and cell fate specification (reviewed in (Schmidt, D and Muller, S, 2003)). In addition to this, cellular functions of Pias proteins out of their SUMO ligase activity have also been described (Garcia-Dominguez, M *et al.*, 2006) and the numerous post-translational modifications and mechanisms that account for the regulation of Pias activity should also be taken into consideration (review in (Rytinki, MM *et al.*, 2009)).

5.4 Senp7 accounting for proper neuronal differentiation.

In the previously mentioned expression analyses, we have observed an important upregulation of Senp5 and Senp7 proteases (Figure R-25 and R-26), which have been associated with SUMO2/3 deconjugation (Di Bacco, A *et al.*, 2006; Gong, L and Yeh, ET, 2006; Shen, LN *et al.*, 2009). In this regard, as expected, our results show that the knockdown of Senp7 impairs neurogenesis-mediated SUMO2/3 deconjugation during neuronal differentiation of P19 cells (Figure R-28), while has no appreciable effects on SUMO1 conjugation levels. However, the fact that also free SUMO1 increases during neurogenesis suggests that all neurogenesis-mediated SUMO deconjugation cannot be exclusively attributed to these proteases. Interestingly, our results indicate that, while increased free SUMO2/3 during neurogenesis correlates with a decrease of high molecular mass SUMOylated products, increased free SUMO1 seems to mostly correlate with a decrease of SUMOylated RanGAP1 levels (Figure R-28), though additional experiments should be performed to assess a specific decrease in the levels of SUMOylated RanGAP1 and discard differentiation-induced RanGAP1 degradation (Figure D-2). However, apart from the impact that lower levels of SUMOylated RanGAP1 may have on neuronal differentiation, we cannot rule out that SUMO1 deconjugation from other targets has an important function in the process. Interestingly, although not directly related to neurogenesis, it has been previously reported that the SUMO1 associated protease Senp1 is necessary for normal development of the mouse embryo (Sharma, P *et al.*, 2013). To this point, we have not observed significant changes on the expression levels of Senp1 during P19 neuronal differentiation, but this does not exclude that Senp1 plays a role in the process. Differential regulation under proliferative and neuronal differentiation conditions of Senp proteins at different levels, other than the expression degree, may account for the net balance of conjugated SUMO during neurogenesis. As an example, SENP3 stabilization against proteasomal-mediated degradation has been reported following oxidative stress (Huang, C *et al.*, 2009; Yan, S *et al.*, 2010). We have demonstrated an increased expression of Senp7 both at mRNA and protein levels following induction of neuronal differentiation (Figures R25 and R26), and knocking down experiments unambiguously demonstrate the involvement of Senp7 in neuronal

differentiation (Figures R-29). A scaffolding function, essential for proper chromosome segregation and not directly related to its SUMO-specific protease activity, has been reported for Senp7 mediating HP1 enrichment at pericentric heterochromatin (Maison, C *et al.*, 2012; Romeo, K *et al.*, 2015). We have not investigated Senp7 enzymatic activity but, regarding this aspect, it is interesting to remark that neurogenesis-mediated increase of Senp7 expression correlates with increased SUMO deconjugation, what points to the involvement of its protease activity in the process (Figure D-2).

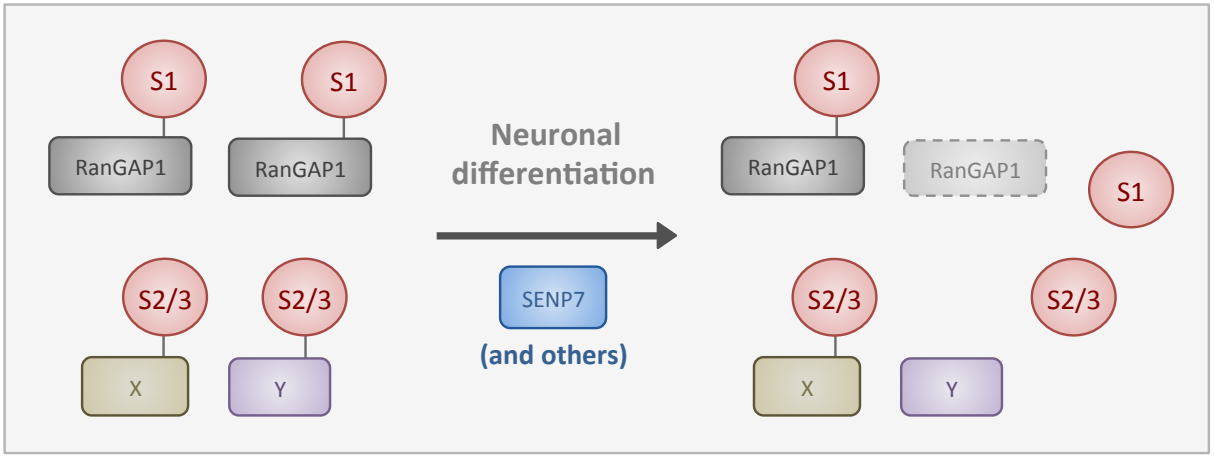

Figure D-2: General model for changes in protein SUMOylation during neuronal differentiation. Schematics showing how neuronal differentiation proceeds with SUMO1 (S1) deconjugation from modified targets, being mostly appreciable in deSUMOylation of RanGAP1, and with SUMO2/3 (S2/3) deconjugation from modified targets (unidentified X and Y proteins). Lower levels of SUMOylated RanGAP1 detected under neuronal differentiation could be related to partial degradation of RanGAP1 following differentiation (dashed box).

As previously mentioned, in addition to Senp7, Senp5 is also upregulated following induction of neurogenesis in P19 cells. At this point, the question about Senp5 and Senp7 redundancy of function or specificity of targets during this process arises. We have performed preliminary loss-of-function analyses that reveal less dramatic effects in neurogenesis in the absence of Senp5 than those observed in the absence of Senp7 (not shown). Interestingly, Senp5 has been recently involved in neutrophil differentiation of myeloid leukemic cells, being also upregulated upon induction of differentiation in blast cells

from acute myeloid leukemia patients (Federzoni, EA *et al.*, 2015). Thus, it is tentative to assign a role to a subset of SUMO proteases in the onset of diverse differentiation processes.

To further investigate the way in which Senp7 expression is upregulated during neuronal differentiation, expression analysis of a GFP reporter driven by the Senp7 5'-upstream region encompassing its promoter has permitted us to monitor transient expression of the reporter upon induction of neuronal differentiation in the neural tube of chick embryos. These results, together with Senp7 peaking its expression at day 4 of the RA treatment to differentiate P19 cells (before cells extend dendritic and axonal processes) (Figure R-25), point to a role of Senp7 at very early stages of neurogenesis. As previously mentioned during the introduction of this work, Neurogenins are proneural genes placed at the earliest stages in the cascade of factors involved in neurogenesis (Ma, Q *et al.*, 1999; Ma, Q *et al.*, 1996; Perez, SE *et al.*, 1999). Other proneural factors like NeuroM are transiently expressed in neural progenitors that have just exited the cell cycle and start migrating from the VZ to the ML (Roztocil, T *et al.*, 1997). This transient expression prefigures a "frontier" region between VZ and ML, designated as subventricular zone (SVZ). In our experiments with the Senp7 expression report, when naturally occurring neurogenesis is permitted, we have observed localization of reporter positive cells close to the SVZ, which may suggest that Senp7 displays an expression pattern similar to that of NeuroM. However, neither Neurogenin2 nor NeuroM were able to sustain reporter expression over the time when used to induce neurogenesis, indicating that the promoter sequence is not directly regulated by these factors (Figures R-31 and R-32). Thus, other factors, transiently activated when triggering neurogenesis by overexpression of Neurogenin2 or NeuroM in the neural tube, should account for early and transient activation of the reporter. When inducing neurogenesis by overexpression of neurogenic factors, virtually all transfected cells migrate into the ML and end up localizing to the most distal part from the VZ. Accordingly, upon induction of neurogenesis following the electroporation of neurogenic factors, although reporter was switched off with time, electroporated cells normally migrated to the ML, as revealed by localization of cells expressing the CMV-mCherry construct that we used to monitorize electroporated cells (Figure R-31 and R-32).

In conclusion, this work describes for the first time that proper neuronal differentiation requires Senp7, a SUMO specific protease, as a regulatory component of SUMOylation. Interfering with the expression of Senp7 impairs neurogenesis in a similar way

to overexpressing SUMO molecules. Senp7 is transiently activated at early stages of neurogenesis, correlating with significant and general deSUMOylation of proteins. Hence, Senp7 appears as a key regulator of neuronal differentiation and adds to the list of factors involved in this process. This finding opens new and exciting research lines to try to identify the targets associated to Senp7 in the context of neurogenesis.

5.5 Cellular functions of SUMO targets in the process of neuronal differentiation

The identification of target proteins that change their SUMOylation state in cells between proliferative and differentiating conditions has always been an attracting endeavour during progression of this work, focusing our efforts in the purification of SUMOylated products in both conditions and their subsequent identification by mass spectrometry (MS). Problems associated to the highly dynamic fashion of the SUMO conjugation and the low amount of SUMOylated forms of target proteins have hindered our progression to this point, till the establishment of a purification protocol in the group of Prof. Frauke Melchior that allows for the elution of SUMOylated proteins with specific peptides after immunoprecipitation with SUMO antibodies (Barysch, SV *et al.*, 2014; Becker, J *et al.*, 2013). The application of this purification protocol in the analysis of proteins that get SUMOylated or deSUMOylated during neuronal differentiation of P19 cells has reverted in the identification of hundreds of target proteins.

After the MS data processing, a further analysis to get a sight into the functional associations in cellular processes that these proteins have was mandatory. To this purpose, gene ontology (GO) analyses were conducted over genes coding for targets that were selected because of remarkable differences in their SUMOylation states compared to their expression levels between the studied conditions (relative SILAC) (Figure R-38). GO performed over genes encoding for targets that are presumably modified by SUMO1 shows that a high number of them (34%) are related to transcriptional regulation, with an also high number of genes implicated in general transcriptional processes (28%) (Table D-1). It is important to mention that a significant percentage of genes are also associated with a variety of functions generally related to negative regulation of distinct processes in the cell.

According to this point, it has been previously discussed how transcriptional regulation by SUMO1 is often associated to a repressor activity ((Ceballos-Chavez, M *et al.*, 2012) and reviewed in (Garcia-Dominguez, M and Reyes, JC, 2009)). With genes encoding for proteins presumably modified by SUMO2/3, GO analysis shows that most of them are also associated to transcriptional functions, mostly regulatory (41.5%). However, a high number of functions attributed to chromatin organization stand out regarding these targets modified by SUMO2/3 (Table D-1), which is interesting, taking into consideration that modification by SUMO2/3 has been classically associated to stress response.

Table D-1: Gene Ontology analysis of SUMO1 and SUMO2/3 SILAC relative targets. The number of genes included in each term is represented graphically by percentages. P-values for statistical signification of each term are also indicated.

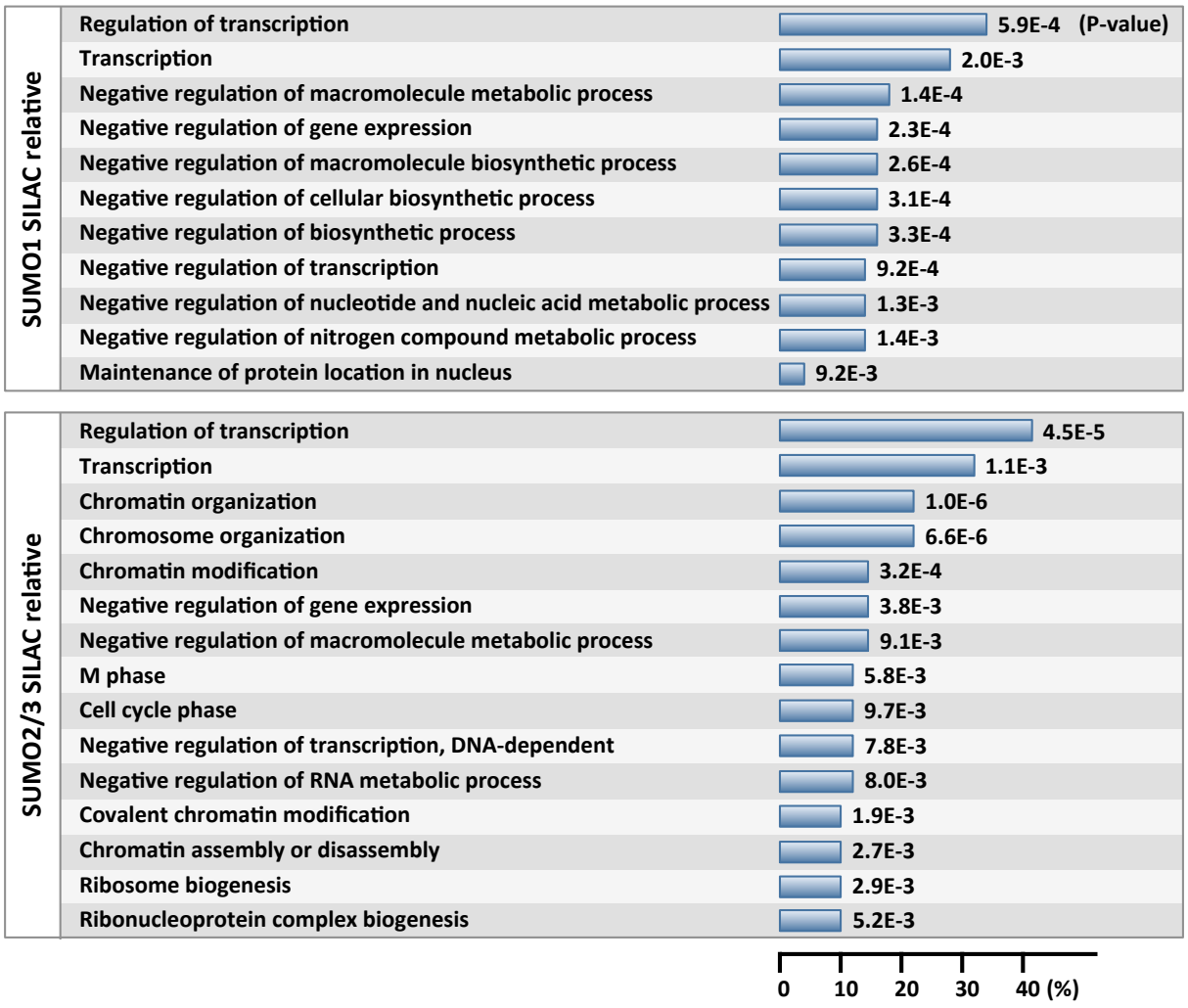

It is worth to further investigate whether SUMO2/3 is clearly involved in the remodelling processes that take place over specific regions of the chromatin that need to be silenced for cell cycle exit and neuronal differentiation of cells, together with relaxation of the chromatin regions that need to be accessible for the transcription machinery in order to express neuronal differentiation genes. When performing an additional GO analysis taking into consideration both sets of SILAC relative targets that are modified by SUMO1 and by SUMO2/3, we find that also most of the analysed genes are implicated in transcription or transcriptional regulation and other functions in the cell that might be of interest regarding neuronal differentiation (Table D-2).

Table D-2: Gene functions of SILAC relative SUMO targets. Genes from an additional GO analysis comprising SILAC relative SUMO1 and SUMO2/3 targets are classified into five general categories. Note that a given gene can fit with more than one category.

Transcription and its regulation		
Ajuba	Kmt2d	Suz12
Atrx	Nacc1	Tet1
Baz1b	Nrip1	Trim24
Bptf	Pml-like	Trim33
Dnttip2	Prox1	Utf1
Etv6	Psip1	Zfp423
Gon4l	Sall2	Zfp445
Gtf2i	Sall4	Zfp512
Hp1bp3	Sap130	Zfp518b
Kctd1	Sarnp	

Ribosome biogenesis and RNA metabolism	
Aatf	Nop58
Krr1	Nup214
Mphosph10	Ranbp2
Ncbp2	Utp14a

Epigenetics and chromatin structure	
Atrx	Hp1bp3
Baz1b	Kmt2d
Bptf	Rlf
Dnmt3b	Suz12
Ehmt2	Tet1
H1fx	Utp3

Mitosis
Cdca8
Incenp
Nup214
Rad21
Ube2i

Nuclear bodies
Morc3
Pml-like

As previously mentioned, targets identified in the MS analysis change the ratio in which they show to be modified by SUMO, according to a remarkable change in their SUMOylation levels in comparison to their expression levels between both conditions or due to a high change in their expression levels. To this last point, it would be important to study why SUMOylation of a specific target is important in one of the analysed conditions, and why the target is dumped or degraded in the opposite condition. These scenarios have to be taken into consideration to further validate and investigate the identified targets. In this regard, it is important to state that some targets might be mistakenly excluded from the lists of SILAC relative candidates, when they indeed change their SUMOylation levels in a significant way compared to changes in their expression, but not fulfilling the strict criteria applied for the relative candidates in a quantitative way. This has been the case for the Interferon regulatory factor-2-binding protein-1 (IRF2BP1). Our validation experiments unambiguously show that, although being excluded from the list of SILAC relative candidates, IRF2BP1 is indeed more efficiently SUMOylated following neuronal differentiation than under proliferative conditions, without great changes in its expression level (Figure R-39). Thus, we do not exclude that additional proteins, not fitting with the established criteria to be considered as SILAC relative candidates, are indeed SILAC relative candidates. IRF2BP1 was initially described to mediate corepressor activity, together with its interaction partner Interferon regulatory factor-2 (IRF-2), over interferon (IFN) genes expression (Childs, KS and Goodbourn, S, 2003). In later works, IRF2BP1 has been associated to regulation of the transforming growth factor (TGF) signalling pathway. In this regard, IRF2BP1 has been shown to antagonise the repressor activity of the Transforming growth interacting factor (TGIF), thus promoting the TGF-ß-mediated growth arrest and gene expression (Faresse, N *et al.*, 2008).

On the other hand, we cannot rule out the possibility that some of the proteins identified as differentially SUMOylated are false positives. The fundament of mass spectrometry, which undergoes peptide digestion of the protein samples prior to the analysis, permits the detection of peptides corresponding to proteins that are not SUMOylated but have been recognized by the SUMO antibodies in an unspecific way and therefore eluted in the immunoprecipitation protocol. Validation of the different candidates, one by one, by using specific antibodies will unambiguously indicate which candidates are relevant to be considered differentially modified by SUMO. For instance, validation

experiments have shown that the iron storage protein subunit ferritin light chain (FLC) has resulted to be a false positive, not being modified by SUMO1 as was firstly indicated by the MS data (Figure R-39).

To assess the implication of the SUMO modification of the selected targets in neuronal differentiation, functional experiments are required. The identification of the target lysines for SUMO modification is critical for each of the selected proteins. As mutation of the identified target lysines to arginine for the obtainment of effective SUMOylation mutants will contribute to get information from functional analyses, either on P19 cells or chicken embryos. The interpretation of the results will greatly depend on the neuronal differentiation phenotype obtained, thus arising a variety of possible scenarios. This way, a mutant protein, whose SUMOylation is necessary for proper differentiation of neural progenitors, may have an effect in disrupting or somehow impairing neuronal differentiation, but in the case that SUMOylation of this protein is needed in neural progenitors for the maintenance of a proliferative state, the mutant may promote and increase differentiation upon induction of neurogenesis with neurogenic factors. It is likely to think that the obtainment of analysable phenotypes will depend in a great manner on the degree of implication that this factors would have in neuronal differentiation and their function on early stages of the differentiation cascade. A function on later stages will presumably do necessary the analysis of specific neuron subtypes for the detection of a given phenotype.

As has been previously shown, we have currently validated SUMOylation of some interesting proteins identified by MS (Figure R-39). Our interest has been initially focused into proteins related to transcriptional regulation like TRIM24, MORC3 or ATRX, or the previously mentioned IRF2BP2, taking into consideration that some of them have never been showed to be SUMOylated. TRIM24 is a member of a large family of proteins that contain a tripartite-motif (TRIM) in their N-terminal region and is comprised by a RING finger, one or two zinc-binding motifs named B-Box and an associated coiled-coil region. The C-terminal region is variable and has been used to catalogue the TRIM proteins into twelve subgroups. TRIM24 is a member of the transcriptional intermediary factor-1 (TIF1) subgroup and has been associated to cell signalling by RA (reviewed in (Gudas, LJ and Wagner, JA, 2011)) and to regulation of the tumour suppressor factor p53 (reviewed in (Jain, AK and Barton, MC, 2009)). C-terminal parts of TIF1 proteins share the presence of a tandem PHD

domain and a Bromo domain. Interestingly, the PHD domain of TRIM28 (also termed as KAP1) has been shown to confer this protein an intramolecular E3 SUMO ligase function (Zeng, L *et al.*, 2008), raising the possibility of TRIM24 also acting as an E3 ligase, proteins that often tend to be modified by SUMO.

The transcriptional regulator ATRX is an ATP-dependent helicase protein comprised by two zinc-finger domains and an ATPase domain. This protein has been implicated in the silencing of certain regions in the genome, thus been described that ATRX associates with Daxx (Death-associated protein 6) to form a chaperone complex that recruits histone H3.3 to regions of the genome were heterochromatin state must be maintained. H3.3 recruitment to these regions has been correlated with accumulation of H3K9me3, therefore associating the action of the ATRX/Daxx complex to the maintenance of H3K9me3 in telomeres, pericentric heterochromatin, methylated CpG islands and other regions of the genome (reviewed in (Voon, HP and Gibbons, RJ, 2016; Voon, HP and Wong, LH, 2016)). Interesting associations between ATRX function and the maintenance of synaptic plasticity and homeostasis have been established when analysing the pathobiology of the mental retardation Rett syndrome. Mutations in the methyl-CpG binding protein 2 (MeCP2) have been classically associated with this syndrome (Bellini, E *et al.*, 2014), and it has been proposed how the disorganized structure of this protein allows for a variety of post-translational modifications, including SUMOylation (Cheng, J *et al.*, 2014; Tai, DJ *et al.*, 2016), that orchestrate the transcriptional regulatory functions attributed to this protein.

Microrchidia family CW-type zinc-finger 3 (MORC3) is a zinc-finger protein that belongs to the family of MORC proteins, characterized by the presence of an N-terminal ATPase domain, a zinc-finger domain, a NLS and a coiled-coil domain located to the C-terminal part (Kimura, Y *et al.*, 2002). MORC3 has been associated to p53 regulation, mediating the recruitment of the tumour suppressor protein into promyelocytic leukemia nuclear bodies (PML-NB) in an ATP-dependent manner, to activate p53 for induction of cellular senescence (Takahashi, K *et al.*, 2007). A mechanism has been described where the formation of PML-independent MORC3 nuclear domains is achieved through MORC3 ATPase activity and then, SUMOylation of MORC3 leads to its association with PML by interaction of SUMO1 with a SUMO-interacting motif (SIM) located in PML proteins (Mimura, Y *et al.*, 2010). Interestingly, recent studies have associated mutations in mice *Morc3* with defects in bone cells differentiation (Hong, G *et al.*, 2017; Jadhav, G *et al.*, 2016).

SUMOylation has been also described for additional targets that seem promising to us because of their association with cellular differentiation. This is the case of the potassium channel tetramerization domain-containing 15 (Kctd15) protein, which has been associated to inhibition of the neural crest formation and whose SUMOylation has been described, though the relationship between these two features is not clear (Zarelli, VE and Dawid, IB, 2013a; Zarelli, VE and Dawid, IB, 2013b). In the same direction, association of the Prospero-related homeobox 1 (Prox1) protein with cell differentiation has been widely studied, but an interesting role in neuronal differentiation emerges from its capability of regulating an important subset of genes to promote cell cycle exit and neuronal differentiation, while inhibiting astrogliogenesis (Stergiopoulos, A *et al.*, 2014).

In conclusion, the further establishment of functional roles for the SUMO modification of identified proteins in the process of neuronal differentiation will help us to understand the signalling mechanisms involved in this process. A subset of identified proteins start to arise as promising candidates to perform more detailed experiments that allow for the establishment of specific connections between SUMOylation and neuronal development.

6 Conclusions

1) The transcription factor Krox20 interacts in a direct and specific manner with the SUMO conjugating enzyme Ubc9 through the zinc-finger domain present in Krox20. Since Krox20 interaction with Nab corepressors occurs through the R1 domain, Krox20 interacts with Nab proteins and Ubc9 through different domains.

2) Krox20 acts as an E3 SUMO ligase for the modification of Nab proteins (Nab1 and Nab2) with SUMO1. Ligase activity depends on physical interaction between Krox20 and Nab.

3) Nab2 is modified by SUMO1 in lysines 379 and 517, accounting for the recruitment of SUMO to chromatin regions under the transcriptional control of Krox20.

4) Krox20-mediated SUMOylation of Nab proteins leads to repression of Krox20 transcriptional activity during hindbrain formation.

5) Levels of SUMOylated proteins decrease, while levels of free SUMO pools increase, following induction of neuronal differentiation. This agrees with impairment in neuronal differentiation provoked by SUMO overexpression.

6) Expression levels of Senp7 and Senp5 are upregulated following induction of neuronal differentiation, while expression levels of other components of the SUMOylation pathway are not significantly altered.

7) Senp7 is required for proper progression of neuronal differentiation, being its expression activated at the onset of the process.

8) SUMO immunoprecipitation following specific peptide elution can efficiently purify SUMOylated proteins from proliferative and differentiating P19 cells grown under SILAC conditions.

9) Morc3, Atrx, Trim24 and Irf2bp1 change their SUMOylation state following neuronal differentiation of P19 cells with retinoic acid.

10) A significant number of proteins that change their SUMOylation state during neuronal differentiation are associated with transcription regulation, according to the functions attributed to SUMO and to tight regulation required for neuronal differentiation.

7 Materials and Methods

7.1 Materials

7.1.1 Vectors

Table M-1: bacterial vectors

Name	Prom.	Res.	Information	Source
pBS-SK (+)	T3/T7	Amp	Cloning backbone RNA probe synthesis	Stratagene
pBS KS (+)	T3/T7	Amp	Cloning backbone	Stratagene
pET28a	T7	Km	Cloning backbone	Novagen
pET28a-His-Nab2-Flag	T7	Km	His-Nab2-Flag expression for purification	This work (Garcia-Gutierrez, P *et al.*, 2011)
pGEX-6P-3	tac	Amp	Cloning backbone	GE Healthcare
pGEX-6P-3-Ubc9	tac	Amp	Ubc9 expression for purification	This work (Garcia-Gutierrez, P *et al.*, 2011)
pGEX-6P-3-Aos1	tac	Amp	Aos1 expression for purification	This work (Garcia-Gutierrez, P *et al.*, 2011)
pGEX-6P-3-Uba2	tac	Amp	Uba2 expression for purification	This work (Garcia-Gutierrez, P *et al.*, 2011)
pGEX-6P-3-Krox20	tac	Amp	Kox20 expression for purification	This work (Garcia-Gutierrez, P *et al.*, 2011)
pGEX-6P-3-SUMO1GG	tac	Amp	SUMO1GG expression for purification	This work (Garcia-Gutierrez, P *et al.*, 2011)

Prom: promoter. Res: resistance cassette.

Table M-2: yeast vectors

Name	Prom.	Comp.	Res.	Information	Source
pDBLeu-Krox20*	ADH	Leu	Km	Two-hybrid (bait)	Invitrogen
pPC86	ADH	Trp	Amp	Two-hybrid (prey)	Invitrogen

* Deletion mutants in Figure R-2 were obtained through standard PCR techniques based on this construct. Prom: promoter. Comp: auxotrophy complementation. Res: resistance cassette.

Table M-3: mammalian vectors (cell transfection and chick embryo electroporation)

Name	Prom.	Res.	Information	Source
pAdRSV-Sp	RSV	Amp	Cloning backbone	Dr. Patrick Charnay (Giudicelli, F *et al.*, 2003)
pAdRSV-Sp-Krox20	RSV	Amp	Krox20 overexpression	Dr. Mario Garcia (Garcia-Dominguez, M *et al.*, 2006)
pAdRSV-Sp-HA-Krox20	RSV	Amp	HA-Krox20 overexpression	Dr. Mario Garcia (Garcia-Dominguez, M *et al.*, 2006)
pAdRSV-Sp-HA-Krox20IF	RSV	Amp	HA-Krox20 I268F overexpression	This work (Garcia-Gutierrez, P *et al.*, 2011)
pAdRSV-Sp-HA-NeuroM	RSV	Amp	HA-NeuroM overexpression	Dr. Mario Garcia (Garcia-Dominguez, M *et al.*, 2003)
pAdRSV-Sp-HA-CHD4	RSV	Amp	HA- truncated CHD4 overexpression	This work (Garcia-Gutierrez, P *et al.*, 2011)
pAdRSV-Sp-Flag-Nab1	RSV	Amp	Flag-Nab1 overexpression	This work (Garcia-Gutierrez, P *et al.*, 2011)
pAdRSV-Sp-Flag-Nab2	RSV	Amp	Flag-Nab2 overexpression	This work (Garcia-Gutierrez, P *et al.*, 2011)
pAdRSV-Sp-Flag-Nab2QRHQ	RSV	Amp	Flag-Nab2 Q64RH95Q overexpression	This work (Garcia-Gutierrez, P *et al.*, 2011)
pAdRSV-Sp-Flag-Nab2KR2	RSV	Amp	Flag-Nab2 K379R/K517R overexpression	This work (Garcia-Gutierrez, P *et al.*, 2011)
pAdRSV-Sp-Flag-RanGAP1Cter	RSV	Amp	Flag-RanGAP1 Cter overexpression	This work (Garcia-Gutierrez, P *et al.*, 2011)
pAdRSV-Sp-Flag-Ubc9C93S	RSV	Amp	Flag-Ubc9 C93S overexpression	This work (Garcia-Gutierrez, P *et al.*, 2011)
pAdRSV-Sp-Neurogenin2	RSV	Amp	Neurogenin2 overexpression	Dr. Mario Garcia (Garcia-Gutierrez, P *et al.*, 2011)
pAdRSV-Sp-His-SUMO1	RSV	Amp	His-SUMO1 overexpression	This work (Garcia-Gutierrez, P *et al.*, 2011)

pAdRSV-Sp-His-SUMO2	RSV	Amp	His-SUMO2 overexpression	This work (Garcia-Gutierrez, P *et al.*, 2011)
pBS-KS-*EphA4*e-LacZ	Minimal *ß-globin*	Amp	LacZ reporter, *EphA4* enhancer-driven	Dr. Mario Garcia (Garcia-Dominguez, M *et al.*, 2006)
pGL4.51	CMV	Amp	Constitutive Luciferase reporter	Promega
pSuper*	H1	Amp	Cloning backbone for shRNA constructs	Oligoengine
pCS2-MT-NeuroD2	CMV	Amp	NeuroD2 overexpression	Dr. Kristen L. Kroll (Seo, S *et al.*, 2005)
pCS2-MT-E12	CMV	Amp	E12 overexpression	Dr. Kristen L. Kroll (Seo, S *et al.*, 2005)
pmCherry-N1	CMV	Km	Constitutive mCherry reporter	Clontech
pEGFP-N1	CMV	Km	Constitutive GFP reporter	Clontech
pEGFP-C2	CMV	Km	Cloning backbone for GFP fussions	Clontech
pEGFP-C2-SUMO1	CMV	Km	GFP-SUMO1 overexpression	This work (Garcia-Gutierrez, P *et al.*, 2011)
phS7P-GFP	*SENP7p*	Km	GFP reporter, *SENP7* (h) promoter-driven	This work (Juarez-Vicente, F *et al.*, 2016)
pchS7P-GFP	*Senp7p*	Km	GFP reporter, *Senp7* (ch) promoter-driven	This work (Juarez-Vicente, F *et al.*, 2016)

***** All shRNA constructs were cloned in the pSuper vector using annealed oligonucleotides. Prom: promoter. Res: resistance cassette.

7.1.2 Oligonucleotides

Table M-4: RNA interference sequences

Name	Sequence 5'-3'
siRNA mouse Krox20#1	CGCCAAGGCCGUAGACAAA
siRNA mouse Krox20#2	GCCCUUCCAGUGUCGGAUC
siRNA GFP (control)	GGCACAAGCUGGAGUACAA
shRNA mouse *Senp7*#1	TTACAGCCTCCTCATGAGA
shRNA mouse *Senp7*#2	TCAGACTCATTGCCTTCGA
shRNA chicken *Senp7*#1	GGATTCTGTTGCTCAGACA
shRNA chicken *Senp7*#2	GAAGAAAGCTGGAGAAGAA
shRNA Control	CCATCAAGACTCATAGATG

Table M-6: oligonucleotides for qPCR

Name	Forward 5'-3'	Reverse 5'-3'
Nab2	AGGAAGAGGAGATCCGGAAG	GTGTTGTCCCTCATGCAGAA
Krox20	CAGGAGTGACGAAAGGAAGC	GACCAGAGGCTGAAGACTGG
GAPDH	AACTTTGGCATTGTGGAAGG	GGATGCAGGGATGATGTTCT
Id4 promoter	GCGCGGCTCTACAAATACTGC	AACCGCGCCTCCCAGCTCAAC
GFP	CAAGATCCGCCACAACATCG	GTCCATGCCGAGAGTGATCC
Sumo1	GGCGATAAGAAGGAAGGAGAA	CATTGGAACTCCCTGTCTTTG
Sumo2	GGACAGGATGGTTCTGTGGT	CGGAATCTGATCTGCCTCA
Sumo3	ATTCCGGTTTGATGGACAAC	GAGGCTGATCCTCCTGTCTG
Sae1	GCTGGACCACGAACAGGTAT	CCCACAGACCCAGTCTGAAT
Uba2	GCATCGTATGGGCCAAGTAT	GCTTCAGCCTCTGTTGGTTC
Ubc9	GTCCCAACAAAGAACCCTGA	GGTGGTGAGGACGGATAGTC

Pias1	TCACCTCACTTGTCCGATTG	CCCTTTGCTCGTAACCTCTG
Pias2	AGTCCAACCAAAGGGGTTCT	CGTGTGGTGGAATGGTACTG
Pias3	AGTTTCGATGCTGCCCTTTA	TCATCACAATCCGAACAGGA
Pias4	CACTGAACTGGTCCCACAGA	CTGCACAGCTTTCACTCCAG
Senp1	CAGAGGCGACATTTCAGCAC	AGAACTGCTTCCCTGTGACC
Senp2	AAGGTTCTCGGCACCATTCTT	TTTGGCTGGGATCTCATCAGT
Senp3	TTTGACTCCCAGCGAACTCT	TTTGACTGCCTCTGCCTGTA
Senp5	GGCGAGCTGATAATGGATGC	ACAAGTCCACCTTCTTCGTCC
Senp6	TGGAACTGTGGTTCATGGGAG	ACCTTGGCCATGACTTAGCA
Senp7	ACAGTTCCAGGGTCAGCAGT	ATGGCCGCTTACACATTTTC
Desi1	GCGGTATTTCCAGCTGTACC	CAGGGAGGACAGGTATTCCA
Pou5f1 (Oct4)	CCAATCAGCTTGGGCTAGAG	CTGGGAAAGGTGTCCCTGTA
Tubb3	TGGAGCGCATCAGCGTATAC	GCCCTGGGCACATACTTGTG
Rn18S	GTAACCCGTTGAACCCCATT	CCATCCAATCGGTAGTAGCG

Table M-5: oligonucleotides for cloning strategies

Name	Forward 5’-3’	Reverse 5’-3’
h*Senp7* promoter	GATCACGAGGTCAGGAGATCG	ATGTTCAGCCCTTCTCTGACC
ch*Senp7* promoter	GAAGTTCCAGCAATACATATGCG	TAAGGCTAGCAATTTGTATTTCATTT ATTCAGAAGG

7.1.3 Antibodies and peptides

Table M-7: primary antibodies

Name	Antigen	Host	Source	Dilution
(M2) Anti-FLAG	FLAG peptide (DYKDDDDK)	Mouse, monoclonal	Sigma-Aldrich (F1804)	1:200 (IF) 1:2000 (WB) 2/250 µg (ChIP)
(M2) Anti-FLAG affinity gel	FLAG peptide (DYKDDDDK)	Mouse, monoclonal	Sigma-Aldrich (A2220)	–
Anti-HA	HA-tag (YPYDVPDYA) from human influenza virus HA (hemaggltinin)	Rat, monoclonal	Roche (11-867-431-001)	1:2000 (WB)
Anti-HA	KLH conjugated HA-tag (YPYDVPDYA) of human influenza virus HA	Rabbit, polyclonal	Sigma-Aldrich (H6908)	1:2000 (WB)
Anti-Krox20	Amino acids 8 to 95 from human Krox20 fused to GST	Rabbit, polyclonal	Covance (PRB-236P)	1:1000 (WB)
(1C4) Anti-Nab2	Recombinant human Nab2	Mouse, monoclonal	Santa Cruz Btg. (sc-23867)	1:1000 (WB)
(D-11) Anti-SUMO1	Amino acids 1 to 101 from human SUMO1	Mouse, monoclonal	Santa Cruz Btg. (sc-5308)	2/250 µg of protein (ChIP)
(21C7) Anti-SUMO1	Recombinant 6x His-tagged human SUMO1	Mouse, monoclonal	DSHB, Iowa, IA, USA	1:1000 (WB)
(8A2) Anti-SUMO2/3	Recombinant human SUMO2	Mouse, monoclonal	DSHB, Iowa, IA, USA	1:1000 (WB)
Anti-Fluorescein	Fluorescein	Sheep, polyclonal	Roche (11426338910)	1:2000 (ISH)
Anti-Digoxigenin	Digoxigenin	Sheep, polyclonal	Roche (11093274910)	1:2000 (ISH)
Anti-SENP7	Internal peptide from human SENP7	Rabbit, polyclonal	Abcam (ab58422)	1:1000 (WB)
(P18) Anti-SENP3	Internal peptide from human SENP3	Goat, polyclonal	Santa Cruz Btg. (sc-46640)	1:1000 (WB)
(DM1A) Anti-α-tubulin	Microtubules from chicken embryo brain	Mouse, monoclonal	Sigma-Aldrich (T9026)	1:5000 (WB)
(H-134) Anti-Oct3/4	Amino acids 1 to 134 from human Oct-4	Rabbit, polyclonal	Santa Cruz Btg. (sc-9081)	1:1000 (WB)

Anti- neuron specific βIII-tubulin	KLH-conjugated amino acids 350 to C-terminus from human βIII-tubulin	Rabbit, polyclonal	Abcam (ab18207)	1:2000 (WB) 1:500 (IF)
(3A10) Anti-neurofilaments	Chicken neurofilaments	Mouse, monoclonal	DSHB, Iowa, IA, USA	1:200 (IF)
Anti-Morc3	Internal peptide from human MORC3 protein	Rabbit, polyclonal	Santa Cruz Btg. (sc-83730)	1:500 (WB)
(H-300) Anti-ATRX	Amino acids 2193 to 2492 from human ATRX	Rabbit, polyclonal	Santa Cruz Btg. (sc-15408)	1:1000 (WB)
Anti-Trim24	Recombinant 6x His-tagged human TRIM24	Rabbit, polyclonal	Proteintech (14208-1-AP)	1:2000 (WB)
Anti-Irf2bp1	Human IRF2BP1 protein (Accession NM_182972)	Rabbit, polyclonal	Proteintech (18847-1-AP)	1:1000 (WB)
Anti-Ubc9	Amino acids 1 to 81 from human Ubc9	Rabbit, polyclonal	Santa Cruz Btg. (sc- 10759)	1:1000 (WB)

Table M-8: secondary antibodies

Name	Conjugate	Host	Source	Dilution
Anti-mouse IgG	HRP	Goat, polyclonal	Sigma-Aldrich (A4416)	1:10000 (WB)
Anti-rabbit IgG	HRP	Goat, polyclonal	Sigma-Aldrich (A6154)	1:10000 (WB)
Anti-rat IgG	HRP	Goat, polyclonal	Sigma-Aldrich (A9037)	1:10000 (WB)
Anti-goat IgG	HRP	Donkey, polyclonal	Bethyl (A50-201P)	1:10000 (WB)
Anti-rabbit IgG	DyLight 549	Donkey, polyclonal	Jackson Immunoresearch (711-505-152)	1:800 (IF)
Anti-rabbit IgG	DyLight 488	Donkey, polyclonal	Jackson Immunoresearch (711-485-152)	1:800 (IF)
Anti-mouse IgG	DyLight 649	Donkey, polyclonal	Jackson Immunoresearch (715-495-151)	1:800 (IF)
Anti-mouse IgG	DyLight Cy3	Donkey, polyclonal	Jackson Immunoresearch (715-165-150)	1:800 (IF)

Table M-9: elution peptides for SUMO immunoprecipitation.

Peptide	Sequence
SUMO1	VPMNSLRFLFE
SUMO2/3	IRFRFDGQPI

7.1.4 Organisms

Table M-10: bacterial or yeast strains and mammal cell lines employed in this work.

Organism	Strain/Line	Information
Bacteria	DH5α	Cloning strategies
	BL21	Heterologous protein expression
Yeast	MaV203	Two-hybrid (His-, Leu-, Trp-, LacZ+)
Mammals	HEK-293T	Transformed human embryonic kidney cells for protein expression
	P19	Mouse teratocarcinoma for RA- or transfection-mediated neuronal differentiation

7.2 Methods

7.2.1 Culture conditions of employed organisms

- Bacterial culture and maintenance

DH5α and BL21 strains from *E. coli* were grown at 37° C in constant agitation at 200 rpm. The culture medium employed was LB (*Luria-Bertani*) medium consisting on 0.5% (w/v) yeast extract, 1% (w/v) bacto-tryptone, 1% (w/v) NaCl, pH 7.0. For agar plates, LB medium was supplemented with 2% (w/v) agar prior to sterilization.

- Yeast culture and maintenance

The yeast strain MaV203 from *S. cerevisiae* was grown at 30° C in constant agitation at 250 rpm. The culture medium employed was YPD consisting on 10 g/l yeast extract, 20 g/l of tryptone and 20 g/l of glucose. For growing restrictions, essential minimal medium (Q-BIOgene) commercially available was employed, being supplemented with 0.8 mM leucine, 0.64 mM histidine and 0.32 mM triptophane, when required.

- Mammal cell lines culture and maintenance

HEK 293T cells were cultured in DMEM (*Dulbecco's Modified Eagle's Medium*) commercially supplemented with 4.5 g/l D-glucose, L-glutamine, sodium pyruvate and sodium bicarbonate (Sigma-Aldrich). 500 ml of medium were supplemented with 10% (v/v) fetal bovine serum (FBS) and 10 ml of a solution consisting on 100 U/ml penicillin and 100 µl/ml streptomycin (P/S). The cells were subcultured for weekly maintenance at 1/10 dilution from an almost confluent plate washing the cells with PBS, detaching with Trypsine-EDTA and diluting them in fresh medium.

P19 cells were cultured in αMEM (*alpha modification Minimum Eagle's Medium*) commercially supplemented with 4.5 g/l D-Glucose, L-glutamine, sodium pyruvate, sodium bicarbonate, ribonucleosides and deoxyribonucleosides (HyClon). 500 ml of medium were supplemented with 7.5% (v/v) newborn calf serum (NCS), 2.5% (v/v) FBS and 10 ml of a P/S solution. The cells were subcultured for weekly maintenance at 1/20 dilution from an almost confluent plate washing the cells with PBS, detaching with Trypsine-EDTA and diluting them in fresh medium.

All the cell lines were cultured in *HEPA Class 100* (Thermo Fisher) incubators with humid atmosphere at 37° C and 5% CO_2. 10 cm ø plates, in addition to 6x and 12x well plates (Nunc) were used to culture the cells in adherent conditions.

7.2.2 DNA/RNA techniques

7.2.2.1 DNA/RNA manipulation and analysis

- PCR (Polymerase Chain Reaction)

The polymerase chain reaction was employed when amplification of DNA fragments was necessary. It was performed using the *Expand High Fidelity* (Roche) kit and a *TC3000* (Techne) thermal cycler. Each PCR reaction was conducted in a total volume of 50 µl, containing 20-50 ng of template DNA, 1 µM of each primer, 2 mM of each deoxy-ribonucleotide, 1 mM $MgCl_2$ and 2.5 units of DNA polymerase in 1x supplied PCR buffer.

The PCR program consisted on an initial denaturing step at 94° C for 5 min, followed by 30 amplification cycles and a final elongation step at 72° C for 10 min. Each amplification cycle was initiated by a denaturing step at 94° C for 1 min, followed by a DNA hybridization step at variable temperature (depending on the Tm for each primer) for 1 min and a final polymerization step at 72° C for a time dependant on the elongated fragment size (1 min/Kb).

- Enzymatic manipulation of DNA fragments

For DNA fragments digestion, diverse restriction enzymes (Fermentas, Takara, New England Biolabs) were employed following the manufacturer's instructions, in addition to the appropriate restriction buffer and digestion temperature. For blunt end production starting from cohesive 5' end fragments, the Klenow fragment from the *E. coli* DNA polymerase I (Promega) was used. For cloning purposes, 1 µg of plasmid DNA or 1/10 from the total volume of a PCR was digested with 5-10 units of restriction enzyme for 2 h at the required temperature.

Prior to DNA ligation, dephosphorylation of the required vector was performed using the calf intestinal alkaline phosphatase (Promega) according to the manufacturer's instructions.

For the ligation of DNA fragments, the T4 DNA ligase (Promega) was employed, following the manufacturer's instructions. Ligations were performed over night at 15° C, following transformation of DNA in competent *E. coli* DH5α.

- Synthesis of RNA probes

Antisense RNA probes were synthesized for *in situ* hybridization experiments. For this, cDNA constructs for *EphA4, HoxB1 and Krox2*0 were linearized with NotI, XbaI and HindIII restriction enzymes (Fermentas), respectively, analysing the restriction efficiency by electrophoresis in 0.8% (w/v) agarose gels, as further explained. RNA probes were obtained by transcription of the linearized plasmids, using the RNA T3 or T7 polymerases with a mixture of fluorescein- or digoxigenin-labelled ribonucleotides (Roche). Transcription reactions were conducted in the presence of RNAse inhibitors (Invitrogen) for 2 h at 37° C. Synthesized probes were then recovered by phenol-chloroform extraction and precipitated with 2 vol of ethanol + 1/10 vol 3 M of lithium chloride (LiCl) for 30 min at -20° C. Integrity of the probes was checked by electrophoresis in 0.8% (w/v) agarose gels, as further described.

- RNA isolation

Total RNA isolation from mammal cells was performed with the *RNeasy® mini Kit* (QIAGEN), according to the manufacturer's instructions. For RNA quality monitoring, 1 µl of each RNA sample was supplemented with 1 µl of 10x loading buffer in a total volume of 10 µl, filled with DEPC H_2O. Integrity of the samples was checked by electrophoresis in 1% (w/v) agarose gels, as further described.

- Retro-transcription (RT) for cDNA obtainment

Prior to cDNA synthesis, contaminant DNA was erased with the *RQ1 RNase-Free DNase* (Promega) kit, according to the manufacturer's instructions. For these cases, 1 µg of RNA was treated with 1 unit of DNase. For the obtainment of cDNA, the *SuperScript® First-Strand Synthesis System* (Invitrogen) kit was employed, following the manufacturer's instructions for the use of random hexamers as reaction primers. Each PCR reaction was performed in a total volume of 20 µl using 0.5-1 µg of RNA.

- DNA/RNA electrophoresis

Electrophoresis of DNA samples in agarose gels was conducted in order to isolate DNA fragments and PCR reactions, or for restriction analysis of DNA constructs. Electrophoresis of RNA fragments was conducted to monitorize the systhesis of RNA probes and quality of total RNA isolation. For this purpose, depending on the DNA or RNA fragment size, 0.5-2% (w/v) agarose gels were prepared by dissolving the required amount of pure agarose in 0.5x TBE buffer (45 mM Tris-borate, 1 mM EDTA pH 8.0). After boiling the suspension in a microwave, 5 µg/ml of ethidium bromide were added to stain the nucleotides. The mixture was placed on electrophoresis chambers with combs and, after cooling down and gelification, covered with 0.5x TBE buffer. DNA and RNA samples were prepared by adding 1/10 volume of 10x loading buffer (0.25% (w/v) bromophenol blue, 0.25% (w/v) xylene cyanol FF, 30% (v/v) glycerol).

For DNA size visualization, 5 µl of *1 Kb Plus Ladder* (Invitrogen) were loaded into one of the lanes. No ladder was employed when analysing RNA. Electrophoresis was conducted at 60-100 V and DNA or RNA was revealed using a *Universal Hood II* (BIO-RAD) trans-illuminator. For image acquisition, the *Quantity One 1-D Analysis Software* (BIO-RAD) was employed.

- DNA/RNA quantification

For nucleic acid quantification, 1 µl of sample was analysed using a *Nanodrop® ND-1000* (Thermo Fisher) spectro-photometer, taking into consideration that values of OD_{260} and OD_{280} should be next to 2.0 for proper nucleic acid purity.

- DNA sequencing

DNA samples were sent to SECUGEN S.L. (Madrid, Spain) for DNA sequencing, according to the company requirements.

7.2.2.2 DNA transformation and isolation

- Bacterial transformation

For routinely transformation, 100 µl of thawed *E. coli* DH5α competent bacteria were mixed with 50-100 ng of plasmid DNA and incubated on ice for 30 min. Then, a heat shock

was applied at 42° C for 75 s and 1 ml of LB was added to the mixture, following incubation at 37° C for at least 1 h to assure the expression of the resistance cassette. Antibiotic selection of transformed bacteria was achieved by seeding them in plates with LB medium supplemented with agar and 100 µg/ml ampicillin or 25 µg/ml kanamycin, depending on the resistance cassette included in the transformed vector, over night at 37° C.

- Bacterial electroporation

Preparation of *E.* coli BL21 (DE3) electrocompetent bacteria was conducted as described in (Green, MR and Sambrook, J, 2012).

For routinely electroporation, 50 µl of thawed electrocompetent bacteria were mixed with up to 25 ng of salt-free DNA and maintained on ice. Meanwhile, electroporation cuvettes (VWR) with 0.2 cm spaced electrodes were also chilled on ice and a *MicroPulser*^{TM} (Biorad) electroporator was set for bacteria, selecting program 2 for the mentioned cuvettes. The cold mixture of bacteria and DNA was then placed on a cuvette and an electrical pulse was applied, immediately resuspending the bacteria in LB medium at room temperature. Cells were then incubated at 37° C for at least 1 h to assure the expression of the resistance cassette.

- DNA preparation from bacteria

For DNA amplification in *E. coli* DH5α, a colony of transformed bacteria was inoculated into 1.5 ml or 100 ml of LB medium supplemented with antibiotics, depending on the preparation scale, and incubated over night at 37° C with constant agitation at 200 rpm. Then, the cultures were harvested by centrifugation for 1-5 min at 10000x g.

The alkaline lysis method was followed (Sambrook, J and Gething, MJ, 1989). For small-scale preparations, 1.5 ml of bacterial culture were harvested by centrifugation and the pellet was resuspended in 100 µl of solution I (50 mM glucose, 25 mM Tris-HCl pH 8.0, 10 mM EDTA pH 8.0). After 5 min at room temperature, 200 µl of Solution II (0.2 M NaOH, 1% (w/v) SDS) were added and mixed by inversion of the tube. After 5 min on ice, 150 µl of Solution III (3 M potassium acetate, 11.5% (v/v) glacial acetic acid) were added and the cell debris was removed after centrifugation at 12000x g for 5 min. Precipitation of plasmid DNA was performed by addition of a volume of 96% ethanol in the presence of salt, followed by a wash with 70% ethanol and resuspension of the DNA pellet in 25 µl of TE buffer.

For medium-scale preparations, the *JETStar™* (GENOMED) purification kit was employed, following the manufacturer's instructions. After plasmid elution, DNA precipitation was performed for plasmid concentration by addition of ethanol and sodium acetate, following incubation at -20° C for at least 2 h. After washing with 70% ethanol, plasmid DNA was resuspended in 10 mM Tris-HCl pH 8.0.

For restriction analysis of plasmid preparations, 1 µg of DNA was digested.

- Yeast transformation

For the introduction of plasmid DNA into yeast, a selected yeast colony was amplified in an YPD plate over night at 30° C and the biomass was harvested and resuspended in 1 ml of Milli-Q H_2O. A flask with 20 ml YPD was inoculated with the appropriate volume of suspended yeast and incubated over night at 30° C in order to achieve an OD_{600} of 0.4 the next day. Then, after harvesting the culture by centrifugation at 3000x g for 5 min, yeasts were washed first in 4 ml of Milli-Q H_2O and then in 2 ml of TE/LiAc buffer: 10 mM Tris-HCl pH 7.5, 1 mM EDTA, 0.1 M lithium acetate (LiAc)). Finally, the pellet of competent yeasts was resuspended in 100 µl of TE/LiAc buffer. For each transformation, 100 µl of competent cells were mixed with 5 µl of DNA carrier solution (10 mg/ml of salmon sperm, boiled during 5 min) and at least 100 ng of plasmid DNA. 300 µl of PEG/LiAc solution (40% (v/v) polyethylene glycol-3350 in TE/LiAc) was added and the mixture was incubated at 30° C for 30 min. Yeasts were then subjected to a heat shock at 42° C for 15 min and centrifuged at 3000x g for 30 s. The pellet was resuspended in 100 µl of Milli-Q H_2O and plated in 10 cm ø plates with the corresponding selective medium. Yeasts were incubated at 30° C for 48-72 h.

- DNA purification

For DNA purification from agarose gels, or in the case that higher DNA quality was required from DNA preparations (e.g. for DNA sequencing), the *FavorPrep™ GEL/PCR Purification Kit* (FAVORGEN Biotech Corp.) was employed, following the manufacturer's instructions.

7.2.2.3 Gene expression and chromatin analysis

- ß-gal activity assay in mammal cells

A lacZ reporter construct responsive to Krox20 was tested in P19 cells cotransfected with several expression vectors. Relative units of ß-galactosidase (ß-gal) were normalized to the value of cells cotransfected only with Krox20 (100%). ß-galactosidase activity of reporter construction was determined using a chemiluminescent assay (Roche). The cytomegalovirus promoter driven luciferase expression vector pGL4.51 (Promega) was used for normalization, employing the *Dual-Luciferase® Reporter Assay System* (Promega) as indicated by the manufacturer.

- ChIP (Chromatin Immunoprecipitation)

For protein crosslink to the chromatin, P19 cells were treated on their 10 cm ø adherent plates, supplementing the medium with crosslink buffer (5 mM HEPES pH 8.0, 10 mM NaCl, 0.1 mM EDTA pH 8.0, 50 µM EGTA pH 8.0 and 1% (w/v) PFA) for 10 min at 37°C. Fixation was quenched adding glycine to a final concentration of 0.1 M and incubating for 5 min at room temperature. After washing the cells twice with cold PBS supplemented with 1x *cOmplete™ Protease Inhibitor Cocktail* (Roche), they were harvested with a scrapper and centrifuged for 5 min at 1500x g. The cell pellet was then lysed with 2.5 ml of lysis buffer 1 (5 mM piperazine-N, N'-bis (2-ethanesulfonic acid) (PIPES) pH 8.0, 85 mM KCl, 0.5% (v/v) NP40), following incubation at room temperature for 5 min and centrifugation for 5 min at 3600x g and 4° C. The pellet was resuspended and lysed in 1 ml of lysis buffer 2 (1% (w/v) SDS, 10 mM EDTA pH 8.0, 50 mM Tris-HCl pH 8.1) supplemented with protease inhibitors.

The lysates were sonicated on ice to shear DNA, using a *Bioruptor* (Diogenode) sonifier, with eight pulses of 30 s each at high output and a pause of 30 s between each pulse, following centrifugation for 5 min at 3600x g and 4° C to recover the chromatin in the supernatant. An aliquot of 50 µl from the total chromatin was then digested adding 350 µl of lysis buffer 2 + 10 µl of 10 mg/ml recombinant proteinase K (Roche) and incubating over night at 65° C. DNA was then recovered by phenol-chloroform extraction and precipitated with 2 vol of ethanol + 1/10 vol 3 M of sodium acetate for 30 min at -80° C, to later quantify DNA concentration and analyse the fragment sizes of sheared DNA in a 1.2% (w/v) agarose

gel. For input controls from each sample, 10 µl of the total chromatin were taken prior to incubation with the antibodies.

To perform the chromatin immunoprecipitation, 30 µg of quantified chromatin from each sample were diluted 1/10 in IP buffer (0.01% (w/v) SDS, 1.1% (v/v) Triton X-100, 1.2 mM EDTA pH 8.0, 16.7 mM Tris-HCl pH 8.1, 167 mM NaCl) supplemented with protease inhibitors. The monoclonal D-11 SUMO1 antibody (sc-5308, Santa Cruz Biotechnology) or the monoclonal M2 Flag antibody (A2220, Sigma-Aldrich) were then added as requested and incubated over night under rotation at 4° C. An additional non-specific interaction control was included per sample with normal mouse IgG (Sigma-Aldrich). Next, 1 µl protein G beads (Roche) per µg of chromatin, previously washed and equilibrated in IP buffer, was added and incubated for 2 h under rotation at 4° C to collect proteins-DNA complexes. Then, beads were subsequently washed with 1 ml of washing buffer 1 (0.1% (w/v) SDS, 1% (v/v) Triton X-100, 2 mM EDTA, 20 mM Tris-HCl pH 8.1, 150 mM NaCl), 1 ml of washing buffer 2 (0.1% (w/v) SDS, 1% (v/v) Triton X-100, 2 mM EDTA, 20 mM Tris-HCl pH 8.1, 500 mM NaCl), 1 ml of washing buffer 3 (0.25 LiCl, 1% (v/v) NP40, 1% (w/v) sodium deoxycholate, 1 mM EDTA, 10 mM Tris-HCl pH 8.1), as well as two final washes with TE1x buffer (10 mM Tris-HCl pH 8.1, 1 mM EDTA).

The protein-DNA complexes were eluted by incubating the beads with 80 µl of elution buffer (TE1x buffer + 1% (w/v) SDS) for 10 min at 65° C. 60 µl of the supernatant were recovered. 50 µl of elution buffer were also added to the 10 µl of input, and the mix was incubated for 10 min at 65° C. Then, 90 µl of elution buffer were added to the 60 µl from the immunoprecipitation or the input resulting from the previous step. The resulting 150 µl from each sample were incubated over night at 65° C.

To decrosslink DNA from proteins, immunoprecipitation and input samples were digested with proteinase K for 1 h at 37° C, following phenol-chloroform DNA extraction and precipitation, as previously indicated to finally resuspend the DNA in 50 µl of MilliQ H_2O.

- qPCR (quantitative PCR)

Quantitative PCR analysis was used in this work to analyse gen expression and to monitor incorporation of proteins to specific DNA sequences by chromatin immuno-precipitation. The Primer3Plus tool was employed for the design of qPCR primers (see Table M-6). The parameters were set for an amplicon length of 50-150 pb and a Tm for both

primers of 60° C. Primers were synthesized by Sigma-Aldrich and tested by analysis of a standard curve with five serial dilutions 10x from one cDNA sample. Curves with values about -3.3 or -3.4 indicated adequate amplification efficiency.

The qPCR analysis was performed using 96x well plates (Applied Biosystems) with a total volume of 20 µl of PCR reaction per well. The *SensiMix™ SYBR® Low-ROX* (BIOLINE) kit was employed for the preparation of each PCR reaction, following the manufacturer's instructions and in cold conditions. For ChIP analysis, 3 µl from a 1/10 dilution of the obtained final DNA samples were included in each reaction. For the P19 cDNA analysis, 3 µl from a 1/10 dilution of the total cDNA were included in each reaction, performed in triplicates. For plate sealing, adhesive film (VWR) was used. For Ct values normalization, *GAPDH* was analysed in ChIP experiments and r18S RNA was analysed in gene expression experiments. The reactions were conducted in a *7500 FAST Real-Time PCR* (Applied Biosystems) thermal cycler, as indicated by the manufacturer. The PCR program consisted on an initial denaturing step at 95° C for 10 min, followed by 40 amplification cycles, each one consisting on a first step at 95° C for 15 s and a second at 65° C for 1 min. A final dissociation cycle consisting on 15 s at 95° C, 1 min at 65° C, 15 s at 95° C and 15 s at 60° C, was performed to detect possible contaminants. Algorithms for calculation of relative units and normalization of values according to primer efficiency have been previously described in (Pfaffl, MW, 2001).

- *In situ* mRNA hybridization

This technique was employed to monitorize gene expression in the chick hindbrain, by the use of specific RNA probes. For this purpose, following rehydration of chicken embryos in PBS, hindbrains were dissected from the embryos and digested in 1.5 ml tubes with 20 µg/ml of proteinase K (Roche) in PBTr 0.1 (0.1% (v/v) Triton X-100 in PBS) for 12 min and then washed with PBTr 0.1. Hindbrains were then fixed with fixing solution (4% (w/v) PFA and 0.1% (v/v) glutaraldehyde in PBTr 0.1) and washed with PBTr 0.1.

For hybridization of the probes to mRNA, hindbrains were previously incubated with pre-hybridizing solution (50% (v/v) formamide, SSC 5x (0.75 M NaCl, 75 mM sodium citrate pH 7.0), 5 mM EDTA, 2% (w/v) blocking reagent (Roche), 50 µg/ml heparin, 50 µg/ml yeast tRNA, 0.1% (v/v) CHAPS and 0.1% (w/v) SDS) for 2 h at 65° C under agitation. Then, hybridization was performed by incubation of the hindbrains with fresh pre-hybridizing

solution supplemented with 1:100 vol of the required RNA probes, over night at 65° C under agitation. After three washes of 20 min each with 2x SSC + 0.1% (v/v) CHAPS and three additional washes with 0.2x SSC + 0.1 (v/v) CHAPS, hindbrains were equilibrated in KTBT solution (50 mM Tris-HCl pH 7.5, 150 mM NaCl, 20 mM KCl, 0.1% (v/v) Triton X-100) for 10 min at room temperature.

For hybridization with specific antibodies for digoxigenin or fluorescein, hindbrains were previously incubated with blocking solution (20% (v/v) FBS in KTBT solution) for 2 h at room temperature and then incubated with digoxigenin or fluorescein antibodies (Roche) at a 1:2000 dilution in blocking solution over night at 4° C under rotation. Next, nine washes of 20 min each were performed with KTBT at room temperature.

Revelation of hybridized probes was conducted by equilibrating the hindbrains in NTMTL solution (0.1 M Tris-HCl pH 9.5, 50 mM $MgCl_2$, 0.1 M NaCl, 0.1% (v/v) Triton X-100 and 0.5 mg/ml Levamisole (Sequoia Research Products Ltd)), following incubation with fresh NTMTL supplemented with NBT or BCIP substrate (Roche) for digoxigenin or fluorescein staining, respectively, in darkness at room temperature till tissue staining was appreciable. Revelation was stopped with subsequent washes with PBTr 0.1 and then hindbrains were mounted on cover slides for image acquisition with a epifluorescence DM6000 microscope (Leica Microsystems GmbH).

In the cases where double *in situ* RNA hybridization was necessary, sequential hybridization was performed, revealing in the first place the fluorescein antibody.

7.2.3 Model organisms

7.2.3.1 Cell culture techniques

- Transient transfection of mammal cells

To perform transient transfection of P19 growing in αMEM + 7.5% (v/v) NCS + 2.5% (v/v) FBS + P/S or HEK-293T cells growing in DMEM + 10% (v/v) FBS + P/S, a number of cells were seeded in adherent 10 cm ø plates, 6x or 12x well plates and transfected after 24 h with 1 µg, 2 µg or 10 µg of DNA respectively. For this purpose, the *Lipofectamine® 2000* (Invitrogen) reagent and the *OptiMEM®* (Gibco) medium were employed according to the manufacturers instructions. Cells were harvested 24-48 h after transfection.

Transient transfection of small interfering RNA (siRNA) molecules was performed using the *Oligofectamine® 2000* (Invitrogen) transfection reagent and the *OptiMEM®* (Gibco) medium, according to the manufacturers instructions. The transfected cells were harvested 48-72 h after transfection, depending on the experiment.

- P19 neuronal differentiation with RA

To obtain neuron differentiated P19 cells, $5 \cdot 10^5$ cells were seeded in non-adherent sterile 10 cm ø plates (Monolab) and grown in suspension with αMEM + 5% (v/v) FBS + P/S + 2 µM RA during 4 d, refreshing the medium the second day. The fourth day, when embryonic bodies were properly formed, they were harvested into 15 mL tubes and centrifuged at 1,500x g for 5 min and media was removed, resuspending the embryonic bodies in fresh αMEM + 7.5% NCS + 2.5% FBS + P/S without any RA. Embryonic bodies were then mechanically disaggregated with a 10 ml pipette and seeded in adherent 10 cm ø plates (Nunc) for three more days. During this last period, axon and dendrite-like processes start to form during the final differentiation. The complete experiment took 7 days but cells were harvested at various time points during the process.

- P19 large-scale SILAC experiment for neuronal differentiation

To perform a Stable Isotope Labelling with Amino acids in Cell culture (SILAC) experiment in proliferating and neural differentiating P19 cells, the cells were amplified for four days in 10 cm ø adherent plates and grown in light amino acids (AA) medium (Silantes DMEM (*Dulbecco's Modified Eagle's Medium*) + 2 mM L-Glutamine + 10 U/ml of penicillin + 10 µg/ml streptomycin + 146 µg/ml Lys + 84 µg/ml Arg) supplemented with 10% (v/v) dialysed FBS, or grown in heavy AA medium (Silantes DMEM + 2 mM L-Glutamine + 10 ml of penicillin/streptomycin + 146 µg/ml D4 Lys + 84 µg/ml [^{13}C]Arg) supplemented with 10% (v/v) dialysed FBS. During these four days, sufficient to achieve around six cell division rounds, the cells incorporated the SILAC specific amino acids.

For the first experiment, $2 \cdot 10^6$ of the cells grown in the heavy AA condition were seeded in 45 adherent plates for proliferation, and still grown in heavy AA medium supplemented with 10% (v/v) dialysed FBS for two more days before harvesting them. Also, 10^6 of the cells grown in the light AA condition were seeded in 90 non-adherent plates for differentiation, and grown in light AA medium supplemented with 5% (v/v) dialysed FBS and

2 µM RA during 4 d, refreshing the medium the second day. The harvesting procedure was conducted as indicated in (Barysch, SV *et al.*, 2014). Briefly, a total amount of approximately $9 \cdot 10^8$ proliferative adherent cells were washed in cold PBS + 10 mM NEM and then directly lysed on the plates with 170 µl of 2x lysis buffer (2% (w/v) SDS, 10 mM EDTA, 10 mM EGTA, 20 mM NEM, 2 mM Pefabloc and 2 mg/ml of protease inhibitors (aprotinin, leupeptin and pepstatin) in PBS) by scrapping the cells directly on the plates with the lysis buffer and obtaining a total lysate volume of approximately 15 ml. In the case of differentiating cells, a total amount of approximately $9 \cdot 10^8$ suspended cells were harvested by centrifugation at 500x g for 5 min, washed in cold PBS + 10 mM NEM and resuspended in a total volume of 16 ml of PBS. Then, cells were lysed adding 16 ml of 2x lysis buffer. The cell lysates were snap-freezed with liquid nitrogen and stored at -80° C.

To perform the reverse experiment, $2 \cdot 10^6$ of the cells grown in the light AA condition were seeded in 45 adherent plates for proliferation, and still grown in light AA medium supplemented with 10% (v/v) dialysed FBS for two more days before harvesting them. Additionally, 10^6 of the cells grown in the heavy AA condition were seeded in 90 non-adherent plates for differentiation, and grown in heavy AA medium supplemented with 5% (v/v) dialysed FBS and 2 µM RA during 4 d, also refreshing the medium the second day. The harvesting procedure was conducted as previously described for the first experiment.

- P19 serum stimulation

To induce protein expression dependent on serum stimulation in P19 cells, $1.5 \cdot 10^5$ cells were seeded in 6x well plates and initially grown in αMEM + 0.1% (v/v) FBS + P/S for 48 h. Then, the medium was replaced with fully supplemented αMEM + 7.5% (v/v) NCS + 2.5% (v/v) FBS + P/S for 2 h to trigger serum-induced responses prior to cell harvesting.

7.2.3.2 Chicken embryos

- Electroporation of the chicken hindbrain and neural tube

This technique was used to introduce DNA expression vectors and silencing constructs in the neural progenitors and cells present in the hindbrain and neural tube of the chick embryo, as described in (Itasaki, N *et al.*, 1999) and (Giudicelli, F *et al.*, 2001).

For this purpose, fertilized eggs were incubated at 38° C in a *Heraeus* (Thermo Fisher) incubator till the desired developmental stage was reached. DNA plasmids were suspended in 10 mM Tris-HCl pH 8.0 at the required concentration and 0.05% (v/v) Fast-Green FCF was added to visualize the DNA solution during the injections. A GFP expression vector was also included in all DNA solutions at a concentration of 0.3 µg/µl to monitor electroporated cells by immunofluorescence. The DNA solution was injected in the lumen of the neural tube using a glass capillary and the embryos were electroporated at the hindbrain or the neural tube level with a *BTX820* (Quantum) electroporator, employing 4 or 6 pulses, respectively, of 50 ms at 25 V and 1 Hz with 500 ms between pulses. Following reincubation for 24 h in hindbrain analyses and for 10 to 40 h for spinal cord analyses, the embryos were extracted from the egg in PBS and fixed in a 4% (w/v) PFA solution for 3 h at room temperature or over night at 4° C. After four washes of 15 min each using PBS to remove traces of PFA solution, the electroporated section of the embryo was dissected by visualization of GFP in a fluorescence magnifier (Nikon). Finally, the embryos were dehydrated in subsequent washes of 5 min using increasing concentrations of methanol in PBS (25%, 50%, 75% and 100% (v/v)) for long term storage at -20° C.

7.2.4 Protein techniques

7.2.4.1 Protein induction and extraction

- *In vitro* protein translation

In vitro translation in the presence of [^{35}S]Met was performed with the *TnT® Quick Coupled Transcription/Translation Systems* (Promega) kit, following the manufacturer's instructions for a standard reaction.

- Protein expression in *E. coli*

Heterologous expression of GST- or polyhistidine-tagged proteins was performed in *E. coli* by cloning the cDNA sequence into a pGEX-6P-3 (GE Healthcare) vector for the GST constructs, or a pET28a+ (Novagen) vector for the polyhistidine-tagged construct. For this purpose, the vectors were electroporated in *E. coli* BL21 (DE3) electrocompetent bacteria and 15-100 µl of this culture was inoculated to 1-2 l of LB medium supplemented with the

requested antibiotic. The bacterial culture was grown to reach an OD_{600} of about 0.5 and 1 ml of bacteria was then harvested as non-induced control. To induce protein expression, 1 mM isopropyl-ß-D-1-thiogalactopyranoside (IPTG) was added to the culture, which was grown at 24° C for 4 h, prior to harvest it by centrifugation for 10 min at 10000x g.

- Protein extraction by sonication

This technique was typically conducted to purify proteins expressed in *E. coli*. For this purpose, the cell pellet was resuspended in 30 ml of 1 mM phenylmethylsulfonyl (PMSF) in PBS to avoid protease action. Then, the cells were sonicated using a *Digital Sonifier S-450D* (Branson) with a 3 mm microtip. The parameters were set to 6 pulses of 30 s each at 40% amplitude, with a pause of 30 s between each pulse and maintaining cold conditions. Once sonicated, the protein extract was centrifuged for 10 min at 15000x g and 4° C, recovering the supernatant to remove cell debris.

- Protein extraction with urea buffer

This technique was performed in the cases that denaturing conditions had to be achieved during protein extraction to preserve protein extracts from the action of peptidases. For this purpose, thorough lysis of harvested cells was conducted in urea buffer (8 M urea, 10 mM Tris-HCl pH 8.0), using a 1 ml syringe with a 0.5 mm ø needle (BD) to mechanically break DNA. After protein quantification of the lysates and boiling in Laemmli buffer (0.1 M Tris-HCl pH 6.8, 8% (v/v) glycerol, 1.6% (w/v) SDS, 4% (v/v) 2-mercaptoethanol, 12.5‰ (w/v) bromophenol blue) (Laemmli, UK, 1970), samples were analysed by SDS-PAGE.

- Protein extraction with SDS buffer

Alternatively, for also preserving protein extracts from the action of peptidases, harvested cells were lysed in SDS buffer (1% SDS wt/v, 5 mM EDTA, 5 mM EGTA, 10 mM N-ethylmaleimide (NEM), 1x *cOmplete™ Protease Inhibitor Cocktail* (Roche) in PBS) and sonicated using a *Digital Sonifier S-450D* (Branson) with a 3 mm microtip. The parameters were set to 6 pulses of 30 s each at 10% amplitude, with a pause of 30 s between each pulse. Protein extracts were then centrifuged for 15 min at 15000x g and supernatant was recovered to eliminate cell debris. After protein quantification, samples were boiled in Laemmli buffer and analysed by SDS-PAGE.

- Protein extraction with Triton/NP40 buffer

When non-denaturing conditions had to be maintained, harvested cells were lysed with Triton buffer (50 mM Tris-HCl pH 7.5, 150 mM NaCl, 1% (v/v) Triton X-100, 1 mM EDTA and 1x *cOmplete™ Protease Inhibitor Cocktail* (Roche)) or NP-40 buffer (50 mM Tris-HCl pH 8.0, 150 mM NaCl, 1% (v/v) Nonidet P-40, 0.5% (w/v) sodium deoxycholate and 1x *cOmplete™ Protease Inhibitor Cocktail* (Roche)) as indicated. Lysates were then kept on ice for 30 min. After centrifugation and protein quantification of the supernatants, protein samples were boiled in Laemmli buffer and analysed by SDS-PAGE or used for other purposes.

7.2.4.2 Protein purification, pull-down and immunoprecipitation

- Purification of GST-tagged proteins

GST-tagged proteins were heterologously expressed in bacteria by induction with IPTG and then purified by glutathione-affinity chromatography using a *Glutathione Sepharose™ 4B* (GE Healthcare) matrix, following the manufacturer's instructions. Then, the adsorbed proteins were eluted with 10 mM reduced glutathione or cleavaged from GST using the *PreScission* (GE Healthcare) enzyme according to the manufacturer's instructions. Protein purification was checked by SDS-PAGE and staining with Coomassie blue (0.25% (w/v) Coomassie Brilliant blue, 40% (v/v) methanol, 10% (v/v) glacial acetic acid).

- GST *in vitro* pull-down

For pulling down Krox20 interacting with Ubc9, 0.5-1 µg of GST or GST-Ubc9 bound to a *Glutathione Sepharose™ 4B* (GE Healthcare) matrix were incubated with *in vitro* translated Krox20 (1/10 of the reaction) in 200 µl of binding buffer (20 mM Tris-HCl pH 7.0, 100 mM NaCl, 1 mM EDTA, 10% glycerol, 0.01% Nonidet P40) and washed, first with binding buffer and then with binding buffer supplemented with 0.4 M NaCl. Samples were boiled in Laemmli buffer and analysed by SDS-PAGE.

- Ni^{2+} affinity pull-down for polyhistidine-tagged proteins

This protocol was used for pulling down polyhistidine-tagged proteins, heterologously expressed in mammal cells after transfection or after protein purification from bacteria through expression induction with IPTG.

For pull-down, the cell pellets were thoroughly lysed in lysis buffer (0.1 M phosphate buffer pH 8.0, 8 M urea) with a 1 ml syringe connected to a 0.5 mm ø needle (BD) to mechanically break DNA. After centrifugation for 10 min at 16000x g, protein concentration in the supernatant was determined and inputs taken. Then, 50 µl of *His-Select® Nickel Affinity Gel* (Sigma-Aldrich) were added and incubated for 2-3 h under rotation at room temperature. Beads were centrifuged for 30 s at 2000x g and washed three times with 1 ml of wash buffer (0.1 M phosphate buffer pH 6.3, 8 M urea). Proteins were eluted from the beads incubating them in Laemmli buffer for 20 min at room temperature and centrifuging the beads to recover the supernatants. Inputs and precipitated proteins were analysed by SDS-PAGE, following Coomassie blue staining or Western blot analysis.

For Nab2 purification, the same protocol was conducted using a non-denaturing lysis buffer (0.1 M phosphate buffer pH 8.0, 1% (v/v) Triton X-100, 5 M NaCl and 1x *cOmplete™ Protease Inhibitor Cocktail* (Roche)) and eluting proteins from the beads with increasing concentrations of imidazole, from 5 mM to 200 mM.

- Immunoprecipitation of Flag-tagged proteins

For this procedure, P19 cells were harvested with cold PBS and centrifuged for 5 min at 1500x g, following lysis in IP buffer (50 mM Tris-HCl pH 8.0, 150 mM NaCl, 1.5 mM EDTA pH8.0, 1x *cOmplete™ Protease Inhibitor Cocktail* (Roche)) + 1% (v/v) Triton X-100 by rotating the suspension for 10 min at room temperature. After centrifugation for 10 min at 10000x g, total protein in the supernatants was quantified and inputs were taken. Then, Triton X-100 concentration was lowered to 0.33% (v/v) adding IP buffer without detergent. Flag-tagged proteins were then immunoprecipitated using the *Anti-Flag® M2* (Sigma-Aldrich) affinity gel, according to the manufacturers instructions.

For this, Anti-Flag beads were added to the protein extracts and incubated for 2-3 h at 4° C, following three washes with cold IP buffer + 0.33% (v/v) Triton X-100. Bound proteins were eluted boiling the beads at 96° C for 4 min in the presence of Laemmli buffer. Inputs and immunoprecipitated proteins were analysed by SDS-PAGE.

- SUMO immunoprecipitation and peptide elution

For enrichment of SUMOylated products, an immunoprecipitation protocol that involves specific peptide elution was employed (Barysch, SV *et al.*, 2014), allowing the purification of endogenously SUMOylated proteins.

Briefly, denaturing conditions were reached in each lysate batch by addition of DTT at a final concentration of 50 mM and incubating the samples at 60° C for 10 min. Then, lysates were sonicated using a *Digital Sonifier II 450* (Branson) with 6-7 cycles. The parameters were set to cycles of 1 min, performing 1 s pulses at a 45% of amplitude, with 1 s between pulses. Then, RIPA conditions were achieved by diluting each sample 1/10 with RIPA dilution buffer (5 mM EDTA, 5 mM EGTA, 10 mM NEM, 1 mM Pefabloc and 1 mg/ml each of protease inhibitors) and adding 10 mM NEM. For each set of experiments, proliferative and differentiated cell lysates were then mixed in a protein proportion of 1:1, after protein quantification, and inputs from each set of experiments were taken. For the first experiment, 150 ml of lysate from the proliferative condition at a protein concentration of 0.825 mg/ml were mixed with 160.5 ml of lysate from the differentiating condition at a protein concentration of 0.77 mg/ml, resulting in 310.5 ml of combined lysate.

For the second experiment, 150 ml of lysate from the proliferative condition at a protein concentration of 1.2 mg/ml were mixed with 180 ml of lysate from the differentiating condition at a protein concentration of 1.0 mg/ml, resulting in 330 ml of combined lysate.

For the SUMO immunoprecipitation, each combined lysate was equally splitted into three batches and 1 ml of beads, coupled with control IgG or with SUMO1 or SUMO2/3 antibodies, were added per immunoprecipitation and incubated over night at 4° C under rotation. After taking flow-through samples, beads were washed three times with RIPA buffer (0.1% (w/v) SDS, 5 mM EDTA, 5 mM EGTA, 10 mM NEM, 1 mM Pefabloc and 1 mg/ml each of aprotinin, leupeptin and pepstatin) and, after a pre-elution step with pre-elution buffer (20 mM phosphate buffer pH 7.4, 500 mM NaCl, 1% (v/v) Triton X-100, 0.5% (w/v) sodium deoxycholate, 0.1% (w/v) SDS, 5 mM EDTA, 5 mM EGTA, 10 mM NEM, 1 mM Pefabloc and 1 mg/ml of protease inhibitors), elution of SUMOylated proteins was performed in two steps, supplementing fresh pre-elution buffer with 0.5 mg/ml of SUMO1 (VPMNSLRFLFE) or SUMO2 (IRFRFDGQPI) peptides. For control IgG elution, a mixture of 0.25 mg/ml of both SUMO1 and SUMO2 peptides was used.

Eluted proteins were precipitated with 10% trichloroacetic acid (TCA) and washed in cold acetone. To check immunoprecipitation efficiency, inputs, flow-throughs and 0.05% of the total eluted volume were analysed by SDS-PAGE. The remaining inputs and eluted proteins were loaded into a 4-12% NuPAGE® gel for protein separation and MS analysis.

7.2.4.3 Yeast two-hybrid

The two-hybrid system *ProQuest™ Two-Hybrid System* (Invitrogen) was employed with a Krox20 deletion construct lacking its trans-activation domains and a cDNA library (Invitrogen) from 8.5 days whole mouse embryo, to search for protein-protein interactions with Krox20. The cDNA insert had an average size of 1.2 kb and was directionally cloned.

In this technique, a fusion protein consisting on truncated Krox20 and the DNA binding domain (DB) of the transcription factor Gal4 (included in the pDBLeu vector, which allows growth in leucine-free medium) is cloned. An additional fusion protein encompassing the second protein of interest coded in the cDNA library and the transactivation domain (AD) of the Gal4 transcription factor (in the pPC86 vector, which allows growth in tryptophan-free medium) is also obtained. If there is an interaction between both proteins of interest in the MaV203 strain of *S. cerevisiae*, the chimeric transcription factor is reconstituted and activates the expression of reporter genes *HIS3* (that allows growth in histidine-free medium) and *LacZ* (whose expression leads to colour appearance when treating with 5-bromo-4-chloro-3-indolyl-ß-D-galactopyranoside (X-Gal)). For this experiment, a 3-amino-1, 2, 4-triazole (3AT) concentration of 10 mM was determined to block basal activation of the *HIS3* reporter gen.

- ß-galactosidase activity assay

Yeast to be tested and their controls were plated in 10 cm ø sterile plates (Monolab) with minimal non-selective medium and grown at 30° C for 72 h till required biomass was obtained. Then, 5 ml of 1 M phosphate buffer pH 7.0 (174,2 g/l K_2HPO_4 and 136,1 g/l KH_2PO_4) and 5 ml of agarose 1% w/v were heated to 50° C. This was combined with 100 µl of SDS 10% w/v, 600 µl of N, N'-dimethylformamide (DMF) and 100 µl of X-Gal 4% w/v in DMF and the mixture was poured over the yeast. Plates were dried for 5 min and incubated at 30° C in darkness. Results were visible after 30 min-12 h.

7.2.4.4 Protein analysis

- Protein quantification

Protein extracts were quantified by Bradford method. For this purpose, 3 µl of protein extract were mixed to 1 ml of *Dye Reagent Concentrate* (Bio-Rad). After incubating the mixture for 5 min, absorbance was measured at 595 nm with a DU® 800 spectrophotometer (Beckman Coulter) and protein concentration was obtained using a calibration curve of bovine serum albumin (BSA). Alternatively, purified proteins were quantified by comparing Coomassie blue staining of serial 1:3 dilutions of BSA in polyacrylamide gels.

- SDS-PAGE

SDS polyacrylamide gel electrophoresis was employed for molecular weight-dependent separation of proteins and conducted as described by (Laemmli, UK, 1970), following the Tris-Glycine method.

For this purpose, discontinuous 7.5 to 15% mini-gels were prepared using the *Mini-PROTEAN® Tetra Cell* casting system, pouring the separating buffer (0.375 M Tris-HCl pH 8.8, 7.5 or 15% (v/v) polyacrylamide (acrylamide and bis-acrylamide 29:1), 0.1% (w/v) SDS, 0.1% APS and 0.05% (v/v) TEMED) with an overlay of 2-propanol. Once the separating buffer was polymerized 2-propanol was removed, stacking buffer (0.125 M Tris-HCl pH 6.8, 4% polyacrylamide (acrylamide and bis-acrylamide 29:1), 0.1% (w/v) SDS, 0.1% (v/v) ammonium persulfate (APS) and 0.05% (v/v) tetramethylethylenediamine (TEMED)) added and combs placed. Once stacking buffer was polymerized, gels were stored at 4° C under high humidity conditions.

Prior to protein migration, Laemmli buffer was added to the samples and they were boiled for 1 min at 96° C. Samples were loaded into the gels, submerged in running buffer (25 mM Tris, 192 mM Glycine pH 8.3 and 0.1% (p/v) SDS). A pre-stained 10-170 kDa marker (Fermentas, Thermo Fisher), unstained 10-200 kDa marker (Thermo Fisher) or unstained 10-200 kDa (Biorad) was loaded in one of the lanes to monitorize the protein molecular weights. Samples were migrated for around 45 min at 190 V.

- Western blot

This method is used to transfer proteins from an SDS-PAGE to a membrane for further visualization of proteins using antibodies against specific proteins of interest or against commercial tags.

In this work, proteins were transferred to a nitrocellulose *Trans-Blot® Transfer Medium* membrane or to a methanol activated *Immun-Blot® PVDF* membrane (Bio-Rad) using a *Trans-Blot® Turbo™* (Biorad) semi-dry transfer apparatus. For this purpose, the membrane was placed underneath the gel and four Whatman sheets were placed on the gel and under the membrane, all soaked in transfer buffer (20% (v/v) methanol in running buffer). Transference was performed at 25 V and 1 A per mini-gel during 30 min, following a quick wash in PBS and protein staining with Ponceau (1% (w/v) Ponceau S red, 5% (v/v) glacial acetic acid). The stain excess was removed with subsequent washes with Milli-Q H_2O. Then, membrane was blocked with blocking solution (5% (w/v) skim dried milk (Central Lechera Asturiana) in PBTw (0.1% (v/v) Tween 20 in PBS)) for 1 h. Primary antibodies were added to a new volume of blocking solution at the indicated concentration and incubated with the membrane for 2h at room temperature or overnight at 4° C in a humid chamber. To remove the excess of primary antibodies, five washes of 10 min each were performed with PBTw.

Horseradish peroxidase (HRP) coupled antibodies were prepared in PBTw at the indicated concentration and incubated with the membrane for at least 45 min at room temperature, following three more washes of 10 min with PBTw. The proteins of interest were revealed by chemiluminescence with the *Clarity™ Western ECL Substrate* (Biorad) kit on *Hyperfilm MP* (GE Healthcare) photographic films using a Hyperprocessor SRX-101A (GE Healthcare) apparatus.

- Immunofluorescence of mammal cells

To visualize proteins endogenously expressed in mammal cells or after transfection of expression vectors, immunofluorescence experiments were performed using specific antibodies against the desired protein or against commonly used tags.

Cells cultured for immunofluorescence experiments were seeded in 12x well plates (Nunc) with one 1.9 cm ø cover slide (Thermo Fisher) per well. Prior to seeding from 10^4 to $9{\cdot}10^4$ P19 cells, depending on the experiment, each well was washed with 96% EtOH and

rinsed three times with PBS. After the corresponding experiments with mammal cells were performed, growing medium was removed and the wells were washed with PBS. Then, 1 ml of PFA solution (4% (w/v) paraformaldehyde (PFA) in PBS) was added to each well for cellular fixation during 10 min. Following three washes of 5 min each under gentle agitation, the cells were permeabilized with 1 ml of PBTr 0.5 (0.5% (v/v) Triton X-100 in PBS) for 15 min and then rinsed with PBTr 0.1 (0.1% (v/v) Triton X-100 in PBS).

For further steps, coverslips were placed on a flat surface in a dark humid chamber. Cells were blocked adding a volume of 100 µl of blocking solution (10% (v/v) donkey serum in PBTr 0.1) during at least 30 min. Cells were then incubated for at least 1 h with a new volume of blocking solution supplemented with primary antibodies at the indicated dilution. After three washes of 5 min with PBTr 0.1, secondary antibodies conjugated with the requested fluorophores were supplemented to a new volume of PBTr 0.1 and incubated with the cells for at least 30 min. After three washes with PBTr 0.1, a last wash including 0.1 µg/ml 4', 6-diamidino-2-phenylindol (DAPI) was performed to stain the nuclei. Following a last wash with Milli-Q H_2O, the coverslips were mounted on a microscope slide using *VECTASHIELD®* (Vector) and nail polish to seal the coverslips and slides. Once sealed, samples were stored at 4° C in darkness till image acquisition using an epifluorescence DM6000 microscope (Leica Microsystems GmbH).

- Immunofluorescence of chicken embryos

Immunofluorescence was also employed to visualize proteins expressed in flat mounts from the hindbrain or transversal sections from the neural tube of chicken embryos.

For this purpose, electroporated structures were rehydrated through subsequent washes of 5 min using decreasing concentrations of methanol (75%, 50% and 25% (v/v)), and a final wash using PBTr 0.25 (0.25% (v/v) Triton X-100 in PBS) was performed. Then, in the case of transversal sections be needed, the structures were included in 4% (w/v) pure agarose in PBS and, 40 µm sections were obtained using a Leica VT 1000 S vibratome. The following procedures were performed in darkness. Sections were blocked during 1 h 30 min using 1 ml of blocking solution (5% (v/v) donkey serum in PBTr 0.25), following incubation over night at 4° C with a new volume of blocking solution supplemented with primary antibodies at the indicated dilution. After six washes of 15 min each with 1 ml of PBTr 0.25, the sections were incubated during 2 h with a new volume of PBTr 0.25 supplemented with

the corresponding secondary antibodies conjugated to fluorophores. After six washes of 15 min with PBTr 0.25, a final wash including 0.1 µg/ml 4', 6-diamidino-2-phenylindol (DAPI) was performed to stain the cell nuclei. Finally, samples were mounted on a microscope slide using *VECTASHIELD®* (Vector) and nail polish to seal the coverslips and slides. In the case of flat mounts, the sections were dorsally dissected, prior to mounting them on the slides. Once sealed, the sections were stored at 4° C in darkness till image acquisition using a confocal TCS SP5 microscope (Leica Microsystems GmbH).

7.2.5 Other techniques

- *In vitro* SUMOylation assays

To test *in vitro* protein SUMOylation, 200 µM ATP, 1 mM dithiothreitol (DTT), 4 mM $MgCl_2$ were added to the following purified proteins: 200 ng Sae1/Uba2, 500 ng Ubc9, 1 µg SUMO1GG, 100 ng Nab2 and 25 ng of Krox20. All this components were incubated in the SUMOylation buffer (20 mM HEPES (N-2-hydroxyethylpiperazine-N'-2-ethanesulfonic acid) pH 7.6, 50 mM NaCl, 0.05% Tween) for 90-180 min at 30° C.

- Preparation of beads coupled to SUMO antibodies for immunoprecipitation

Antibody-coupled beads were needed to perform the SUMO immunoprecipitation of P19 protein extracts. As starting material, batches of antibody supernatants from SUMO1-21C7 and SUMO2-8A2 hybridoma cells (The Developmental Studies Hybridoma Bank at the University of Iowa) were obtained after growing the cells in a *CELLine CL350* (Integra) two-compartments bioreactor, according to the manufacturer's instructions.

After protein quantification of each batch of supernatant, 1 ml of protein G-agarose beads (Roche) were prepared for each 8 mg of SUMO1 or SUMO2/3 antibody to be coupled, in addition to control beads prepared with mouse normal IgG (Life Technologies). Crosslink of the antibodies to the beads was preformed as described in (Barysch, SV *et al.*, 2014), as well as tests to check crosslink between beads and antibodies. For this, control samples of beads coupled to the antibodies prior and after cross-link (Non X-link and X-link, respectively) were taken and, after centrifugation, bead pellets were incubated with 2x SDS sample buffer (125 mM Tris pH 6.8, 5% (w/v) SDS, 0.2% (w/v) bromophenol blue, 25% (v/v) glycerol) for 30 min at 37° C. After centrifugation, supernatant was collected and 2x SDS

sample buffer was added to the bead pellets. As a final step, 200 mM DTT was added to both supernatant and bead samples and they were boiled for 5 min at 96° C. Then, the presence of light and heavy antibody chains in the samples was analysed by SDS-PAGE and further staining with Coomassie blue. Beads coupled to antibodies were stored at 4° C for further immuno-precipitation experiments.

- Fetal bovine serum dialysis

To supplement the culture media used for the SILAC experiment, dialyzed serum is necessary in order to avoid contamination with undesired non-labelled amino acids.

For this SILAC experiment, the necessary amount of FBS was dialyzed using a 10 kDa pore dialysis membrane and diluting three times 1:10 in PBS during 48 h at 4° C. The dialyzed serum aliquots were stored at -20° C till needed.

- Mass Spectrometry analysis and data processing

Mass spectrometry (MS) analysis was performed in the Core Facility for Mass Spectrometry and Proteomics (CFMP) at the Center for Molecular Biology of the University of Heidelberg (ZMBH). The obtained data was analysed and filtered by Dr. Sina Barysch and Dr. Annette Flotho in the group of Prof. Dr. Frauke Melchior, at the ZMBH.

7.2.6 Data processing

- Statistical analysis

Student's-t test was performed to assess the statistical significance when comparing samples with the same variance. For the showed data, *P* values were indicated as follows: *P < 0.05; **P < 0.01; ***P < 0.001.

- Bioinformatics tools

For the design of oligonucleotides, the Primer3Plus tool (www.bioinformatics.nl/cgi-bin/primer3plus/primer3plus.cgi) was employed. For the analysis of oligonucleotides, Amplify 3.1 software designed by B. Engels (Department of Genetics, University of Wisconsin, WI) was employed.

For DNA sequence analysis and post-sequencing verification, DNA Strider 1.3 (Service de Biochemie, Centre d'Etudes Nucléaires de Saclay, France) and 4 Peaks 1.7.2 (Nucleobytes) softwares were used, respectively. qPCR experiments were performed and analysed using FAST 7500 Real-Time PCR 2.0.6 software (Applied Biosystems).

Adquisition and analysis of microscopy images was conducted with Leica Application Suite AF 2.7.0.9329 (Leica Microsystems GmbH), while quantification of Western blot bands was performed with ImageJ32 1.50i (National Institute of Health, Bethesda, MD). Any further image processing was conducted on Adobe Photoshop 11.0 (Adobe Systems Software).

Gene Ontology analysis was performed with DAVID 6.8 (Huang da, W *et al.*, 2009). Prediction of putative SUMOylation sites was performed with GPS-SUMO 1.0 (Zhao, Q *et al.*, 2014).

Statistical analysis was conducted on Prism5 5.0a (GraphPad Software). Microsoft Office 2011 for Mac (Microsoft) was also employed in this work.

8 Abbreviations

- General abbreviations

AA	Amino acids
ADP	Adenosine-5'-diphosphate
APS	Ammonium persulfate
ATP	Adenosine-5'-triphosphate
BSA	Bovine serum albumine
C-	Carboxyl- (proteins)
cDNA	Complementary DNA
CMV	Cytomegalovirus
Da	Dalton
DMF	N, N'-dimethylformamide
DMEM	Dulbeccos's modified Eagles medium
DMSO	Dimethyl sulfoxideç
DNA	Deoxyribonucleic acid
DTT	Dithiotreitol
E. coli	*Escherichia coli*
ECL	Enhanced chemical luminescence
EDTA	Ethylenediaminetetraacetic acid
EGTA	Ethyleneglycoltetraacetic acid
FBS	Fetal bovine serum
GFP	Green fluorescence protein
GO	Gene ontology
GST	Glutathione-S-transferase
HA	Hemagglutinin
HCl	Hydrochloric acid
HECT	Homologous to the E6-AP Carboxyl Terminus
HEPES	(4-(2-hydroxyethyl)-1-piperazine)ethanesulfonic acid
His-	Hexahistidine tag

HRP	Horseradish peroxidase
IP	Immunoprecipitation
IgG	Immunoglobuline G
IPTG	Isopropyl-beta-D-thiogalactopyranoside
LB	Luria-Bertani
mRNA	Messenger ribonucleic acid
MS	Mass spectrometry
N-	Amino- (protein)
NCS	Newborn calf serum
NEM	N-ethylmaleimide
PAGE	Polyacrylamide gel electrophoresis
PBS	Phosphate buffered saline
PBTr	PBS + Triton-X100
PBTw	PBS + Tween 20
PCR	Polymerase chain reaction
PMSF	Phenylmethylsulphonyl fluoride
RNA	Ribonucleic acid
rRNA	Ribosomal ribonucleic acid
RSV	Human respiratory syncytial virus
S. cerevisiae	*Saccharomyces cerevisiae*
SDS	Sodium dodecyl sulfate
SILAC	Stable Isotope Labelling with Amino acids in Cell culture
TBE	Tris-borate + EDTA
TE	Tris + EDTA
TEMED	Tetramethylethylenediamine
Tris	Tris(hydroxymethyl)aminomethane
Triton-X100	4-octylphenol polyethoxylate
Tween-20	Polyoxylethylene (20) sorbitan monolaurate
(v/v)	Volume per volume
(w/v)	Weight per volume

- Physical units

A	Ampere
°C	Degree Celsius
d	Day
g	Gram
x g	Gravitational acceleration on Earth
h	Hour
l	Liter
m	Meter
M	Molar (mol/L)
min	Minute
OD	Optical density
pH	Negative common logarithm for proton concentration
s	Second
V	Volt

- Prefixes

k	Kilo- 10^{3}
c	Centi- 10^{-2}
m	Mili- 10^{-3}
µ	Micro- 10^{-6}
n	Nano- 10^{-9}

- Nucleic acids code

A	Adenine
T	Thymine
C	Cytosine
G	Guanine
U	Uracile

- Amino acids code

A	Ala	Alanine
C	Cys	Cysteine
D	Asp	Aspartate
E	Glu	Glutamate
F	Phe	Phenylalanine
G	Gly	Glycine
H	His	Histidine
I	Iso	Isoleucine
K	Lys	Lysine
L	Leu	Leucine
M	Met	Methionine
N	Asn	Asparagine
P	Pro	Proline
Q	Gln	Glutamine
R	Arg	Arginine
S	Ser	Serine
T	Thr	Threonine
V	Val	Valine
W	Trp	Triptophane
Y	Tyr	Tyrosine

9 Appendix

The enclosed CD contains the data obtained from the MS analysis performed to identify proteins that change their SUMOylation levels between proliferative and neuronal differentiating conditions, comprised in the following appendix tables:

Table A-1: Total identified proteins. Include the number of Razor plus unique peptides and SILAC intensity ratios from all proteins identified in this MS analysis.

Table A-2: SUMO1 SILAC candidates. Include data from identified SUMO1 target proteins that show a relevant SILAC intensity ratio.

Table A-3: SUMO2/3 SILAC candidates. Include data from identified SUMO2/3 target proteins that show a relevant SILAC intensity ratio.

Table A-4: SUMO1 SILAC relative candidates. Include data from identified SUMO1 target proteins with SILAC intensity ratios due to a remarkable change in their SUMOylation state and not to significant changes in their expression levels.

Table A-5: SUMO2/3 SILAC relative candidates. Include data from identified SUMO2/3 target proteins with SILAC intensity ratios due to a remarkable change in their SUMOylation state and not to significant changes in their expression levels.

10 Bibliography

Alegre KO and Reverter D (2011) Swapping small ubiquitin-like modifier (SUMO) isoform specificity of SUMO proteases SENP6 and SENP7. J Biol Chem 286: 36142-36151

Azuma Y, Arnaoutov A and Dasso M (2003) SUMO-2/3 regulates topoisomerase II in mitosis. J Cell Biol 163: 477-487

Azuma Y, Tan SH, Cavenagh MM, Ainsztein AM, Saitoh H and Dasso M (2001) Expression and regulation of the mammalian SUMO-1 E1 enzyme. FASEB J 15: 1825-1827

Barysch SV, Dittner C, Flotho A, Becker J and Melchior F (2014) Identification and analysis of endogenous SUMO1 and SUMO2/3 targets in mammalian cells and tissues using monoclonal antibodies. Nat Protoc 9: 896-909

Bayer P, Arndt A, Metzger S, Mahajan R, Melchior F, Jaenicke R and Becker J (1998) Structure determination of the small ubiquitin-related modifier SUMO-1. J Mol Biol 280: 275-286

Becker J, Barysch SV, Karaca S, Dittner C, Hsiao HH, Berriel Diaz M, Herzig S, Urlaub H and Melchior F (2013) Detecting endogenous SUMO targets in mammalian cells and tissues. Nat Struct Mol Biol 20: 525-531

Beg AA and Scheiffele P (2006) Neuroscience. SUMO wrestles the synapse. Science 311: 962-963

Bellini E, Pavesi G, Barbiero I, Bergo A, Chandola C, Nawaz MS, Rusconi L, Stefanelli G, Strollo M, Valente MM, Kilstrup-Nielsen C and Landsberger N (2014) MeCP2 post-translational modifications: a mechanism to control its involvement in synaptic plasticity and homeostasis? Front Cell Neurosci 8: 236

Berdnik D, Torok T, Gonzalez-Gaitan M and Knoblich JA (2002) The endocytic protein alpha-Adaptin is required for numb-mediated asymmetric cell division in Drosophila. Dev Cell 3: 221-231

Bernier-Villamor V, Sampson DA, Matunis MJ and Lima CD (2002) Structural basis for E2-mediated SUMO conjugation revealed by a complex between ubiquitin-conjugating enzyme Ubc9 and RanGAP1. Cell 108: 345-356

Bertrand N, Castro DS and Guillemot F (2002) Proneural genes and the specification of neural cell types. Nat Rev Neurosci 3: 517-530

Blader P, Fischer N, Gradwohl G, Guillemot F and Strahle U (1997) The activity of neurogenin1 is controlled by local cues in the zebrafish embryo. Development 124: 4557-4569

Bohren KM, Nadkarni V, Song JH, Gabbay KH and Owerbach D (2004) A M55V polymorphism in a novel SUMO gene (SUMO-4) differentially activates heat shock transcription factors and is associated with susceptibility to type I diabetes mellitus. J Biol Chem 279: 27233-27238

Bray SJ (2006) Notch signalling: a simple pathway becomes complex. Nat Rev Mol Cell Biol 7: 678-689

Castoralova M, Brezinova D, Sveda M, Lipov J, Ruml T and Knejzlik Z (2012) SUMO-2/3 conjugates accumulating under heat shock or MG132 treatment result largely from new protein synthesis. Biochim Biophys Acta 1823: 911-919

Ceballos-Chavez M, Rivero S, Garcia-Gutierrez P, Rodriguez-Paredes M, Garcia-Dominguez M, Bhattacharya S and Reyes JC (2012) Control of neuronal differentiation by sumoylation of BRAF35, a subunit of the LSD1-CoREST histone demethylase complex. Proc Natl Acad Sci U S A 109: 8085-8090

Cepko CL (1999) The roles of intrinsic and extrinsic cues and bHLH genes in the determination of retinal cell fates. Curr Opin Neurobiol 9: 37-46

Chang CC, Naik MT, Huang YS, Jeng JC, Liao PH, Kuo HY, Ho CC, Hsieh YL, Lin CH, Huang NJ, Naik NM, Kung CC, Lin SY, Chen RH, Chang KS, Huang TH and Shih HM (2011) Structural and functional roles of Daxx SIM phosphorylation in SUMO paralog-selective binding and apoptosis modulation. Mol Cell 42: 62-74

Chavrier P, Zerial M, Lemaire P, Almendral J, Bravo R and Charnay P (1988) A gene encoding a protein with zinc fingers is activated during G0/G1 transition in cultured cells. EMBO J 7: 29-35

Cheng J, Huang M, Zhu Y, Xin YJ, Zhao YK, Huang J, Yu JX, Zhou WH and Qiu Z (2014) SUMOylation of MeCP2 is essential for transcriptional repression and hippocampal synapse development. J Neurochem 128: 798-806

Chenn A and McConnell SK (1995) Cleavage orientation and the asymmetric inheritance of Notch1 immunoreactivity in mammalian neurogenesis. Cell 82: 631-641

Chenn A, Zhang YA, Chang BT and McConnell SK (1998) Intrinsic polarity of mammalian neuroepithelial cells. Mol Cell Neurosci 11: 183-193

Childs KS and Goodbourn S (2003) Identification of novel co-repressor molecules for Interferon Regulatory Factor-2. Nucleic Acids Res 31: 3016-3026

Chomette D, Frain M, Cereghini S, Charnay P and Ghislain J (2006) Krox20 hindbrain cis-regulatory landscape: interplay between multiple long-range initiation and autoregulatory elements. Development 133: 1253-1262

Chung CD, Liao J, Liu B, Rao X, Jay P, Berta P and Shuai K (1997) Specific inhibition of Stat3 signal transduction by PIAS3. Science 278: 1803-1805

Davis RL and Turner DL (2001) Vertebrate hairy and Enhancer of split related proteins: transcriptional repressors regulating cellular differentiation and embryonic patterning. Oncogene 20: 8342-8357

Desmazieres A, Charnay P and Gilardi-Hebenstreit P (2009) Krox20 controls the transcription of its various targets in the developing hindbrain according to multiple modes. J Biol Chem 284: 10831-10840

Desmazieres A, Decker L, Vallat JM, Charnay P and Gilardi-Hebenstreit P (2008) Disruption of Krox20-Nab interaction in the mouse leads to peripheral neuropathy with biphasic evolution. J Neurosci 28: 5891-5900

Desterro JM, Rodriguez MS and Hay RT (1998) SUMO-1 modification of IkappaBalpha inhibits NF-kappaB activation. Mol Cell 2: 233-239

Desterro JM, Rodriguez MS, Kemp GD and Hay RT (1999) Identification of the enzyme required for activation of the small ubiquitin-like protein SUMO-1. J Biol Chem 274: 10618-10624

Desterro JM, Thomson J and Hay RT (1997) Ubc9 conjugates SUMO but not ubiquitin. FEBS Lett 417: 297-300

Di Bacco A, Ouyang J, Lee HY, Catic A, Ploegh H and Gill G (2006) The SUMO-specific protease SENP5 is required for cell division. Mol Cell Biol 26: 4489-4498

Dohmen RJ (2004) SUMO protein modification. Biochim Biophys Acta 1695: 113-131

Dohmen RJ, Stappen R, McGrath JP, Forrova H, Kolarov J, Goffeau A and Varshavsky A (1995) An essential yeast gene encoding a homolog of ubiquitin-activating enzyme. J Biol Chem 270: 18099-18109

Eaton EM and Sealy L (2003) Modification of CCAAT/enhancer-binding protein-beta by the small ubiquitin-like modifier (SUMO) family members, SUMO-2 and SUMO-3. J Biol Chem 278: 33416-33421

Eckermann K (2013) SUMO and Parkinson's disease. Neuromolecular Med 15: 737-759

Farah MH, Olson JM, Sucic HB, Hume RI, Tapscott SJ and Turner DL (2000) Generation of neurons by transient expression of neural bHLH proteins in mammalian cells. Development 127: 693-702

Faresse N, Colland F, Ferrand N, Prunier C, Bourgeade MF and Atfi A (2008) Identification of PCTA, a TGIF antagonist that promotes PML function in TGF-beta signalling. EMBO J 27: 1804-1815

Federzoni EA, Gloor S, Jin J, Shan-Krauer D, Fey MF, Torbett BE and Tschan MP (2015) Linking the SUMO protease SENP5 to neutrophil differentiation of AML cells. Leuk Res Rep 4: 32-35

Flotho A and Melchior F (2013) Sumoylation: a regulatory protein modification in health and disease. Annu Rev Biochem 82: 357-385

Garcia-Dominguez M, Gilardi-Hebenstreit P and Charnay P (2006) PIASxbeta acts as an activator of Hoxb1 and is antagonized by Krox20 during hindbrain segmentation. EMBO J 25: 2432-2442

Garcia-Dominguez M, March-Diaz R and Reyes JC (2008) The PHD domain of plant PIAS proteins mediates sumoylation of bromodomain GTE proteins. J Biol Chem 283: 21469-21477

Garcia-Dominguez M, Poquet C, Garel S and Charnay P (2003) Ebf gene function is required for coupling neuronal differentiation and cell cycle exit. Development 130: 6013-6025

Garcia-Dominguez M and Reyes JC (2009) SUMO association with repressor complexes, emerging routes for transcriptional control. Biochim Biophys Acta 1789: 451-459

Garcia-Gutierrez P, Juarez-Vicente F, Gallardo-Chamizo F, Charnay P and Garcia-Dominguez M (2011) The transcription factor Krox20 is an E3 ligase that sumoylates its Nab coregulators. EMBO Rep 12: 1018-1023

Garcia-Gutierrez P, Juarez-Vicente F, Wolgemuth DJ and Garcia-Dominguez M (2014) Pleiotrophin antagonizes Brd2 during neuronal differentiation. J Cell Sci 127: 2554-2564

Garcia-Gutierrez P, Mundi M and Garcia-Dominguez M (2012) Association of bromodomain BET proteins with chromatin requires dimerization through the conserved motif B. J Cell Sci 125: 3671-3680

Gareau JR and Lima CD (2010) The SUMO pathway: emerging mechanisms that shape specificity, conjugation and recognition. Nat Rev Mol Cell Biol 11: 861-871

Ghosh H, Auguadri L, Battaglia S, Simone Thirouin Z, Zemoura K, Messner S, Acuna MA, Wildner H, Yevenes GE, Dieter A, Kawasaki H, M OH, Zeilhofer HU, Fritschy JM and Tyagarajan SK (2016) Several posttranslational modifications act in concert to regulate gephyrin scaffolding and GABAergic transmission. Nat Commun 7: 13365

Giudicelli F, Gilardi-Hebenstreit P, Mechta-Grigoriou F, Poquet C and Charnay P (2003) Novel activities of Mafb underlie its dual role in hindbrain segmentation and regional specification. Dev Biol 253: 150-162

Giudicelli F, Taillebourg E, Charnay P and Gilardi-Hebenstreit P (2001) Krox-20 patterns the hindbrain through both cell-autonomous and non cell-autonomous mechanisms. Genes Dev 15: 567-580

Gong L and Yeh ET (2006) Characterization of a family of nucleolar SUMO-specific proteases with preference for SUMO-2 or SUMO-3. J Biol Chem 281: 15869-15877

Goodson ML, Hong Y, Rogers R, Matunis MJ, Park-Sarge OK and Sarge KD (2001) Sumo-1 modification regulates the DNA binding activity of heat shock transcription factor 2, a promyelocytic leukemia nuclear body associated transcription factor. J Biol Chem 276: 18513-18518

Goridis C and Brunet JF (1999) Transcriptional control of neurotransmitter phenotype. Curr Opin Neurobiol 9: 47-53

Gotz M and Huttner WB (2005) The cell biology of neurogenesis. Nat Rev Mol Cell Biol 6: 777-788

Green MR and Sambrook J (2012) Molecular Cloning: A Laboratory Manual. Cold Spring Harbor Laboratory Press, New York

Gregoire S and Yang XJ (2005) Association with class IIa histone deacetylases upregulates the sumoylation of MEF2 transcription factors. Mol Cell Biol 25: 2273-2287

Gudas LJ and Wagner JA (2011) Retinoids regulate stem cell differentiation. J Cell Physiol 226: 322-330

Guillemot F (1999) Vertebrate bHLH genes and the determination of neuronal fates. Exp Cell Res 253: 357-364

Guo D, Li M, Zhang Y, Yang P, Eckenrode S, Hopkins D, Zheng W, Purohit S, Podolsky RH, Muir A, Wang J, Dong Z, Brusko T, Atkinson M, Pozzilli P, Zeidler A, Raffel LJ, Jacob CO, Park Y, Serrano-Rios M, Larrad MT, Zhang Z, Garchon HJ, Bach JF, Rotter JI, She JX and Wang CY (2004) A functional variant of SUMO4, a new I kappa B alpha modifier, is associated with type 1 diabetes. Nat Genet 36: 837-841

Hamada M, Haeger A, Jeganathan KB, van Ree JH, Malureanu L, Walde S, Joseph J, Kehlenbach RH and van Deursen JM (2011) Ran-dependent docking of importin-beta to RanBP2/Nup358 filaments is essential for protein import and cell viability. J Cell Biol 194: 597-612

Hammer E, Heilbronn R and Weger S (2007) The E3 ligase Topors induces the accumulation of polysumoylated forms of DNA topoisomerase I in vitro and in vivo. FEBS Lett 581: 5418-5424

Hasegawa Y, Yoshida D, Nakamura Y and Sakakibara S (2014) Spatiotemporal distribution of SUMOylation components during mouse brain development. J Comp Neurol 522: 3020-3036

Hatakeyama J, Tomita K, Inoue T and Kageyama R (2001) Roles of homeobox and bHLH genes in specification of a retinal cell type. Development 128: 1313-1322

Hay RT (2005) SUMO: a history of modification. Mol Cell 18: 1-12

Hay RT (2007) SUMO-specific proteases: a twist in the tail. Trends Cell Biol 17: 370-376

Hecker CM, Rabiller M, Haglund K, Bayer P and Dikic I (2006) Specification of SUMO1- and SUMO2-interacting motifs. J Biol Chem 281: 16117-16127

Hickey CM, Wilson NR and Hochstrasser M (2012) Function and regulation of SUMO proteases. Nat Rev Mol Cell Biol 13: 755-766

Hietakangas V, Anckar J, Blomster HA, Fujimoto M, Palvimo JJ, Nakai A and Sistonen L (2006) PDSM, a motif for phosphorylation-dependent SUMO modification. Proc Natl Acad Sci U S A 103: 45-50

Hochstrasser M (2001) SP-RING for SUMO: new functions bloom for a ubiquitin-like protein. Cell 107: 5-8

Hong G, Qiu H, Wang C, Jadhav G, Wang H, Tickner J, He W and Xu J (2017) The Emerging Role of MORC Family Proteins in Cancer Development and Bone Homeostasis. J Cell Physiol 232: 928-934

Hong Y, Rogers R, Matunis MJ, Mayhew CN, Goodson ML, Park-Sarge OK and Sarge KD (2001) Regulation of heat shock transcription factor 1 by stress-induced SUMO-1 modification. J Biol Chem 276: 40263-40267

Huang C, Han Y, Wang Y, Sun X, Yan S, Yeh ET, Chen Y, Cang H, Li H, Shi G, Cheng J, Tang X and Yi J (2009) SENP3 is responsible for HIF-1 transactivation under mild oxidative stress via p300 de-SUMOylation. EMBO J 28: 2748-2762

Huang da W, Sherman BT and Lempicki RA (2009) Systematic and integrative analysis of large gene lists using DAVID bioinformatics resources. Nat Protoc 4: 44-57

Inoue T, Hojo M, Bessho Y, Tano Y, Lee JE and Kageyama R (2002) Math3 and NeuroD regulate amacrine cell fate specification in the retina. Development 129: 831-842

Itasaki N, Bel-Vialar S and Krumlauf R (1999) 'Shocking' developments in chick embryology: electroporation and in ovo gene expression. Nat Cell Biol 1: E203-207

Ivanov AV, Peng H, Yurchenko V, Yap KL, Negorev DG, Schultz DC, Psulkowski E, Fredericks WJ, White DE, Maul GG, Sadofsky MJ, Zhou MM and Rauscher FJ, 3rd (2007) PHD domain-mediated E3 ligase activity directs intramolecular sumoylation of an adjacent bromodomain required for gene silencing. Mol Cell 28: 823-837

Jackson SP and Durocher D (2013) Regulation of DNA damage responses by ubiquitin and SUMO. Mol Cell 49: 795-807

Jadhav G, Teguh D, Kenny J, Tickner J and Xu J (2016) Morc3 mutant mice exhibit reduced cortical area and thickness, accompanied by altered haematopoietic stem cells niche and bone cell differentiation. Sci Rep 6: 25964

Jain AK and Barton MC (2009) Regulation of p53: TRIM24 enters the RING. Cell Cycle 8: 3668-3674

Johnson ES and Blobel G (1997) Ubc9p is the conjugating enzyme for the ubiquitin-like protein Smt3p. J Biol Chem 272: 26799-26802

Johnson ES, Schwienhorst I, Dohmen RJ and Blobel G (1997) The ubiquitin-like protein Smt3p is activated for conjugation to other proteins by an Aos1p/Uba2p heterodimer. EMBO J 16: 5509-5519

Johnson JE, Birren SJ, Saito T and Anderson DJ (1992) DNA binding and transcriptional regulatory activity of mammalian achaete-scute homologous (MASH) proteins revealed by interaction with a muscle-specific enhancer. Proc Natl Acad Sci U S A 89: 3596-3600

Joseph J, Tan SH, Karpova TS, McNally JG and Dasso M (2002) SUMO-1 targets RanGAP1 to kinetochores and mitotic spindles. J Cell Biol 156: 595-602

Juarez-Vicente F, Luna-Pelaez N and Garcia-Dominguez M (2016) The Sumo protease Senp7 is required for proper neuronal differentiation. Biochim Biophys Acta 1863: 1490-1498

Kagey MH, Melhuish TA and Wotton D (2003) The polycomb protein Pc2 is a SUMO E3. Cell 113: 127-137

Kageyama R and Nakanishi S (1997) Helix-loop-helix factors in growth and differentiation of the vertebrate nervous system. Curr Opin Genet Dev 7: 659-665

Kerscher O (2007) SUMO junction-what's your function? New insights through SUMO-interacting motifs. EMBO Rep 8: 550-555

Kerscher O, Felberbaum R and Hochstrasser M (2006) Modification of proteins by ubiquitin and ubiquitin-like proteins. Annu Rev Cell Dev Biol 22: 159-180

Kimura Y, Sakai F, Nakano O, Kisaki O, Sugimoto H, Sawamura T, Sadano H and Osumi T (2002) The newly identified human nuclear protein NXP-2 possesses three distinct domains, the nuclear matrix-binding, RNA-binding, and coiled-coil domains. J Biol Chem 277: 20611-20617

Knecht AK and Bronner-Fraser M (2002) Induction of the neural crest: a multigene process. Nat Rev Genet 3: 453-461

Kotaja N, Karvonen U, Janne OA and Palvimo JJ (2002) PIAS proteins modulate transcription factors by functioning as SUMO-1 ligases. Mol Cell Biol 22: 5222-5234

Laemmli UK (1970) Cleavage of structural proteins during the assembly of the head of bacteriophage T4. Nature 227: 680-685

Lange C, Huttner WB and Calegari F (2009) Cdk4/cyclinD1 overexpression in neural stem cells shortens G1, delays neurogenesis, and promotes the generation and expansion of basal progenitors. Cell Stem Cell 5: 320-331

Le N, Nagarajan R, Wang JY, Svaren J, LaPash C, Araki T, Schmidt RE and Milbrandt J (2005) Nab proteins are essential for peripheral nervous system myelination. Nat Neurosci 8: 932-940

Lee JE (1997) Basic helix-loop-helix genes in neural development. Curr Opin Neurobiol 7: 13-20

Lee L, Sakurai M, Matsuzaki S, Arancio O and Fraser P (2013) SUMO and Alzheimer's disease. Neuromolecular Med 15: 720-736

Lewis KE (2006) How do genes regulate simple behaviours? Understanding how different neurons in the vertebrate spinal cord are genetically specified. Philos Trans R Soc Lond B Biol Sci 361: 45-66

Li SJ and Hochstrasser M (1999) A new protease required for cell-cycle progression in yeast. Nature 398: 246-251

Lima CD and Reverter D (2008) Structure of the human SENP7 catalytic domain and poly-SUMO deconjugation activities for SENP6 and SENP7. J Biol Chem 283: 32045-32055

Lin CH, Stoeck J, Ravanpay AC, Guillemot F, Tapscott SJ and Olson JM (2004) Regulation of neuroD2 expression in mouse brain. Dev Biol 265: 234-245

Liu B, Liao J, Rao X, Kushner SA, Chung CD, Chang DD and Shuai K (1998) Inhibition of Stat1-mediated gene activation by PIAS1. Proc Natl Acad Sci U S A 95: 10626-10631

Loriol C, Parisot J, Poupon G, Gwizdek C and Martin S (2012) Developmental regulation and spatiotemporal redistribution of the sumoylation machinery in the rat central nervous system. PLoS One 7: e33757

Lukaszewicz AI and Anderson DJ (2011) Cyclin D1 promotes neurogenesis in the developing spinal cord in a cell cycle-independent manner. Proc Natl Acad Sci U S A 108: 11632-11637

Lumsden A and Krumlauf R (1996) Patterning the vertebrate neuraxis. Science 274: 1109-1115

Luo J, Ashikaga E, Rubin PP, Heimann MJ, Hildick KL, Bishop P, Girach F, Josa-Prado F, Tang LT, Carmichael RE, Henley JM and Wilkinson KA (2013) Receptor trafficking and the regulation of synaptic plasticity by SUMO. Neuromolecular Med 15: 692-706

Ma Q, Fode C, Guillemot F and Anderson DJ (1999) Neurogenin1 and neurogenin2 control two distinct waves of neurogenesis in developing dorsal root ganglia. Genes Dev 13: 1717-1728

Ma Q, Kintner C and Anderson DJ (1996) Identification of neurogenin, a vertebrate neuronal determination gene. Cell 87: 43-52

MacPherson PA, Jones S, Pawson PA, Marshall KC and McBurney MW (1997) P19 cells differentiate into glutamatergic and glutamate-responsive neurons in vitro. Neuroscience 80: 487-499

Maden M (2006) Retinoids and spinal cord development. J Neurobiol 66: 726-738

Mager GM, Ward RM, Srinivasan R, Jang SW, Wrabetz L and Svaren J (2008) Active gene repression by the Egr2.NAB complex during peripheral nerve myelination. J Biol Chem 283: 18187-18197

Mahajan R, Delphin C, Guan T, Gerace L and Melchior F (1997) A small ubiquitin-related polypeptide involved in targeting RanGAP1 to nuclear pore complex protein RanBP2. Cell 88: 97-107

Maison C, Romeo K, Bailly D, Dubarry M, Quivy JP and Almouzni G (2012) The SUMO protease SENP7 is a critical component to ensure HP1 enrichment at pericentric heterochromatin. Nat Struct Mol Biol 19: 458-460

Martin S, Wilkinson KA, Nishimune A and Henley JM (2007) Emerging extranuclear roles of protein SUMOylation in neuronal function and dysfunction. Nat Rev Neurosci 8: 948-959

Massari ME and Murre C (2000) Helix-loop-helix proteins: regulators of transcription in eucaryotic organisms. Mol Cell Biol 20: 429-440

Matic I, Schimmel J, Hendriks IA, van Santen MA, van de Rijke F, van Dam H, Gnad F, Mann M and Vertegaal AC (2010) Site-specific identification of SUMO-2 targets in cells reveals an inverted SUMOylation motif and a hydrophobic cluster SUMOylation motif. Mol Cell 39: 641-652

Matunis MJ, Coutavas E and Blobel G (1996) A novel ubiquitin-like modification modulates the partitioning of the Ran-GTPase-activating protein RanGAP1 between the cytosol and the nuclear pore complex. J Cell Biol 135: 1457-1470

McConnell SK (1988) Development and decision-making in the mammalian cerebral cortex. Brain Res 472: 1-23

Mechta-Grigoriou F, Garel S and Charnay P (2000) Nab proteins mediate a negative feedback loop controlling Krox-20 activity in the developing hindbrain. Development 127: 119-128

Mei D, Song H, Wang K, Lou Y, Sun W, Liu Z, Ding X and Guo J (2013) Up-regulation of SUMO1 pseudogene 3 (SUMO1P3) in gastric cancer and its clinical association. Med Oncol 30: 709

Melchior F (2000) SUMO--nonclassical ubiquitin. Annu Rev Cell Dev Biol 16: 591-626

Melchior F, Schergaut M and Pichler A (2003) SUMO: ligases, isopeptidases and nuclear pores. Trends Biochem Sci 28: 612-618

Mellitzer G, Xu Q and Wilkinson DG (2000) Control of cell behaviour by signalling through Eph receptors and ephrins. Curr Opin Neurobiol 10: 400-408

Meulmeester E, Kunze M, Hsiao HH, Urlaub H and Melchior F (2008) Mechanism and consequences for paralog-specific sumoylation of ubiquitin-specific protease 25. Mol Cell 30: 610-619

Mimura Y, Takahashi K, Kawata K, Akazawa T and Inoue N (2010) Two-step colocalization of MORC3 with PML nuclear bodies. J Cell Sci 123: 2014-2024

Mizuguchi R, Sugimori M, Takebayashi H, Kosako H, Nagao M, Yoshida S, Nabeshima Y, Shimamura K and Nakafuku M (2001) Combinatorial roles of olig2 and neurogenin2 in the coordinated induction of pan-neuronal and subtype-specific properties of motoneurons. Neuron 31: 757-771

Mossessova E and Lima CD (2000) Ulp1-SUMO crystal structure and genetic analysis reveal conserved interactions and a regulatory element essential for cell growth in yeast. Mol Cell 5: 865-876

Nieto M, Schuurmans C, Britz O and Guillemot F (2001) Neural bHLH genes control the neuronal versus glial fate decision in cortical progenitors. Neuron 29: 401-413

Novitch BG, Chen AI and Jessell TM (2001) Coordinate regulation of motor neuron subtype identity and pan-neuronal properties by the bHLH repressor Olig2. Neuron 31: 773-789

Okuma T, Honda R, Ichikawa G, Tsumagari N and Yasuda H (1999) In vitro SUMO-1 modification requires two enzymatic steps, E1 and E2. Biochem Biophys Res Commun 254: 693-698

Olsen SK, Capili AD, Lu X, Tan DS and Lima CD (2010) Active site remodelling accompanies thioester bond formation in the SUMO E1. Nature 463: 906-912

Olson JM, Asakura A, Snider L, Hawkes R, Strand A, Stoeck J, Hallahan A, Pritchard J and Tapscott SJ (2001) NeuroD2 is necessary for development and survival of central nervous system neurons. Dev Biol 234: 174-187

Perez SE, Rebelo S and Anderson DJ (1999) Early specification of sensory neuron fate revealed by expression and function of neurogenins in the chick embryo. Development 126: 1715-1728

Pfaffl MW (2001) A new mathematical model for relative quantification in real-time RT-PCR. Nucleic Acids Res 29: e45

Picard N, Caron V, Bilodeau S, Sanchez M, Mascle X, Aubry M and Tremblay A (2012) Identification of estrogen receptor beta as a SUMO-1 target reveals a novel phosphorylated sumoylation motif and regulation by glycogen synthase kinase 3beta. Mol Cell Biol 32: 2709-2721

Pichler A, Knipscheer P, Saitoh H, Sixma TK and Melchior F (2004) The RanBP2 SUMO E3 ligase is neither HECT- nor RING-type. Nat Struct Mol Biol 11: 984-991

Reverter D and Lima CD (2006) Structural basis for SENP2 protease interactions with SUMO precursors and conjugated substrates. Nat Struct Mol Biol 13: 1060-1068

Reyes-Turcu FE, Ventii KH and Wilkinson KD (2009) Regulation and cellular roles of ubiquitin-specific deubiquitinating enzymes. Annu Rev Biochem 78: 363-397

Rodriguez MS, Dargemont C and Hay RT (2001) SUMO-1 conjugation in vivo requires both a consensus modification motif and nuclear targeting. J Biol Chem 276: 12654-12659

Rodriguez-Boulan E and Nelson WJ (1989) Morphogenesis of the polarized epithelial cell phenotype. Science 245: 718-725

Romeo K, Louault Y, Cantaloube S, Loiodice I, Almouzni G and Quivy JP (2015) The SENP7 SUMO-Protease Presents a Module of Two HP1 Interaction Motifs that Locks HP1 Protein at Pericentric Heterochromatin. Cell Rep

Roztocil T, Matter-Sadzinski L, Alliod C, Ballivet M and Matter JM (1997) NeuroM, a neural helix-loop-helix transcription factor, defines a new transition stage in neurogenesis. Development 124: 3263-3272

Russo MW, Sevetson BR and Milbrandt J (1995) Identification of NAB1, a repressor of NGFI-A- and Krox20-mediated transcription. Proc Natl Acad Sci U S A 92: 6873-6877

Rytinki MM, Kaikkonen S, Pehkonen P, Jaaskelainen T and Palvimo JJ (2009) PIAS proteins: pleiotropic interactors associated with SUMO. Cell Mol Life Sci 66: 3029-3041

Saitoh H and Hinchey J (2000) Functional heterogeneity of small ubiquitin-related protein modifiers SUMO-1 versus SUMO-2/3. J Biol Chem 275: 6252-6258

Saitoh H, Pizzi MD and Wang J (2002) Perturbation of SUMOlation enzyme Ubc9 by distinct domain within nucleoporin RanBP2/Nup358. J Biol Chem 277: 4755-4763

Sambrook J and Gething MJ (1989) Protein structure. Chaperones, paperones. Nature 342: 224-225

Savare J, Bonneaud N and Girard F (2005) SUMO represses transcriptional activity of the Drosophila SoxNeuro and human Sox3 central nervous system-specific transcription factors. Mol Biol Cell 16: 2660-2669

Schmidt D and Muller S (2003) PIAS/SUMO: new partners in transcriptional regulation. Cell Mol Life Sci 60: 2561-2574

Schneider-Maunoury S, Topilko P, Seitandou T, Levi G, Cohen-Tannoudji M, Pournin S, Babinet C and Charnay P (1993) Disruption of Krox-20 results in alteration of rhombomeres 3 and 5 in the developing hindbrain. Cell 75: 1199-1214

Schoenwolf GC and Kelley RO (1980) Characterization of intercellular junctions in the caudal portion of the developing neural tube of the chick embryo. Am J Anat 158: 29-41

Schulz S, Chachami G, Kozaczkiewicz L, Winter U, Stankovic-Valentin N, Haas P, Hofmann K, Urlaub H, Ovaa H, Wittbrodt J, Meulmeester E and Melchior F (2012) Ubiquitin-specific protease-like 1 (USPL1) is a SUMO isopeptidase with essential, non-catalytic functions. EMBO Rep 13: 930-938

Schwamborn JC, Berezikov E and Knoblich JA (2009) The TRIM-NHL protein TRIM32 activates microRNAs and prevents self-renewal in mouse neural progenitors. Cell 136: 913-925

Seeler JS and Dejean A (2003) Nuclear and unclear functions of SUMO. Nat Rev Mol Cell Biol 4: 690-699

Seo S, Herr A, Lim JW, Richardson GA, Richardson H and Kroll KL (2005) Geminin regulates neuronal differentiation by antagonizing Brg1 activity. Genes Dev 19: 1723-1734

Sharma P, Yamada S, Lualdi M, Dasso M and Kuehn MR (2013) Senp1 is essential for desumoylating Sumo1-modified proteins but dispensable for Sumo2 and Sumo3 deconjugation in the mouse embryo. Cell Rep 3: 1640-1650

Shen L, Tatham MH, Dong C, Zagorska A, Naismith JH and Hay RT (2006) SUMO protease SENP1 induces isomerization of the scissile peptide bond. Nat Struct Mol Biol 13: 1069-1077

Shen LN, Dong C, Liu H, Naismith JH and Hay RT (2006) The structure of SENP1-SUMO-2 complex suggests a structural basis for discrimination between SUMO paralogues during processing. Biochem J 397: 279-288

Shen LN, Geoffroy MC, Jaffray EG and Hay RT (2009) Characterization of SENP7, a SUMO-2/3-specific isopeptidase. Biochem J 421: 223-230

Shin EJ, Shin HM, Nam E, Kim WS, Kim JH, Oh BH and Yun Y (2012) DeSUMOylating isopeptidase: a second class of SUMO protease. EMBO Rep 13: 339-346

Song J, Zhang Z, Hu W and Chen Y (2005) Small ubiquitin-like modifier (SUMO) recognition of a SUMO binding motif: a reversal of the bound orientation. J Biol Chem 280: 40122-40129

Srinivasan R, Mager GM, Ward RM, Mayer J and Svaren J (2006) NAB2 represses transcription by interacting with the CHD4 subunit of the nucleosome remodeling and deacetylase (NuRD) complex. J Biol Chem 281: 15129-15137

Stergiopoulos A, Elkouris M and Politis PK (2014) Prospero-related homeobox 1 (Prox1) at the crossroads of diverse pathways during adult neural fate specification. Front Cell Neurosci 8: 454

Suh HY, Kim JH, Woo JS, Ku B, Shin EJ, Yun Y and Oh BH (2012) Crystal structure of DeSI-1, a novel deSUMOylase belonging to a putative isopeptidase superfamily. Proteins 80: 2099-2104

Sun Y, Goderie SK and Temple S (2005) Asymmetric distribution of EGFR receptor during mitosis generates diverse CNS progenitor cells. Neuron 45: 873-886

Sun Y, Nadal-Vicens M, Misono S, Lin MZ, Zubiaga A, Hua X, Fan G and Greenberg ME (2001) Neurogenin promotes neurogenesis and inhibits glial differentiation by independent mechanisms. Cell 104: 365-376

Svaren J, Sevetson BR, Apel ED, Zimonjic DB, Popescu NC and Milbrandt J (1996) NAB2, a corepressor of NGFI-A (Egr-1) and Krox20, is induced by proliferative and differentiative stimuli. Mol Cell Biol 16: 3545-3553

Svaren J, Sevetson BR, Golda T, Stanton JJ, Swirnoff AH and Milbrandt J (1998) Novel mutants of NAB corepressors enhance activation by Egr transactivators. EMBO J 17: 6010-6019

Swiss VA and Casaccia P (2010) Cell-context specific role of the E2F/Rb pathway in development and disease. Glia 58: 377-390

Tai DJ, Liu YC, Hsu WL, Ma YL, Cheng SJ, Liu SY and Lee EH (2016) MeCP2 SUMOylation rescues Mecp2-mutant-induced behavioural deficits in a mouse model of Rett syndrome. Nat Commun 7: 10552

Takahashi K, Yoshida N, Murakami N, Kawata K, Ishizaki H, Tanaka-Okamoto M, Miyoshi J, Zinn AR, Shime H and Inoue N (2007) Dynamic regulation of p53 subnuclear localization and senescence by MORC3. Mol Biol Cell 18: 1701-1709

Tatham MH, Jaffray E, Vaughan OA, Desterro JM, Botting CH, Naismith JH and Hay RT (2001) Polymeric chains of SUMO-2 and SUMO-3 are conjugated to protein substrates by SAE1/SAE2 and Ubc9. J Biol Chem 276: 35368-35374

Tatham MH, Kim S, Jaffray E, Song J, Chen Y and Hay RT (2005) Unique binding interactions among Ubc9, SUMO and RanBP2 reveal a mechanism for SUMO paralog selection. Nat Struct Mol Biol 12: 67-74

Tempe D, Piechaczyk M and Bossis G (2008) SUMO under stress. Biochem Soc Trans 36: 874-878

Theil T, Frain M, Gilardi-Hebenstreit P, Flenniken A, Charnay P and Wilkinson DG (1998) Segmental expression of the EphA4 (Sek-1) receptor tyrosine kinase in the hindbrain is under direct transcriptional control of Krox-20. Development 125: 443-452

Tomita K, Moriyoshi K, Nakanishi S, Guillemot F and Kageyama R (2000) Mammalian achaete-scute and atonal homologs regulate neuronal versus glial fate determination in the central nervous system. EMBO J 19: 5460-5472

Topilko P, Schneider-Maunoury S, Levi G, Baron-Van Evercooren A, Chennoufi AB, Seitanidou T, Babinet C and Charnay P (1994) Krox-20 controls myelination in the peripheral nervous system. Nature 371: 796-799

Vertegaal AC, Andersen JS, Ogg SC, Hay RT, Mann M and Lamond AI (2006) Distinct and overlapping sets of SUMO-1 and SUMO-2 target proteins revealed by quantitative proteomics. Mol Cell Proteomics 5: 2298-2310

Voon HP and Gibbons RJ (2016) Maintaining memory of silencing at imprinted differentially methylated regions. Cell Mol Life Sci 73: 1871-1879

Voon HP and Wong LH (2016) New players in heterochromatin silencing: histone variant H3.3 and the ATRX/DAXX chaperone. Nucleic Acids Res 44: 1496-1501

Wang L, Wansleeben C, Zhao S, Miao P, Paschen W and Yang W (2014) SUMO2 is essential while SUMO3 is dispensable for mouse embryonic development. EMBO Rep 15: 878-885

Wang X, Tsai JW, Imai JH, Lian WN, Vallee RB and Shi SH (2009) Asymmetric centrosome inheritance maintains neural progenitors in the neocortex. Nature 461: 947-955

Watanabe M, Takahashi K, Tomizawa K, Mizusawa H and Takahashi H (2008) Developmental regulation of Ubc9 in the rat nervous system. Acta Biochim Pol 55: 681-686

Weger S, Hammer E and Heilbronn R (2005) Topors acts as a SUMO-1 E3 ligase for p53 in vitro and in vivo. FEBS Lett 579: 5007-5012

Wei W, Yang P, Pang J, Zhang S, Wang Y, Wang MH, Dong Z, She JX and Wang CY (2008) A stress-dependent SUMO4 sumoylation of its substrate proteins. Biochem Biophys Res Commun 375: 454-459

Werner A, Flotho A and Melchior F (2012) The RanBP2/RanGAP1*SUMO1/Ubc9 complex is a multisubunit SUMO E3 ligase. Mol Cell 46: 287-298

Wilkinson KD (1997) Regulation of ubiquitin-dependent processes by deubiquitinating enzymes. FASEB J 11: 1245-1256

Willardsen MI and Link BA (2011) Cell biological regulation of division fate in vertebrate neuroepithelial cells. Dev Dyn 240: 1865-1879

Wong KA, Kim R, Christofk H, Gao J, Lawson G and Wu H (2004) Protein inhibitor of activated STAT Y (PIASy) and a splice variant lacking exon 6 enhance sumoylation but are not essential for embryogenesis and adult life. Mol Cell Biol 24: 5577-5586

Xu Z and Au SW (2005) Mapping residues of SUMO precursors essential in differential maturation by SUMO-specific protease, SENP1. Biochem J 386: 325-330

Yamashita M (2013) From neuroepithelial cells to neurons: changes in the physiological properties of neuroepithelial stem cells. Arch Biochem Biophys 534: 64-70

Yan S, Sun X, Xiang B, Cang H, Kang X, Chen Y, Li H, Shi G, Yeh ET, Wang B, Wang X and Yi J (2010) Redox regulation of the stability of the SUMO protease SENP3 via interactions with CHIP and Hsp90. EMBO J 29: 3773-3786

Yang SH, Galanis A, Witty J and Sharrocks AD (2006) An extended consensus motif enhances the specificity of substrate modification by SUMO. EMBO J 25: 5083-5093

Yang W, Thompson JW, Wang Z, Wang L, Sheng H, Foster MW, Moseley MA and Paschen W (2012) Analysis of oxygen/glucose-deprivation-induced changes in SUMO3 conjugation using SILAC-based quantitative proteomics. J Proteome Res 11: 1108-1117

Yokota Y (2001) Id and development. Oncogene 20: 8290-8298

Yunus AA and Lima CD (2009) Structure of the Siz/PIAS SUMO E3 ligase Siz1 and determinants required for SUMO modification of PCNA. Mol Cell 35: 669-682

Zarelli VE and Dawid IB (2013a) The BTB-containing protein Kctd15 is SUMOylated in vivo. PLoS One 8: e75016

Zarelli VE and Dawid IB (2013b) Inhibition of neural crest formation by Kctd15 involves regulation of transcription factor AP-2. Proc Natl Acad Sci U S A 110: 2870-2875

Zeng L, Yap KL, Ivanov AV, Wang X, Mujtaba S, Plotnikova O, Rauscher FJ, 3rd and Zhou MM (2008) Structural insights into human KAP1 PHD finger-bromodomain and its role in gene silencing. Nat Struct Mol Biol 15: 626-633

Zhan Y, Liu Y, Wang C, Lin J, Chen M, Chen X, Zhuang C, Liu L, Xu W, Zhou Q, Sun X, Zhang Q, Zhao G and Huang W (2016) Increased expression of SUMO1P3 predicts poor prognosis and promotes tumor growth and metastasis in bladder cancer. Oncotarget 7: 16038-16048

Zhang FP, Mikkonen L, Toppari J, Palvimo JJ, Thesleff I and Janne OA (2008) Sumo-1 function is dispensable in normal mouse development. Mol Cell Biol 28: 5381-5390

Zhao Q, Xie Y, Zheng Y, Jiang S, Liu W, Mu W, Liu Z, Zhao Y, Xue Y and Ren J (2014) GPS-SUMO: a tool for the prediction of sumoylation sites and SUMO-interaction motifs. Nucleic Acids Res 42: W325-330

Zhu J, Zhu S, Guzzo CM, Ellis NA, Sung KS, Choi CY and Matunis MJ (2008) Small ubiquitin-related modifier (SUMO) binding determines substrate recognition and paralog-selective SUMO modification. J Biol Chem 283: 29405-29415

11 Agradecimientos

Mi más sincero agradecimiento va dirigido a mi director de tesis, el Dr. Mario García Domínguez, por la oportunidad brindada para el abordaje de este trabajo y por toda la experiencia y guía brindadas durante su desarrollo, y extenderlo también a mi tutor de tesis, el Dr. Andrés Aguilera López.

Quisiera expresar también mi agradecimiento a los compañeros de laboratorio, en especial al Dr. Pablo García Gutiérrez, cuya aportación científica ha sido esencial para el desarrollo del primer capítulo de esta tesis, y a todos los compañeros y personal técnico del Centro Andaluz de Biología Molecular y Medicina Regenerativa (CABIMER) en Sevilla.

También quisiera expresar mi agradecimiento a la Profesora Frauke Melchior, por darme la oportunidad de establecer una colaboración que ha sido de vital importancia para el desarrollo del tercer capítulo de esta tesis, y extender mi agradecimiento a su grupo en el Centro de Biología Molecular de la Universidad de Heidelberg (ZMBH), en especial a las Dras. Sina Barysch y Annette Flotho, que han realizado el análisis de los datos obtenidos por espectrometría de masas.

Finalmente, no podría terminar sin agradecer a mi familia y amigos el apoyo recibido durante todo este trabajo. Gracias por todo el cariño y comprensión que habéis mostrado conmigo. Este trabajo no tendría sentido sin vosotros.

Este trabajo ha sido financiado por los siguientes proyectos y becas concedidas:

Plan Nacional del MICINN (BFU 2009-10986)

Junta de Ampliación de Estudios del CSIC (JAEPre010)

Plan Nacional del MINECO (BFU 2012-37304)

EMBO Short Term Fellowship (ASTF Nº 399-2014)

Plan Nacional del MINECO (BFU 2015-64721-P)

Consejería de Economía, Innovación y Ciencia de la Junta de Andalucía (P12-CTS-2064)